

# **Creating a Fluorescent *Pseudomonas aeruginosa* Biofilm Reporter**

Harry Meades



MSc by Research: Microbiology

2022-2023



## ACKNOWLEDGEMENTS

I would like to extend my sincere gratitude to my co-supervisors Dr. Marina Ezcurra & Dr. Simon Moore for their continued support and guidance throughout the duration of this project. I also extend my thanks to my friends in the Ezcurra and Moore labs who provided valuable teaching and insight, especially in the toughest moments of this project.

I would also like to thank my family for their patience and for encouraging me to pursue this MSc in the first place.

## ABSTRACT

*Pseudomonas aeruginosa* is a Gram-negative bacterium that forms three dimensional communities, called biofilms, within immunocompromised hosts to sustain its infection cycle. Communication within these structures is essential as they enable a synchronised reaction from all cells within the biofilm in response to an environmental stimulus. Biofilms are of particular interest in research as they enable production of virulence factors and provide a level of protection against widely used antimicrobials, leading researchers to use a combination of *in vitro* and *in vivo* methods to research them.

In this study, we used a combination of biofilm assays and *C. elegans* imaging of already existing *P. aeruginosa* strains to design a red fluorescing *P. aeruginosa* biofilm reporter construct. We then built our desired tool using Gibson Assembly which was transformed into *P. aeruginosa* using electroporation. The strain was then tested *in vitro* and *in vivo* for functionality. The resulting strain appears to produce a strong red fluorescence in response to C4-HSL based upon initial trials. This red fluorescence was then seen in low levels in *C. elegans* fluorescence microscopy in the lumen indicating QS/biofilm formation was occurring.

Moving forward, further studies are required due to a lack of biological replicates on the *in vitro* and *in vivo* work. Once that is completed, this tool could be used in a variety of ways such as an indicator when looking at novel antimicrobials.

## Table of Contents

<b>ACKNOWLEDGEMENTS</b> .....	<b>3</b>
<b>ABSTRACT</b> .....	<b>4</b>
<b>Chapter 1: Introduction</b> .....	<b>10</b>
<b>1.1. <i>Pseudomonas aeruginosa</i></b> .....	<b>10</b>
<b>1.2. <i>P. aeruginosa</i> Biofilms</b> .....	<b>10</b>
1.2.1. Formation Stages.....	11
1.2.2. Structure of biofilms.....	12
1.2.3. Function of Biofilms .....	16
<b>1.3. Quorum Sensing</b> .....	<b>19</b>
1.3.1. The Las QS System .....	21
1.3.2. The Rhl QS System.....	26
1.3.3. The PQS QS System.....	30
1.3.4. The lqs QS System .....	33
<b>1.4. Studying Biofilms with Synthetic Biology</b> .....	<b>34</b>
1.4.1. An Introduction to Synthetic Biology .....	35
1.4.2. Synthetic Biology and <i>P. aeruginosa</i> Biofilms .....	36
<b>1.5. Studying Biofilms In vitro</b> .....	<b>40</b>
1.5.1. Methods .....	40
<b>1.6. In vivo Biofilm Study</b> .....	<b>43</b>
1.6.1. An Introduction to Model Organisms .....	43

1.6.2. <i>Caenorhabditis elegans</i> as a Model Organism .....	44
1.6.3. Biofilm Studies of <i>C. elegans</i> .....	46
1.7. Aims .....	49
<b>Chapter 2: Methods</b> .....	<b>51</b>
2.1. Strains.....	51
2.2 Solutions .....	52
2.3 Reagents.....	53
2.4. Kits .....	55
2.5. Bacterial Growth Conditions .....	55
2.6. Preliminary <i>C. elegans</i> Work .....	55
2.6.1. Worm Husbandry .....	55
2.6.2. Synchronisation.....	56
2.6.3. <i>P. aeruginosa</i> Infection.....	57
2.6.4. Microscopy .....	57
2.7. Biofilm Assay.....	57
2.8. Recombinant DNA Assembly.....	59
2.8.1. Software DNA Analysis .....	59
2.8.2 Primer Design.....	59
2.9. Recombinant DNA cloning.....	60
2.9.1. Preparation of chemically competent cells .....	60

2.9.2. Transformation of chemically competent cells.....	61
2.9.3. Plasmid purification .....	61
2.9.4. DNA concentration estimation by Nanodrop absorbance.....	62
2.9.5. Gel Electrophoresis of DNA .....	62
2.9.6. <i>P. aeruginosa</i> gDNA Purification.....	63
2.9.7. PCR.....	64
2.9.8. Gel Extraction of DNA .....	64
2.9.9. Gibson Assembly.....	65
<b>2.10. DNA Sequencing .....</b>	<b>66</b>
<b>2.11. Transformation of <i>P. aeruginosa</i> .....</b>	<b>66</b>
2.11.1. <i>E. coli</i> ET12567 Conjugation.....	66
2.11.2 <i>E. coli</i> S17 Conjugation .....	69
2.11.3. Electroporation.....	70
<b>2.12. In Vitro &amp; In Vivo Testing of <i>P. aeruginosa</i> HM09.....</b>	<b>71</b>
2.12.1. Ensuring Biofilm Control of HM09.....	71
2.12.2. Microscopy Images of <i>P. aeruginosa</i> HM09 on LB Agar Containing C4-HSL .....	71
2.12.3. <i>C. elegans</i> Imaging on <i>P. aeruginosa</i> HM09 .....	72
<b>Chapter 3: Results.....</b>	<b>73</b>
<b>3.1. Existing GFP biofilm reporter <i>P. aeruginosa</i> strains showed significantly more GFP production when compared to PA14 in vitro but signal lost when imaging <i>C. elegans</i> intestine.....</b>	<b>73</b>

<b>3.2. Constructing <i>prhIA-mScarlet-I</i> using Gibson Assembly .....</b>	<b>76</b>
3.2.1. RFP bioreporter was designed using Benchling .....	76
3.2.2. Bioreporter fragments were collected by PCR and agarose gel extraction successfully .....	78
3.2.3. Successful Gibson Assembly of the RFP bioreporter .....	81
<b>3.3. Sequencing showed successfully constructed biofilm reporter .....</b>	<b>82</b>
<b>3.4. Successful transformation of <i>P. aeruginosa</i> PA14 .....</b>	<b>83</b>
3.4.1. Initial conjugation transformation of <i>P. aeruginosa</i> PA14 was unsuccessful .....	84
3.4.2. Alternate transformation method (electroporation) of <i>P. aeruginosa</i> PA14 successfully produced RFP bioreporter <i>P. aeruginosa</i> strain .....	87
<b>3.5. HM09 biofilm reporter in <i>P. aeruginosa</i> PA14 produces proportional fluorescence depending on the amount of C4-HSL .....</b>	<b>89</b>
<b>3.6. Fluorescent microscopy of HM09 colonies showed brighter red fluorescence when compared to PA14 in the presence of C4-HSL .....</b>	<b>91</b>
<b>3.7. HM09 fed <i>C. elegans</i> showed inconclusive red fluorescence in intestinal lumen when compared to PA14 fed <i>C. elegans</i> .....</b>	<b>93</b>
<b>Chapter 4: Discussion .....</b>	<b>96</b>

<b>4.1. The current state of in-vitro and in-vivo modelling for biofilm study.....</b>	<b>96</b>
<b>4.2. Green fluorescing <i>P. aeruginosa</i> as a tool for studying biofilms .....</b>	<b>98</b>
<b>4.3. Using synthetic biology to create a red fluorescing <i>P. aeruginosa</i> strain for studying biofilms.....</b>	<b>101</b>
<b>4.4. Causes for unsuccessful <i>P. aeruginosa</i> conjugation.....</b>	<b>101</b>
<b>4.5. <i>P. aeruginosa</i> HM09 red fluorescence was proportional to autoinducer concentration indicating biofilm control.....</b>	<b>103</b>
<b>4.6. In-vivo modelling for studying red fluorescing <i>P. aeruginosa</i> biofilms .....</b>	<b>104</b>
<b>4.7. Conclusions and future research .....</b>	<b>106</b>
<b>5. References: .....</b>	<b>108</b>

## Chapter 1: Introduction

### 1.1. *Pseudomonas aeruginosa*

*Pseudomonas aeruginosa* is an opportunistic pathogen which was responsible for approximately 4,200 cases of bacteraemia in the UK from April 2022 to April 2023 (UKHSA, 2022). *P. aeruginosa* is a Gram-negative bacterium meaning the cell wall is double enveloped, the first being a thin wall of peptidoglycan and the second, outer membrane, containing lipopolysaccharides (Shilhavy et al., 2010). *P. aeruginosa* is the leading source of mortality and morbidity in cystic fibrosis (CF) patients due to their compromised immune systems (Waters & Goldberg, 2019). Single *P. aeruginosa* cells can colonise the airways in the host by forming a biofilm in the lungs of CF patients and then upregulating their virulence factors causing the host harm (Jennings et al., 2021). The negative effects are compounded with these infections becoming even harder to treat due to the increasing number of multidrug resistant *P. aeruginosa* cases (AbdulWahab et al., 2017). The World Health Organisation (WHO) placed *P. aeruginosa* onto a list of 19 other bacteria which needed urgent research to discover new antimicrobials in response to the large increase in multidrug resistant cases of infection (Tacconelli et al., 2018).

### 1.2. *P. aeruginosa* Biofilms

*P. aeruginosa* possess the ability to form a biofilm where the bacterial cells create a community which can interact and communicate with

each other via messengers in the matrix (Thi et al., 2020). However, before considering anything biofilm related, it is important to understand the stages of biofilm development, the structure of the biofilm and finally the biofilm's function.

### 1.2.1. Formation Stages

As stated above, *P. aeruginosa* cells are motile meaning they possess a flagellum which allows the single bacterium cells to travel within the host to find new surfaces to colonise (Thi et al., 2020).

(Figure 1.2.1) shows the stages of biofilm development.

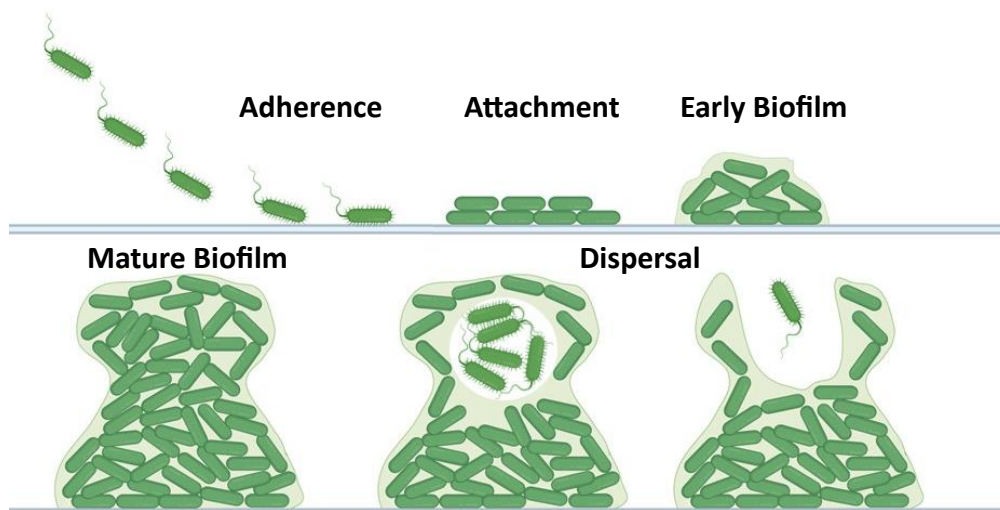


**Figure 1.2.1. Stages of biofilm formation.** Single planktonic cells adhere to the surface before deciding to irreversibly attach. Once this decision is made, the cells enter a growth phase where matrix is produced and surrounds the growing *P. aeruginosa* cells. Once the biofilm matures, motile cells are then produced ready to be dispersed and propagate the biofilm elsewhere within the host. Adapted from (Thi et al., 2020).

From the above figure it can be seen that planktonic single *P. aeruginosa* cells have motility factors such as pili and flagella which allow them to adhere to a surface and start the biofilm forming process (Thi et al., 2020). Once the single cells have adhered a

change occurs where motility factors are downregulated and proliferating and matrix production begins (Maunder & Welch, 2017). With propagation ongoing, the structure of the biofilm begins to take shape as it becomes a 3D structure and is seen as mature (Kaplan, 2010). Once the biofilm has matured, there are several ways in which new cells can disperse according to external or internal factors (Kim & Lee, 2016). Although not tied to one cause, dispersal is an essential part of the biofilm lifecycle as this allows for new cells to continue the bacterial lineage and continue infecting new areas within a host (Kim & Lee, 2016).

### 1.2.2. Structure of biofilms

Generally, the biofilm forms a mushroom-shaped 3D structure into the later stages of development, which is the matrix encompassing many microcolonies (Sauer et al., 2022). This matrix is composed of many different things (Figure 1.2.2).

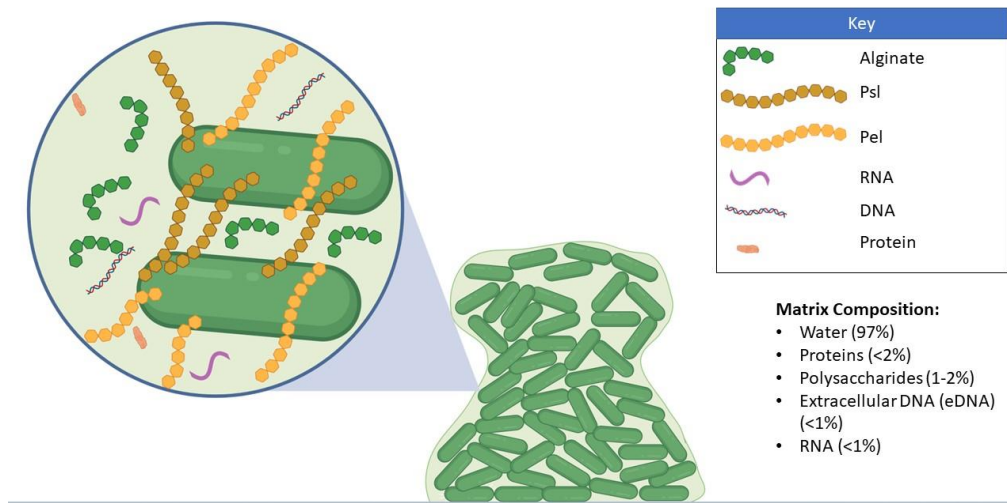


**Figure 1.2.2. Biofilm matrix composition.** Water is the largest component followed by the extracellular polysaccharides alginate, Psl and Pel all of which have their own function. Extracellular DNA and RNA is also present stemming from the lysis of cells in the biofilm following cell death. Image adapted from (Maunder & Welch, 2017).

Water is the largest contributor composing 97% of the entire biofilm matrix (Tuon et al., 2022). The water present in the biofilm matrix plays the role of a circulatory system, osmotic pressure regulator and provides a medium for signalling molecules to pass through (Quan et al., 2022). Growing bacteria need nutrients in a biofilm however there are more populated regions than others, this disparity in population makes it incredibly difficult for nutrients to diffuse to the highly populated regions in the inner biofilm. This is helped by the fact that biofilms have water channels which allow water to find its way to these densely populated regions and for waste produced by bacteria to be removed (Wilking et al., 2013; Costerton et al., 1995). Changes in osmotic pressure in a biofilm have been shown to affect the rate at which a biofilm can expand, this has led people to hypothesise that osmotic pressure regulation acts as a regulator for nutrient uptake by

the bacteria (Seminara et al., 2012; Yan et al., 2017). Signalling molecules being transported within a biofilm is incredibly important. Quorum sensing (QS) is a mechanism where communication occurs between cells within the biofilm and synchronised actions occur, for this to happen there needs to be a stable transport network (water channels) for the signalling molecules to travel longer distances (Rutherford & Bassler, 2012; Darch et al., 2012).

Polysaccharides are a large part of the extracellular matrix (Figure 1.2.2). There are 3 main types of extracellular polysaccharide in *P. aeruginosa* biofilm matrix and they are alginate, Psl and Pel (Colvin et al., 2011). Alginate is coded for by a biosynthetic gene cluster which is activated once the planktonic cells adhere to the surface where the biofilm will form (Boyd & Chakrabarty, 1995). Alginate is the decider between mucoid and non-mucoid biofilms where overproduction results in a slimier biofilm, overproduction of alginate has also been known to influence the architecture of the biofilm and the overall shape (Moradali & Rehm, 2019). Psl polysaccharide is coded for by *polysaccharide synthesis locus (psl)* which encompasses 15 genes where 11 are required for formation and export of the polysaccharide Psl (Byrd et al., 2009). Once formed, Psl plays a key role in the initial attachment of cells to the surface where the biofilm begins to form, later on in development it has been shown that overproduction of Psl resulted in stronger cell-cell interactions within a biofilm due to the mesh matrix it forms holding cells together (Wei & Ma, 2013). The final extracellular polysaccharide in *P.*

*aeruginosa* (Pel) is encoded by a seven gene operon (*pelABCDEFGF*) where each part is required for formation and export (Le Mauff et al., 2022). Pel is greatly relied on in *P. aeruginosa* PA14 and was shown, when overproduced, to increase the amount of aggregation to other cells when PA14 was in culture (Mann & Wozniak, 2012). This shows that Pel is important for cell-cell interactions whereas Psl is needed for initial attachment to surface despite both being able to be the primary extracellular polysaccharide in the matrix of the biofilm (Jennings et al., 2015; Colvin et al., 2012).

Finally, there are a variety of proteins found within the biofilm matrix, which includes extracellular DNA, RNA, and others. Generally, proteins play an important role as the internal scaffold supplying stability and shaping the structure of the biofilm (Fong & Yildiz, 2015). There are a wide variety of proteins in the matrix of the biofilm such as proteins with enzymatic effects, protease effects and DNases present to break down the extracellular DNA and RNA (Fong & Yildiz, 2015). Extracellular DNA and RNA fall into the category of intracellular proteins which have found their way into the biofilm matrix presumably by lysis of dead *P. aeruginosa* cells. This appearance of extracellular DNA is not solely coincidental as it does have a role in the scaffolding of the biofilm matrix by forming G-quadruplex structures which enhance the structural integrity of the matrix (Seviour et al., 2021). Other ways internal proteins can spill out into the external environment was presented by Toyofuku et al. in 2012. The research group presented the idea that some of these

extracellular proteins can escape the inside of cells via outer membrane vesicles (OMVs) where it was found that 30% of matrix proteins had been found in OMVs. Some proteins outside of DNA and RNA also serve structural roles in the biofilm, an example being Cdr-A. Cdr-A is the first reported protein in the extracellular matrix and is coded for by the *cdrAB* Operon, CdrA is able to interact with itself as well as the extracellular polysaccharide Psl and it is through these CdrA-CdrA and CdrA-Psl interactions by which the biofilm matrix structure and stability is provided (Reichhardt et al., 2020).

Overall, the 3 main components discussed here (water, extracellular polysaccharide and proteins) are very good at ensuring the stability and structural integrity of the *P. aeruginosa* biofilm and play a pivotal role in the longevity of the biofilm. The structural support provided occurs through individual interactions or interactions between the different groups which shows how efficient this process is. A persistent biofilm means a chronic infection for the host, however it's important to consider what the biofilm does to the bacterial cells inside.

### 1.2.3. Function of Biofilms

The *P. aeruginosa* biofilm is in place to protect the bacterial cells against external factors looking to halt the infection, e.g., antimicrobials or the hosts immune response (Rather et al., 2021). *P. aeruginosa* biofilms have antimicrobial resistance mechanisms at different stages of the antimicrobials path through the biofilm.

Resistance occurs at the surface of the biofilm because antimicrobials find it hard to penetrate the surface due to binding of some antimicrobials to components on the surface of the biofilm (Ciofu & Tolker-Nielsen, 2019; ASM, 2023). If the antimicrobial passes the surface, the further it penetrates in the less effective it tends to be at killing the bacteria in the biofilm due to the build-up of nutrients, waste and lack of oxygen. Pamp et al. showed using a flow chamber that ciprofloxacin, an antibiotic used in combination with gentamicin to treat CF patients, could not penetrate past the periphery of the *P. aeruginosa* biofilm and hence left the cells at the centre alive (Yin et al., 2022). Finally, another major contributor to the continuance of biofilms is the presence of persister cells. Persister cells are found deep within the biofilm and are bacterial cells that enter a “spore-like” state which are highly resistant (ASM, 2023). Persister cells in *P. aeruginosa* have been found after the introduction of antimicrobials such as gentamicin, ciprofloxacin, and ceftazidime (Patel et al., 2022). Persister cells have a much lower metabolic activity due to the restriction on nutrients and oxygen that occurs deeper into the biofilm and such this low activity results in a decrease in the number of targets present for antimicrobials to bind to (Ciofu & Tolker-Nielsen, 2019). Persister cells production is currently thought to be due to toxin-antitoxin pairs as opposed to a genetic change (Wood et al., 2013). The idea is that a toxin (something disrupting a cellular process) is paired with an antitoxin (RNA or protein) and this removes the target for certain

antimicrobials to work (Wood et al., 2013). The levels of persister cells are determined by cell density also, as the gene *carB*, which codes for the large subunit of CPSase, has been linked to a 2,500x decrease in survivability when knocked out (Cameron et al., 2018). CPSase is responsible for synthesising pyrimidine and arginine for *P. aeruginosa* and a lack of pyrimidine production by the bacterial cells results in cell density not reaching required levels in the stationary phase (Cameron et al., 2018).

Biofilms can cause evasion of the host immune response by two mechanisms. Biofilms are typically large structures and so they act as a physical barrier against detection and removal by immune cells, however there can also be a genetic response activating regulators, switches, or suppressors of the host immune system (González et al., 2018). The blocking functionality comes from the extracellular polysaccharides present in the matrix as the structurally integral part of the matrix provides a barrier stopping entry into the biofilm (Gunn et al., 2016). Also, rhamnolipids can provide a shield against attracted neutrophils by inducing cellular necrosis (Moser et al., 2017). Alginate in the biofilm matrix of *P. aeruginosa* is known to provoke the immune system by causing respiratory burst and cytokine production (Moser et al., 2017).

To conclude, biofilms are complex structures which are very efficient at ensuring sustainability of the cells within. They have a set formation cycle from single planktonic cell, where it adheres, grows into a large bacterial community, and then disperses individual cells

again. The matrix of the biofilm is well built where each part serves an important role based on the availability in the matrix. Finally, the biofilm serves the main purpose to protect the bacterial colony against removal by natural host immune system or antimicrobial treatments.

### 1.3. Quorum Sensing

Quorum sensing is a method of communication between bacterial cells within the biofilm community. In general, the quorum sensing process is deemed “all or nothing”. Every cell within the community produces acyl-homoserine lactones (AHLs) and when a certain concentration threshold is reached there is either an upregulation or downregulation of biofilm specific gene products depending on which signalling pathway is active (Coquant et al., 2020). The concept of quorum sensing was first described in myxobacteria and actinomycetes when it was noticed that communities of cells changed behaviour synchronously, and in response to this Fuqua et al. were looking at *Vibrio fischeri* and discovered the method of communication through LuxI and LuxR proteins (Fuqua et al., 1994). LuxI-type proteins are AHL synthases which catalyse the conversion of an intermediate into the AHL required for the quorum sensing pathway (Miranda et al., 2022). LuxR-type proteins are responsible for perceiving the produced AHLs (Yu et al., 2020). AHLs (Figure 1.3.1) have an *N*-acylated homoserine-lactone ring at the core and have an acyl chain between four and 18 carbons long, the LuxI protein can obtain the lactone ring from *S*-adenosylmethionine, and

the acyl chains are obtained from intermediates of fatty acid synthesis (Pappenfort & Bassler, 2016).

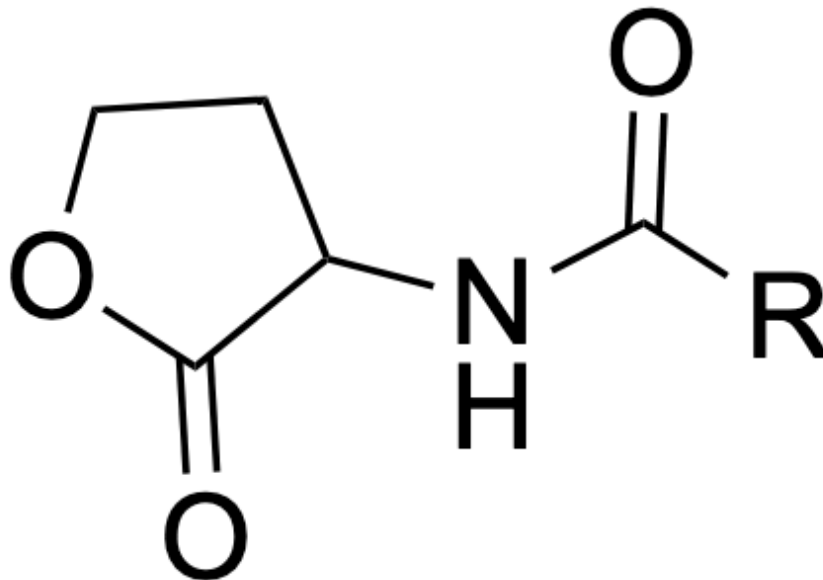


**Figure 1.3.1. AHL general formula.** AHLs have *N*-acylated homoserine-lactone ring core and a variable region (R) which is an acyl chain between four and 18 carbons long (Pappenfort & Bassler, 2016).

Once produced, the LuxR protein can detect the AHLs using the AHL-binding region at the N-terminus which allows the protein to fold correctly and makes the protein stable. Once this occurs the DNA binding domain on the C-terminus is unmasked and allowed to interact with the DNA resulting in transcription of targeted genes (Tsai & Winans, 2010; Rajput & Kumar). LuxR interacts with DNA through *lux* boxes, which are 20 base pair inverted repeats around 42.5 base pairs upstream of start of *lux* operon, where LuxR can either be an activator or a repressor (Antunes et al., 2008; van Kessel et al., 2013). *P. aeruginosa* quorum sensing works in a similar way by using LuxI-type and LuxR-type proteins and AHLs (Figure 1.3.2). There are

four individual systems which fit within a hierarchical structure with each playing a specific role in activating different virulence factor when required (Lee & Zhang, 2015).

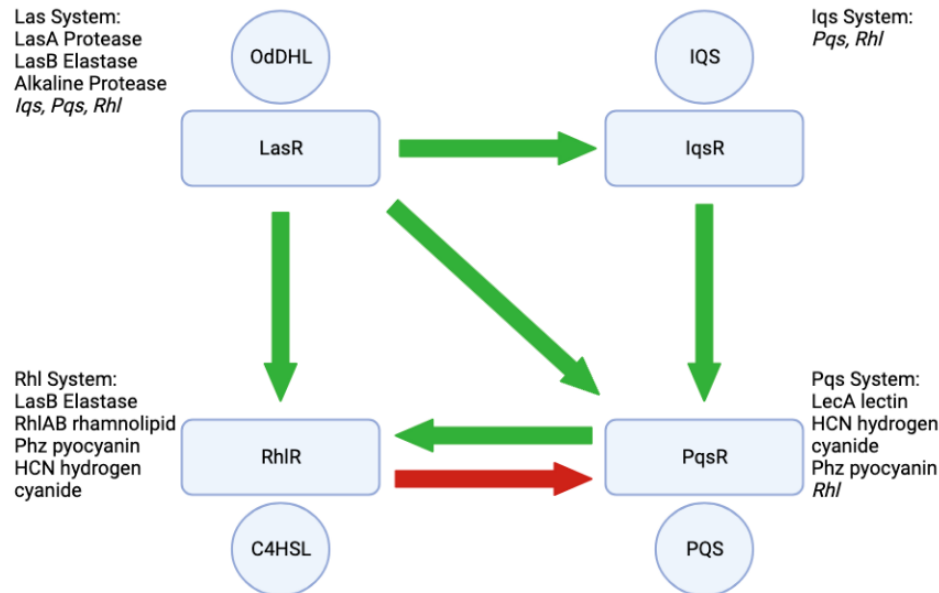


**Figure 1.3.2 The four quorum sensing systems.** Includes signalling molecules, the virulence factors regulated by each system and the interplay between each system. The Las system is responsible for activating the other three downstream systems. Iqs system then activates Pqs which activates Rhl providing a Las independent pathway. Rhl has an inhibitory effect on Pqs Adapted from Lee & Zhang 2015.

### 1.3.1. The Las QS System

The Las system sits at the top of the hierarchy of *P. aeruginosa* quorum sensing as every other systems activation is reliant on it (Dekimpe & Dèziel, 2009). The start of the Las system is triggered when the cell density within a biofilm is increased causing the necessary genes for cells to survive in this situation to be upregulated (Thi et al., 2020). The Las system relies on the AHL *N*-3-oxo-dodecanoyl-L-homoserine lactone, 3OC<sub>12</sub>HSL, which is recognised by the receptor protein LasR (McCready et al., 2019).

The LasR protein is then able to cause the production of LasI which produces more 3OC<sub>12</sub>HSL which then causes a feedforward loop increasing the concentration of the AHL (Wargo & Hogan, 2007). The *lasI* gene has a minor transcriptional start site located -13 from the start codon which can be activated in the absence of LasR:3OC<sub>12</sub>HSL (Seed et al., 1996). Once 3OC<sub>12</sub>HSL is produced it is passively allowed to exit into the extracellular environment where other cells can take up the molecule and their receptors can recognise the AHL and begin upregulating their *lasI/lasR* genes and hence the positive feedback loop continues (Miller & Gilmore, 2020). The Las system is responsible for activating several virulence factors when activated (Figure 1.3). LasA and LasB are secreted by type 2 secretion systems (T2SS) and are a key aspect of the *P. aeruginosa* virulence arsenal (Liao et al., 2022). Both LasA and LasB are activated by the transcription factor LasR when it has bound 3OC<sub>12</sub>HSL (Toder et al., 1994).

The LasA protease is encoded by the *lasA* gene and is a zinc-binding metalloprotease responsible for cleaving peptide bonds after a glycine-glycine sequence (Toder et al., 1994; Vessillier et al., 2001; Barequet et al., 2004). LasA protease function means it plays a role in regulating several processes linked to *P. aeruginosa* virulence such as shedding of the ectodomain of syndecans-1 in the lungs which is thought to increase virulence of a *P. aeruginosa* infection, and LasA has been linked to degrading connective tissue (Spencer et al., 2010). Syndecans are cell surface heparan sulphate

proteoglycans and they play a role in maintaining interactions between cells and between cells and extracellular matrix (Olczyk et al., 2015). When a *P. aeruginosa* infection occurs, it has been shown that shedding of syndecans-1 ectodomains traps cathelicidins, which are proline/arginine-rich antimicrobial peptides, resulting in reduced antimicrobial activity (Park et al., 2000; Duperthuy, 2020). LasA is also able to cause degradation of connective tissue by acting as an enhancer for LasB and helping it break down elastin (Li & Lee, 2019).

The LasB elastase is encoded by the *lasB* gene which is under the control of LasR normally, or can be activated by RhIR under phosphate limiting conditions, and is another zinc-binding metalloprotease which has three main abilities to increase virulence. LasB causes tissue damage and enhances invasion at infection sites, interacts with the immune system causing immunomodulation, and enables biofilm growth (Toder et al., 1994; Cathcart et al., 2011; Soto-Aceves et al., 2021). LasB can cause tissue damage because it has high specificity against elastin in the host. LasB targets elastin lamina, specifically, which is found in the arteries causing haemorrhaging when broken down and elastin in the eye can be broken down causing cornea damage in keratitis (Yang et al., 2015). LasB binds to the hydrophobic domain on elastin surface and uses hydrophobic amino acid residues at P1 and P1' position to cause degradation of the fibre which, when extended along the whole fibre, causes fibre breakage (Yang et al., 2015). LasB helps *P. aeruginosa*

avoid the immune system, degrades cell receptors on eukaryotic cell surface and degrades cytokines which then enables the infection to become chronic (Bastaert et al., 2018). The evasion mechanism is not quite understood yet however it is known that LasB causes increased interleukin-1 $\beta$  production in the lungs which in turn causes increased inflammation which has been known to cause damage for prolonged periods of time (Sun et al., 2020; Dinarello, 2018). Finally, LasB has been linked with alginate production due to its role in cleaving nucleoside diphosphate kinase (NDK) from a 16 kDa to a 12 kDa protein (Kamath et al., 1998). Once this cleavage occurs, the protein becomes membrane associated and forms complexes with other proteins to mainly produce GTP which is required for mannose 1-phosphate to be converted to GDP-mannose (a prerequisite to alginate) (Kamath et al., 1998; Yu et al., 2017).

The Las system is also responsible for the production of alkaline protease (AprA) as LasR also acts as a positive regulator for *aprA* (Coin et al., 1997). AprA is a 50 kDa zinc-metalloprotease which is secreted by type I secretion system (T1SS) (Jing et al., 2021). AprA has a negative effect on the immune system by interfering with complement-mediated lysis of erythrocytes (Laarman et al., 2012). This is key as the immune system uses membrane attack complexes (MAC) to form holes in the membrane of the bacterial cell wall which relies on the production of certain complement (Heesterbeek et al., 2019). AprA has been found to block the production of C3b and C5a

complements as well as cleave C2 compliment (Figure 1.3.3)  
(Laarman et al., 2012).

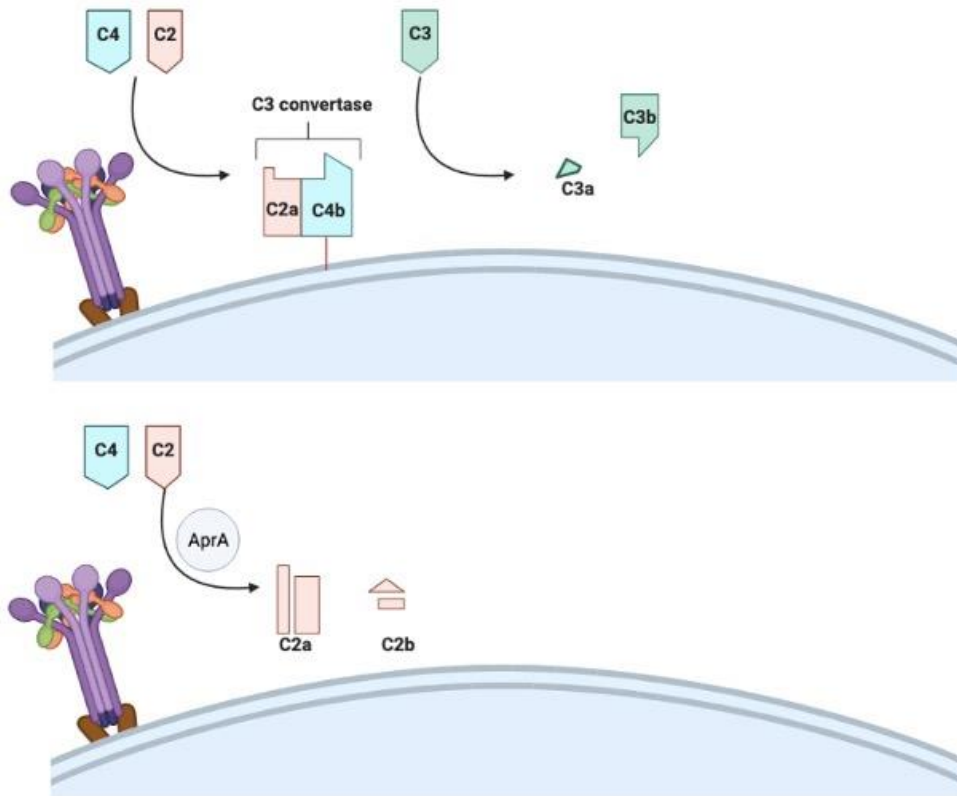


**Figure 1.3.3. The conversion of C4, C2 and C3 compliments.**  
(Top) in the absence of AprA, C4 and C2 are cleaved into C2a and C4b which is then able to combine to form a C3 convertase. The convertase then cleaves C3 into C3a and C3b which later plays a role in cleaving C5 compliment. (Bottom) in the presence of AprA, C2 is cleaved down into C2a and C2b fluid form which is unable to combine with C4 to form the C3 convertase. Image adapted from (Laarman et al., 2012).

C3b is responsible for allowing uptake of bacteria by neutrophils,  
C5a is responsible for neutrophil activation and C2 plays a regulatory  
role as a C3 convertase which allows C3b to be added to the  
bacterial cell surface (Heesterbeek et al., 2018). AprA can also cause  
immune system evasion which enables longevity of infection. It has  
been noted that AprA is able to break down citrullinated histone H3  
and myeloperoxidase which is used by neutrophils to bind to

bacterial DNA causing degradation which is why increased levels of AprA correlates to lower survival chance of patients (Jing et al., 2021).

### 1.3.2. The Rhl QS System

The Las system activates the three other quorum sensing pathways, the most important being Rhl. Specifically, LasR:3OC<sub>12</sub>HSL goes on to upregulate the *rhlR* and *rhlI* genes producing the receptor protein RhlR and the AHL-synthase RhlI (Thomason et al., 2019). Once produced, RhlI produces the AHL *N*-butanoyl-L-homoserine lactone (C4-HSL) which RhlR forms a complex with resulting in upregulation of *rhlI* again to produce more C4-HSL until the required concentration threshold is reached (Mukherjee et al., 2017). RhlR once active, has a negative effect on the Pqs system through an unknown mechanism (Wilder et al., 2011).

Rhamnolipids are biosurfactants which minimise the surface and interfacial tension between two fluid phases (Soberón-Chávez et al., 2021). *P. aeruginosa* can produce both mono- and di-rhamnolipids where a mono- or di-rhamnose group is linked to three variable length fatty acids (Caiazza et al., 2005). Once RhlR registers C4-HSL, it then goes on to activate the *rhlAB* operon and the *rhlC* gene causing rhamnolipid formation which typically occurs during the stationary phase (Chong & Li, 2017; Irorere et al., 2017). RhlA competes with the enzymes of the type 2 fatty acid synthase cycle for the intermediates of the  $\beta$ -hydroxyacyl-acyl carrier protein pathway to

supply the acyl moiety (Zhu & Rock, 2008). RhIB is responsible for the production of both mono-rhamnolipid via dTDP-L-rhamnolipid and  $\beta$ -3-(3-hydroxyalakanoyloxy) alkanolic acid (HAA) as substrates (Kiss et al., 2017). RhIC is needed for the production of di-rhamnolipid and it works by catalysing the breakdown of a mono-rhamnolipid (Reis et al., 2011). The *P. aeruginosa* rhamnolipids have been shown to aid biofilm formation and swarming motility but reduce mucociliary transport in human respiratory system (Soberón-Chávez et al., 2021). Once the channels have formed in biofilm architecture, *P. aeruginosa* is able to use rhamnolipids to maintain the void space surrounding microcolonies, rhamnolipids also reduce cell-cell adhesion within the biofilm (Davey et al., 2003; Wood et al., 2018). Swarming motility in *P. aeruginosa* occurs on semisolid surfaces and results in complex motility patterns (Caiazza et al., 2005). The rhamnolipids in *P. aeruginosa* are known as swarming modulators as they can both inhibit and promote swarming to occur, the current hypothesis being that biosynthesis of rhamnolipids is needed for tendrils to form (Caiazza et al., 2005). Mucociliary transport is required in the respiratory system to clear mucus and anything trapped within from the respiratory tract via the wave like motion of the cilia (Bustamante-Marin & Ostrowski, 2017). The mucosal clearing is slowed in *P. aeruginosa* infected hosts due to rhamnolipids being able to affect the ion transport of epithelial cells by reducing sodium absorption and inhibiting transcellular ion transport (Read et al., 1992; Abdel-Mawgoud et al., 2010).

Pyocyanin is part of a family of compounds called phenazines which have different physical and chemical properties based on structure (Gonçalves & Vasconcelos, 2021). Pyocyanin is made of nitrogen-containing aromatic rings which can act as a zwitterion meaning it has both positive and negative charges on the same molecule (da Silva et al., 2021; Delaviz et al., 2015). When RhIR is activated, it goes on to positively regulate *phzA1B1C1D1E1F1G1* (*phz1*) and *phzA2B2C2D2E2F2G2* (*phz2*) operons which are required for pyocyanin production (Soto-Aceves et al., 2021). Both operons are nearly identical and the seven genes code for enzymes which convert different substrates making up the pyocyanin synthesis pathway (Parsons et al., 2007). Pyocyanin can have a positive or negative impact on *P. aeruginosa* depending on the situation. In a scenario where cells become deficient in nutrients, pyocyanin acts as a redox mediator by providing an alternative electron acceptor, however when carbon or other nutrients are depleted pyocyanin becomes toxic to cells (Meirelles & Newman, 2018). This toxicity to *P. aeruginosa* cells is key in biofilm formation and architecture as this causes eDNA to be released into the biofilm matrix which can act as a scaffold for the matrix (Das & Manefield, 2012). In humans, pyocyanin is also dangerous due to the increase in the levels of reactive oxygen species ( $O_2^{\cdot-}$  and  $H_2O_2$ ) (Figure 1.3.4).

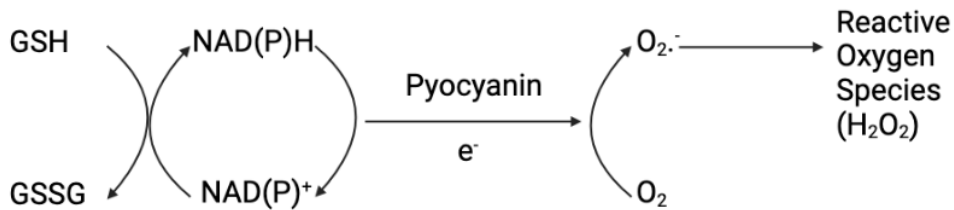


**Figure 1.3.4. Production of reactive oxygen species by pyocyanin.** Pyocyanin acts as an electron acceptor, it receives an electron from NAD(P)H in the mitochondria and donates it to oxygen creating free radicals which go on to form reactive oxygen species. Image adapted from (Rada & Leto, 2012).

The reactive oxygen species generated by pyocyanin causes oxidative damage to parts of the cell cycle, DNA damage, NAD(P)H depletion and inhibition of enzymes in the mitochondria (Hall et al., 2016). Pyocyanin has also been shown to cause disruption to the host immune response resulting in increased inflammatory response and reduced host immune system functionality (Hall et al., 2016). The combination of free radicals and inflammation causes damage to a range of human systems such as the respiratory, urological, central nervous system, endocrine, hepatic and vascular (Hall et al., 2016).

RhIR:C4-HSL also up regulates the expression of the *hcnABC* operon, which encode the enzymes that lead to the production of hydrogen cyanide (HCN) (Pessi & Haas, 2000). HcnABC is a membrane-bound cyanide synthases complex which mediate the conversion of glycine to cyanide by oxidative decarboxylation (Létoffé et al., 2022). HCN is a volatile compound and inhibits the growth of *Staphylococcus aureus*, helping *P. aeruginosa* to compete in the environment and in cystic fibrosis patients (Létoffé et al., 2022).

During infection, HCN causes damage to the host by binding

irreversibly to cytochrome *c* oxidase, the terminal enzyme in mitochondrial oxidative phosphorylation (Yan et al., 2019; Watson & McStay, 2020). HCN binding to cytochrome *c* oxidase prevents the generation of ATP leading to cell death (Zuhra & Szabo, 2022).

### 1.3.3. The PQS QS System

The *Pseudomonas* quinolone signal (PQS) system is controlled by three operons: *pqsABCDE*, *phnAB* and *pqsH* (Wade et al., 2005). The system was first discovered in 1999 by Pesci and colleagues once they had managed to purify the molecule causing the signalling called 2-heptyl-3-hydroxy-4-quinolone also known as PQS (Pesci et al., 1991). The synthesis of PQS is complex and different intermediates play a role in the virulence of the *P. aeruginosa* infection (Figure 1.3.5) (Schütz & Empting, 2018).

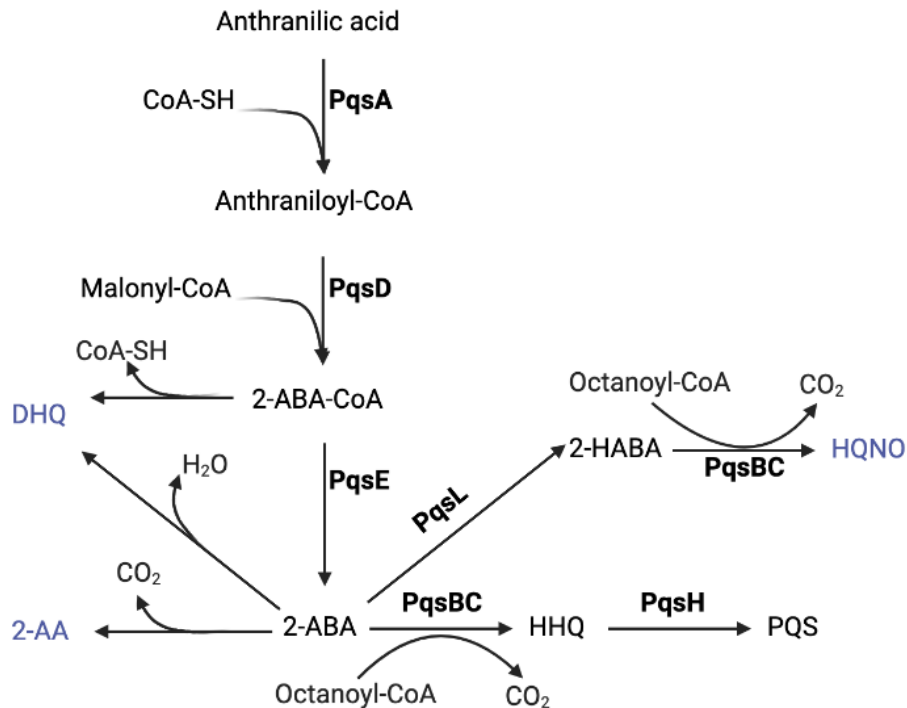


**Figure 1.3.5. Synthesis pathway of Pqs.** Abbreviations: CoA – Coenzyme A, 2-ABA-CoA – 2'-aminobenzoylacetyl-CoA, 2-ABA – 2'-aminobenzoylacetate, DHQ – dihydroxyquinoline, 2-AA – 2'-aminoacetophenone, 2-HABA – 2'-hydroxylaminobenzoylacetate, HHQ – 2-heptyl-4-(1*H*)-quinolone, HQNO – 4-hydroxy-2-heptylquinolone-*N*-oxide, PQS – *Pseudomonas* quinolone signal. Image adapted from (Schütz & Empting, 2018).

PqsA is an anthranilate-coenzyme A ligase which makes anthranilate produce anthraniloyl-CoA, then PqsD regulates the formation of 2-ABA-CoA from the previously made anthraniloyl-CoA and malonyl-CoA (Lin et al., 2018). Once produced, PqsE hydrolyses the 2-ABA-CoA into 2-ABA where PqsBC catalyses the condensation of octanoyl-CoA to convert 2-ABA to HHQ (Lin et al., 2018). Finally, HHQ can convert HHQ to Pqs which then can be used in the quorum sensing pathway (Lin et al., 2018). As shown in figure 1.3.5.

however, there are a few intermediates and alternative metabolites which increase the damage done by *P. aeruginosa* to the host. DHQ is the first alternative produced in the biosynthesis pathway and it

plays a role in pathogenicity as well as maintaining infection in oxygen-limited conditions (Gruber et al., 2016). DHQ has been shown to have an inhibitory effect on epithelial cell growth in the lungs and it has been shown to feed into the signalling pathway of the PQS system by binding to PqsR (Zhang et al., 2008; Gruber et al., 2016). 2-AA is the next intermediate produced which is responsible for persister cell formation which is key for maintaining infection and resisting antimicrobial intervention (discussed in 1.2.3) (Que et al., 2013). Finally, HQNO is a cytochrome inhibitor meaning it inhibits the respiratory electron transport chain resulting in ATP depletion and cell death (Montagut et al., 2022). HQNO causes eDNA production by self-poisoning *P. aeruginosa* cells in biofilm causing cell death by inhibiting respiration, giving *P. aeruginosa* an advantage in situations where cocolonization could occur (Hazan et al., 2016; Radlinski et al., 2017). The PQS system works because HHQ and PQS bind to the PqsR receptor, also referred to as MvfR, which is then able to transcribe a variety of downstream genes as well as regulate the *pqsABCDE* operon (Singh et al., 2022).

The PQS system is responsible for the expression of the galactophilic lectin LecA which is coded for by the *lecA* gene (Diggle et al., 2006). LecA is a tetrameric protein which has been cited as having a key role in initial adhesion as well as biofilm formation since it can interact with tissue cell surfaces (Fu et al., 2015). LecA can bind to the host cell surface by a mechanism known as the lipid zipper which states that Gb3 and glycosphingolipids on host cell

surface are recognised by LecA on bacterial cell surface (Sych et al., 2023). This lipid zipper causes the dispersion of ordered domains on host cell surface allowing for the bacterial invasion into host cells (Sych et al., 2023). When it comes to biofilm formation, the LecA mechanism has not been discovered yet, however studies have been conducted which show LecA-deficient strains of *P. aeruginosa* have thinner biofilms and that LecA production is upregulated when biofilms are formed (Wagner et al., 2017).

The PQS system is responsible for the production of pyocyanin and hydrogen cyanide, Pqs activates the *phz* and *hcn* operons (Groleau et al., 2020). PqsE can bind RhlR, becoming an effector molecule for the receptor when Las system is not active, which provides an alternate activation pathway when Las is defective (Groleau et al., 2020). Further research into this points to PqsE being able to bind to RhlR through an  $\alpha$ -helix containing R243/R246A/R247A (Simanek et al., 2022).

#### 1.3.4. The Iqs QS System

The final quorum sensing pathway in *P. aeruginosa* is the integrated quorum sensing (Iqs) pathway. This is a relatively recent discovery, and is understood to be active under phosphate-limiting conditions when both Pqs and Rhl cannot be activated (Lee et al., 2013). The Iqs system uses 2-(2-hydroxyphenyl)-thiazole-4-carbaldehyde (Iqs) as its messenger (Hemmati et al., 2020). Very little is currently known

about the lqs system apart from the fact it is thought to be produced by the *ambBCDE* gene cluster (Lee & Zhang, 2015).

Overall, the interactions between the four QS systems increases *P. aeruginosa* survivability in the environment. The Las system is at the top of the hierarchy as the first system activated and causes the activation of all others through the LasI/LasR proteins. LasA, LasB and AprA are all products of the Las system. Rhl is the next most important system which is activated via las-dependent or las independent means. Rhamnolipids, pyocyanin and hydrogen cyanide are all produced from the Rhl pathway causing major host damage. The Pqs system is activated by Las and responsible for the production of LecA, hydrogen cyanide and pyocyanin. Finally, lqs is the newest discovered and is yet to be linked to a virulence factor.

#### 1.4. Studying Biofilms with Synthetic Biology

As shown, the quorum sensing pathways of *P. aeruginosa* are extremely complex with four different systems each interlinked via biochemical and genetic interactions resulting in changes to how the bacterial cells/communities behave. The complexity behind biofilms and quorum sensing in *P. aeruginosa* is the reason why modern techniques to study them are everchanging and being modernised. Synthetic biology provides a means in order to develop novel constructs hijacking an organism's natural genetic processes to work in a way that is beneficial to the area of research a group is interested in. Synthetic biology allows for a tailored tool specific to

the needs of the researchers making it an incredibly useful discipline within biosciences. It is well documented that quorum sensing and biofilm formation relies largely on genetic and biochemical elements making it a perfect candidate to be hijacked through novel genetic circuits created using synthetic biology.

#### 1.4.1. An Introduction to Synthetic Biology

Synthetic biology is defined as the engineering of biological systems for useful purposes (National Human Genome Research Institute, 2019). Synthetic biology aims to create advances in a range of applied scenarios. An early use of synthetic biology includes the mass production of insulin (a peptide) using bacterial fermentation instead of harvesting animals (Baeshen et al., 2014). Synthetic biology aims to reprogram organisms through manipulation of genetic code and creation of genetic circuits (Kitano et al., 2023). DNA is seen as a key programmability element which can be manipulated from the natural source or chemically synthesised. Gene expression is then controlled by a range of standardised and modularised DNA parts (Xie & Fussenegger, 2018). There are a variety of components which can be used for constructing a genetic circuit deriving from the host organism's natural genetic pathways or from newly introduced code not natively found in the host organism (Brophy & Voigt, 2014). Different components include plasmid vectors to insert newly synthesised constructs into a host, fluorescing proteins to act as reporters when a certain process has occurred, promoter regions specific to a certain gene in a biological process allowing activation

of a reporter gene, terminators can be inserted between genes to achieve independent gene expression, etc (Chen et al., 2023; Kelly et al., 2019). The vast array of different components and types makes synthetic biology an interesting area of biosciences due to the different applications it can be used for.

Synthetic biology uses the “Design-Build-Test-Learn” (DBTL) cycle which is a conceptual framework for the engineering of biology. The DBTL cycle begins with designing the tool you see fit to solve your issue and this can be done through literature search and detailed modelling (Liu et al., 2015). Building can be done in a variety of ways depending on what you are trying to build but for biofilm related research a genetic assembly method is used to produce a plasmid which can be inserted into the bacterium (iGEM, 2023).

#### 1.4.2. Synthetic Biology and *P. aeruginosa* Biofilms

As discussed previously, a large part of quorum sensing and biofilm formation relies on genetics and the natural processes that occur within the *P. aeruginosa* cells. The reliance on genetics opens the door for intervention via synthetic biology through the construction of a biosensor. A biosensor is described as a device which measures a biological or chemical input and displays a proportional output when detected (Bhalla et al., 2016). In the case of *P. aeruginosa* quorum sensing, a genetic circuit could be constructed which could detect receptor protein activation in response to autoinducer production and displaying an output which could be seen and quantified. The variety

of different components listed in the previous section allow for this theoretical biosensor to be considered. One of the most important parts of the quorum sensing pathway in *P. aeruginosa* is the specificity of the promoter regions. LasR, RhlR and PqsR all recognise and bind a specific autoinducer which causes the upregulation of specific genes related to virulence, motility, biofilm formation, etc (Lee & Zhang, 2015). The promoter regions of the regulated genes have specific sites which are only active when the receptor-ligand complex of that specific QS pathway binds, e.g., LasR binds to the *rhlR* and *pqsR* promoter regions resulting in their upregulation (Jayakumar et al., 2022). Specific branches of the QS systems in *P. aeruginosa* have been linked to biofilm formation and such provides grounds that biofilm specific reporters could be created. An example being that Mukherjee and colleagues created *P. aeruginosa* strains that contained a construct which caused a green fluorescence when the Rhl QS system is active by including the *rhlA* promoter region before the GFP in the construct (Mukherjee et al. 2017). Fluorescent proteins could be an extremely important component for displaying an output in response to promoter activation. Fluorescing proteins are a very good indicator because they allow tracking of a specific process in relation to space and time providing a good model for *in vitro* and *in vivo* application (Kim et al., 2021). It is well understood that *P. aeruginosa* produces green pigments which could make using a GFP difficult and such an alternative colour should be selected (Prince-Whelan et al., 2007).

Finally, the most important part of a synthetic biological tool to consider is the vector backbone which can be used. The backbone of a synthetic tool is where the origin of replication and the antibiotic marker(s) are located (Nora et al., 2019). The origin of replication dictates the copy number of the plasmid (Rouches et al., 2022). The antibiotic marker present on a vector backbone conveys antimicrobial resistance which allows successfully transformed bacteria cells to survive in a selective media (Martinez-Garcia et al., 2015). Previous research using plasmid inserts into *P. aeruginosa* relies on the *pUCP* family of general-purpose vectors as a backbone which were based on *Escherichia coli* plasmids *pUC18* and *pUC19* (Schweizer, 1991). Overall, when designing biosensors, they can be considered in terms of logic gates and genetic circuits (Figure 1.4).

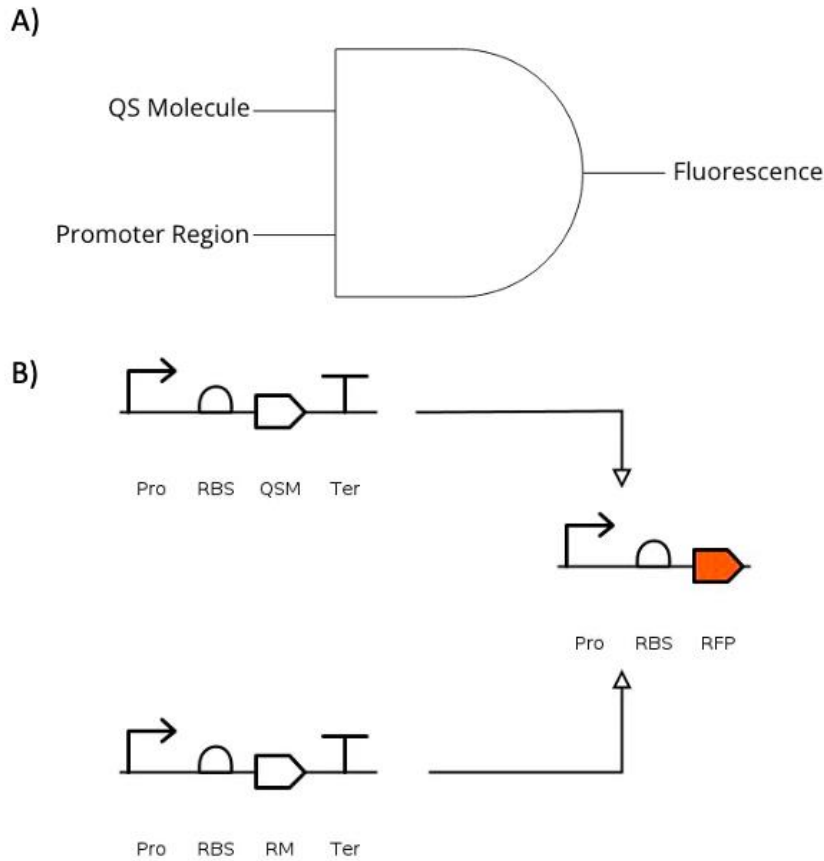


**Figure 1.4. Logic gate and circuit diagram design of *P. aeruginosa* biofilm biosensor.** A) The simplest idea is that if the quorum sensing molecule (QS) and the promoter protein are present and active then you will get fluorescence when a biofilm forms which allows visualisation. B) Circuit diagram showing the same idea as in A but with the necessary genetic components required to make the plasmid work.

The above diagram highlights the importance of understanding the genetic components required to build a successful genetic circuit.

The parts involved are dependent on what your specific needs are.

For a biosensor, a promoter which becomes active when the biomolecule is sensed is required which then allows the upregulation in production of a fluorescent output molecule creating a visual notification when the biomolecule has been sensed and in turn when the biofilm has formed. For this project, biosensors were extremely useful and allowed visualisation of biofilms *in vitro* and *in vivo*.

## 1.5. Studying Biofilms *In vitro*

As covered throughout, a biofilm is a complex architecture that forms on surfaces enabling a bacterial community to survive. To better aid the general understanding of biofilms there are 2 main categories in which biofilm research can fall under, *in vitro* and *in vivo*.

### 1.5.1. Methods

*In vitro* research occurs without the use of a live organism present and such allows for better control of the different variables that would be expected to influence formation (Arango et al., 2013). *In vitro* research provides an easier alternative because doesn't require needing specialist knowledge on a model organism. The two different methods of studying biofilms *in vitro* are through static and dynamic methods (Su et al., 2022).

A static biofilm model is given the name because of the media used to allow the biofilm to form in is unchanged and stationary (Guzmán-Soto et al., 2021). This method of studying biofilms typically is used when looking into the biofilm disrupting capabilities of novel antimicrobials because they are repeatable and inexpensive (Su et al., 2022). Commonly used static methods include microtiter plate assay, Calgary biofilm device and the biofilm ring test (Crivello et al., 2023). The microtiter plate assay is extremely simple, it allows biofilms to be formed at the bottom of the wells (Coffey & Anderson, 2014). This method can be further built upon by using visualisation methods such as confocal laser scanning microscopy and scanning

electron microscopy (Vyas & Mai-Prochnow, 2022). The Calgary device allows biofilms to form on pegs which are on a lid that is placed onto a 96-well plate containing media and inoculum. The lid with pegs and biofilms can then be transferred to new plates containing test antimicrobial compounds and the effects can be studied for biofilm disrupting capabilities (Garrison et al., 2017). Finally, the biofilm ring test works by growing bacterial culture in the presence of magnetic beads that are set in a ring shape. Magnetisation is then applied, if a biofilm has been formed the magnets stay in a ring shape or they will form a spot if no biofilm has formed (Olivares et al., 2016). Despite being easier to set up, static models aren't preferred as they often do not take into consideration the environmental factors a biofilm will face which can have an effect on gene expression (Buhmann et al., 2016). To ensure the data obtained by static models is applicable to hosts, people often use dynamic models.

Dynamic models are named such because they rely on nutrient supply and waste removal occurring throughout creating a flow of media which aim to mimic the environmental conditions of a host (Guzmán-Soto et al., 2021). This replication of host environment means that groups can try and research biofilms without the need for a model organism and still achieve similar conditions for their biofilms to grow in (Gabriliska & Rumbaugh, 2015). Commonly used methods of dynamic biofilm research include flow-cell systems, Robbins devices, a drip flow reactor and microfluidic platforms (Gabriliska &

Rumbaugh, 2015). Flow cell systems are conducted by allowing culture and media to flow over a microscope slide, where the biofilm should form, before being passed into a waste bottle by a peristaltic pump (Wolfaardt et al., 1994). Following on from this, Robbins devices are used similarly to the flow cell systems. The Robbins device has several sampling ports with studs inserted in them. The biofilm is allowed to form on the removable studs whilst the culture is constantly flowed through (Hall-Stoodley et al., 1999). A drip flow reactor has either four or six test chambers each able to hold a microscope slide which is where the biofilm forms. The media is passed along the face of the slide and runs down the 10° angled slant before being passed into waste. The microscope slides are then able to be used to visualise the biofilm formation (Heuschkel et al., 2021). Finally, the microfluidic platform has three separate channels two for culturing media and the centre for bacterial injections. The three channels feed into a central channel where the biofilm formation can occur along the centre of the channel where biofilm formation can be monitored (Straub et al., 2020). The models explained here are more complex but provide a better insight into how biofilms are expected to behave in a host without the use of a model organism. However, even dynamic models cannot replicate some of the structural characteristics that are seen *in vivo* and such it is important to consider which *in vivo* models are used.

## 1.6. *In vivo* Biofilm Study

### 1.6.1. An Introduction to Model Organisms

The issue faced when using *in vitro* methods of research, in the context of biofilms, is that both dynamic and static models lack the complexity of living organisms and such *in vivo* research in model organisms is required to confirm applicability to a living host. A model organism is a non-human species which has been used in experiments with the aim of understanding a biological process for the findings to then be applied to another species (Leonelli, 2013). There are a variety of model organisms which have yielded positive results for furthering our understanding of pathogenic biofilms which can be split into different categories of vertebrates and invertebrates (Lebeaux et al., 2013). The model organisms used most when studying biofilms are *Drosophila melanogaster* (fruit fly), *Danio rerio* (zebrafish) and, the focus of our research, *Caenorhabditis elegans* (nematode worm) (Lebeaux et al., 2013). Currently, *in vivo* model organisms are under used because there are not standard procedures making them widely available for use. This means that a large amount of biofilm research is being done *in vitro* using the static and dynamic models, however there is a wide willing to transition to live organisms should a shift in procedure occur (Weigelt et al., 2021).

### 1.6.2. *Caenorhabditis elegans* as a Model Organism

Research using *C. elegans* started in 1899 with Emile Maupas publishing the first paper using the organism, however popularity and notability came when Sydney Brenner began using *C. elegans* to study behaviour in 1965 and throughout his career (Nigon & Félix, 2017). *C. elegans* is widely used as a model organism because they have a very quick life cycle taking 3 days from egg fertilisation to adult stage (Figure 1.5.1) and their lifespan is around 2.5 weeks fed on their natural lab food source of *Escherichia coli* OP50 (Meneely et al., 2019).

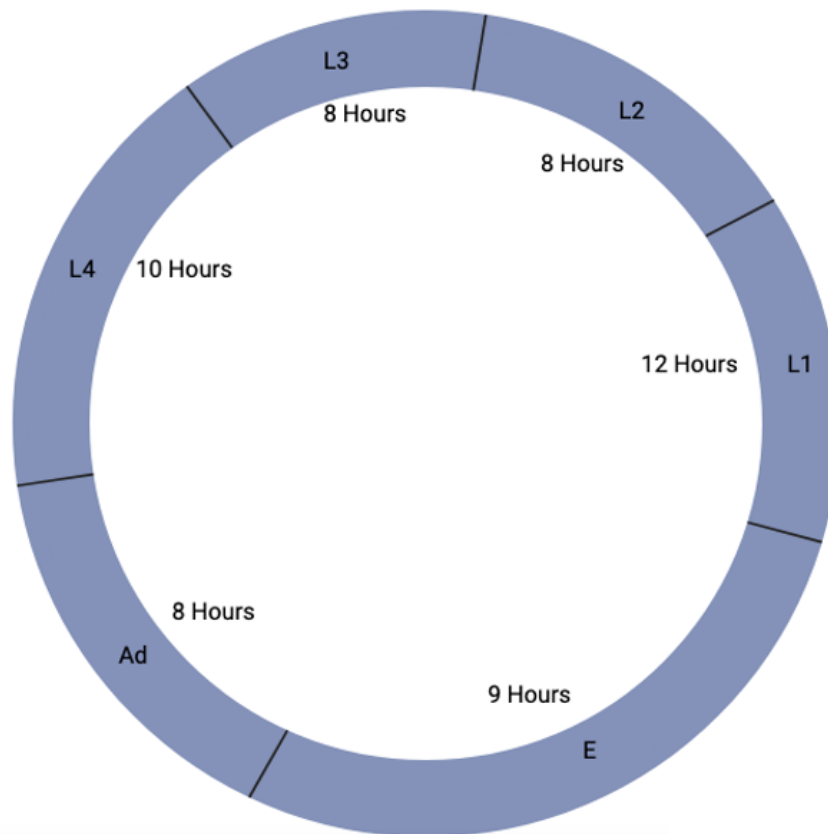


**Figure 1.5.1. Diagrammatic representation of the *C. elegans* life cycle.** The *C. elegans* start in the embryo (E) stage initially after hatching where, 9 hours later, they become L1 stage. L1-L4 development occurs over a 38-hour period until the worms reach young adult stage (Ad). 8 hours after becoming young adults, the worms are able to lay eggs and they cycle then continues with the progeny (Herndon et al., 2018).

Outside of the short life cycle, hermaphroditic *C. elegans* fertilisation produces approximately 300 offspring before sperm depletion, if a hermaphrodite is outcrossed and supplied with enough adult males then up to 1400 progeny can be obtained from 1 worm (Chasnov, 2013). This means large populations of *C. elegans* can be generated in a very short timeframe making them an ideal model organism. *C. elegans* are inexpensive to cultivate and thousands of mutant and transgenic strains are publicly available from the *Caenorhabditis* Genetics Centre (CGC) (CGC, 2023). The N2 worm is the wild type which is typically stored at 20°C. *C. elegans* was the first multicellular

organism to have its entire genome fully sequenced (National Human Genome Research Institute, 2013). The worm genome is 100Mbp in which 42% of human genes have had orthologs found (Coulson et al., 1991; Palikaras & Tavernarakis, 2013). This goes to show that work conducted with *C. elegans* has the potential to be useful across many different disciplines of biology due to the applicability to humans.

### 1.6.3. Biofilm Studies of *C. elegans*

Now that we know why *C. elegans* is widely used it's important to consider the organism in practise. *C. elegans* is a good model organism to review biofilm formation to understand microbe-host interactions and potential new methods of fighting infections (Wang & Zheng., 2022). This is made possible due to the anatomy of the roundworms which can be seen in Figure 1.5.2.

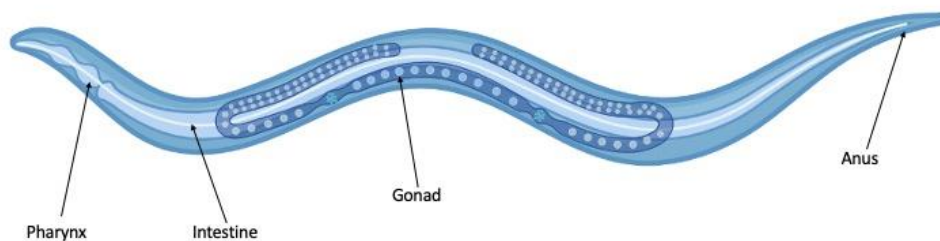


**Figure 1.5.2. Simplified diagram of worm anatomy.** In the pharynx where the bacterial food is crushed before being passed into the intestines until eventually it's passed by the worms through the anus. The gonads are wrapping around the intestine of the worm, and this is where eggs are produced and fertilised before laying. Image adapted from (Mullan & Marsh, 2019).

The intestine provides a good environment for bacterial colonisation which has been observed and is one of the biggest discoveries to come from monitoring the gut colonization (McGhee, 2007). The

body of the *C. elegans* worm is also transparent which means that colonisation of the gut can be monitored in such a way that is non-invasive and unlikely to disrupt any of the formed biofilm (Holt et al., 2017).

*C. elegans* as a model has been used for many years in order to research host microbe interactions via biofilm assays. To conduct the assay, a population of *C. elegans* are fed the bacteria for several days before being visualised to see disease progression or before treating with novel compounds to test antimicrobial activity (Smolentseva et al., 2017).

The biofilm infection assay of *C. elegans* has studied many pathogenic bacterial strains such as *Yersinia pestis*, *Salmonella enterica*, *Burkholderia cenocepacia*, *P. aeruginosa*, etc all of which have shown biofilm formation is, for one reason or another, responsible for killing the worms (Khan et al., 2018). In the case of *P. aeruginosa*, there are a variety of virulence factors that have been linked to biofilm formation causing *C. elegans* death such as pyocyanin, hydrogen cyanide leading to inactivation of *hcnC* gene and exopolysaccharide matrix resulting in induction of NPR-1-neuropeptide receptor (Cezairliyan et al., 2013; Wareham et al., 2005; Reddy et al., 2011). Infecting *C. elegans* with the bacterial strain to study biofilms provides the opportunity to test novel compounds for biofilm disrupting capabilities and toxicity *in vivo* (Desalermos et al., 2011). This has been done previously in several studies in which large libraries of natural products are put through a

screening process of *C. elegans* infected with a pathogenic bacterial strain so that novel antimicrobials can be identified (Kim et al., 2015; Zhou et al., 2011; Lakshmanan et al., 2014). Despite having potential for screening, currently methods available to study biofilms *in vivo* in *C. elegans* are limited. The aim of this project is to develop tools based on fluorescence which can be used to study biofilms in *C. elegans*.

## 1.7. Aims

The overall aim of this project is to develop a transgenic *P. aeruginosa* strain which produces fluorescence when it forms biofilms which can be used to monitor biofilm formation *in vitro* and *in vivo*.

**Aim 1: Use mNeogreen strains of *Pseudomonas aeruginosa* from Mukherjee et al., 2017 to determine suitability for monitoring biofilms.**

This will work by feeding the wildtype N2 *C. elegans* worms *P. aeruginosa* PA14, *P. aeruginosa* SM381 and *P. aeruginosa* SM383 then taking images to determine whether green fluorescence can be seen indicating biofilm formation. This will also be complimented with *in vitro* work via a biofilm assay, then quantifying fluorescence using a plate reader to test the natural biofilm forming capabilities of the strain outside of a host organism.

**Aim 2: Create a plasmid that encodes a red fluorescence protein (RFP) which is activated under the control of a *P. aeruginosa* biofilm marker.**

It is known that the *C. elegans* gut autofluoresces green, due to the lysozymes present within, which means that the green fluorescing bacteria will be hard to distinguish, and such may be difficult to determine biofilm formation. Therefore, we are going to design and build a new plasmid using an RFP variant, mScarlet-I, to increase signal-to-background fluorescence ratio and enable accurate measurement of biofilm formation and colonisation in the *C. elegans* gut.

**Aim 3: Create a *P. aeruginosa* strain containing the RFP plasmid and test suitability as a screening method using *C. elegans*.** The newly formed RFP strain will be tested using *C. elegans* imaging and biofilm assays to compare the newly synthesised strain to the strains obtained from Mukherjee et al. We will also use AHLs to test dose-response and quantify fluorescence using a plate reader proving the plasmid is biofilm activated.

## Chapter 2: Methods

### 2.1. Strains

**Table 2.1.** Table detailing the different bacterial and nematode strains used in this chapter and the sources they were obtained from.

Name	Genotype	Description	Source
<b>Bacterial Strains</b>			
<i>E. coli</i> DH10 $\beta$	F <sup>-</sup> <i>mcrA</i> $\Delta(mrr\text{-}hsdRMS\text{-}mcrBC)$ $\phi 80/lacZ\Delta M15$ $\Delta lacX74$ <i>recA1</i> <i>endA1</i> <i>araD139</i> $\Delta(ara\text{-}leu)7697$ <i>galU</i> <i>galK</i> $\lambda\text{-}rpsL(Str^R)$ <i>nupG</i>	Competent <i>E. coli</i> cells	New England Biolabs
<i>E. coli</i> OP50		Used for maintenance of <i>C. elegans</i>	Caenorhabditis Genetics Center, University of Minnesota
<i>E. coli</i> ET12567	<i>pUZ8002</i>	<i>E. coli</i> strain containing a non-transmissible donor plasmid	Moore lab – Mervyn Bibb, Hopkins et al. Practical book for <i>Streptomyces</i>
<i>E. coli</i> S17-1	<i>PSUP106</i>	<i>E. coli</i> strain containing a non-transmissible donor plasmid	DSMZ
<i>P. aeruginosa</i> PA14	Wild-type	Wild-type <i>P. aeruginosa</i>	(Mukherjee et al., 2017)
<i>P. aeruginosa</i> SM381	<i>prhIA-mNeonGreen</i>	<i>P. aeruginosa</i> that fluoresces green when	(Mukherjee et al., 2017)

		biofilm formed	
<i>P. aeruginosa</i> SM383	<i>prhIA-mNeonGreen</i> $\Delta$ <i>rhIR</i>	<i>P. aeruginosa</i> strain that fluoresce green when biofilm has formed and has had the QS gene <i>rhIR</i> knockout	(Mukherjee et al., 2017)
<i>P. aeruginosa</i> JP1	<i>pTdk-GFP</i> $\Delta$ <i>lasI</i>	Constitutively active GFP plasmid present, <i>lasI</i> QS gene knocked out	Gary Robinson
<i>P. aeruginosa</i> JP2	<i>pTdk-GFP</i> $\Delta$ <i>lasI</i> $\Delta$ <i>rhlI</i>	Constitutively active GFP plasmid present, <i>lasI</i> and <i>rhlI</i> QS genes knocked out	Gary Robinson
<b>Nematode Strains</b>			
N2	Wild-type	Wild-type <i>C. elegans</i>	Caenorhabditis Genetics Center, University of Minnesota

## 2.2 Solutions

**Table 2.2.** Table detailing the common solutions used with their compositions.

<b>Solution Name</b>	<b>Composition</b>
Luria Broth (LB)	(1 L): Dissolve 25 g Luria Broth Base to 1 L Milli-Q H <sub>2</sub> O <b>OR</b> mix 10 g Tryptone, 5 g yeast extract, 5 g NaCl into 1 L Mili-Q H <sub>2</sub> O.
Mueller-Hinton Broth (MHB)	(1 L): Dissolve 21 g Mueller-Hinton Broth powder in 1 L of Milli-Q H <sub>2</sub> O.
1x PBS	(1 L): Mix 100 mL 10x PBS with 900 mL Milli-Q H <sub>2</sub> O.
M9 Solution	(1 L): Dissolve 3 g KH <sub>2</sub> PO <sub>4</sub> , 6 g Na <sub>2</sub> HPO <sub>4</sub> , 5 g NaCl in 1 L Milli-Q H <sub>2</sub> O.

Bleaching Solution	(15 mL): Mix 3 mL bleach (Sodium hypochlorite, 11-15% available chlorine), 2 mL NaOH and 7 mL Milli-Q H <sub>2</sub> O.
TSS Buffer	(50 mL): Mix 1.5 mL 1 M MgCl <sub>2</sub> , 2.5 mL DMSO, 5g PEG 8000 and top up to 50 mL with LB.
50x TAE Buffer	(1 L): Mix 242 g Tris Base, 57.1 mL glacial acetic acid and 100 mL 0.5 M EDTA (pH 8.0). Top up to 1 L using Milli-Q water.
1x TAE Buffer	(1 L): Mix 20 mL 50x TAE, top up to 1 L with Milli-Q H <sub>2</sub> O.
<i>Pseudomonas</i> Isolation Agar	(1 L): Mix 1.4 g MgCl <sub>2</sub> , 20 g peptic digest animal tissue, 10 g K <sub>2</sub> SO <sub>4</sub> , 13.6 g agar, 980 mL Milli-Q H <sub>2</sub> O and 20 mL glycerol. Autoclave and allow to cool before adding 1mL Triclosan (25 mg/mL).
300 mM Sucrose	(1L): 102.69 g sucrose dissolved in 1 L Milli-Q H <sub>2</sub> O

## 2.3 Reagents

**Table 2.3.** Table shows the reagents used along with the supplier which they were purchased from as well as the identification number on the supplier's website.

Reagent Name	Supplier	Identification Number
Luria Broth (LB)	Invitrogen	12795-027
Mueller-Hinton Broth (MHB)	Oxoid	CM0405
10x PBS	Bio-Rad	161-0780
NaCl	Thermo Fisher Scientific	7647-14-5
Bacto Peptone	Thermo Fisher Scientific	211677
Agar	Melford	9002-18-0
KH <sub>2</sub> PO <sub>4</sub>	Thermo Fisher Scientific	011594.A1
MgSO <sub>4</sub>	Melford	7487-88-9
CaCl <sub>2</sub>	Fisher Scientific (Fluka)	31307-500G
Cholesterol	Thermo Fisher Scientific	A11470.18
Bleach	Thermo Fisher Scientific	L14709.AP
NaOH	Thermo Fisher Scientific	134070010
Ethanol	Thermo Fisher Scientific	E/0650DF/08

Tetramisole	Sigma	L9756-5G
DH10 $\beta$	Thermo Fisher Scientific	EC0113
Carbenicillin	Thermo Fisher Scientific	10177012
Buffer D	Promega	R9921
BamHI	Promega	R6021
NdeI	Promega	R6801
Agarose	Melford	9012-36-6
SYBR Safe DNA Gel Stain	Invitrogen	S33102
10x Blue Juice Gel Loading Buffer	Invitrogen	10816015
1 Kb Plus Ladder	Invitrogen	10787018
HindIII	Promega	R6041
EcoRI	Promega	R6011
Buffer B	Promega	R9921
5x Q5 Buffer	New England Biolabs	M04951S
dNTPs	Invitrogen	10534823
Q5 Polymerase	New England Biolabs	M04951S
GC Enhancer	New England Biolabs	M04951S
Buffer - Gibson	New England Biolabs	E2611S
Tango Buffer	Thermo Fisher Scientific	ER0991
AatII	Thermo Fisher Scientific	ER0991
NcoI	Promega	R6153
Kanamycin	VWR	E713-20ML
Chloramphenicol	Thermo Fisher Scientific	10368030
Sucrose	Thermo Fisher Scientific	S/8600/60
C4-HSL	Fluka	98426-48-3
Gentamicin	Sigma Aldrich	G1264-1G
MgCl <sub>2</sub>	Thermo Fisher Scientific	7791-18-6
Triclosan	Sigma Aldrich	72779-5G-F
Peptone from Meat	Gibco	211677
K <sub>2</sub> SO <sub>4</sub>	VWR	BLDPBD148896-100G
Glycerol	Sigma Aldrich	G5516-1L
Tryptone	Oxoid	LP0042B
Yeast Extract	Oxoid	LP0021B

Tris-Base	Thermo Fisher Scientific	77-86-1
Acetic Acid	Fisher Scientific	10171460
EDTA	VWR	60-00-4
Na <sub>2</sub> HPO <sub>4</sub>	Sigma Aldrich	S0876-1KG
PEG 8000	Sigma Aldrich	P2139-500G
DH5α	Thermo Fisher Scientific	EC0112

## 2.4. Kits

**Table 2.4.** Table of the kits used, includes provider of the kit as well as the identification number.

Kit Name	Provider	Identification Number
QIAprep Spin Miniprep Kit	Qiagen	27104
Monarch Genomic DNA Purification Kit #T3010G	New England Biolabs	T3010S
Zymo Research DNA Clean & Concentrator	Zymo Research	D4004

## 2.5. Bacterial Growth Conditions

All bacterial strains were grown in LB, MHB or on LB agar plates containing 1.5% (w/v) agar (Table 2.3). Temperature was set to 37°C overnight, liquid cultures were set to shake at 180 RPM in a Gene Temp-Shaker 300 incubator and plates were left static in a Sanyo MIR-153 incubator.

## 2.6. Preliminary *C. elegans* Work

### 2.6.1. Worm Husbandry

N2 *C. elegans* maintained at 20°C according to the standard protocol set out in which platinum wire was used for transferring the worms (Stiernagle, 2006). Worms fed *E. coli* OP50 as maintenance food

source and NGM plates were also made as specified (Stiernagle, 2006). NGM plates were made up in 1.8 L total aliquots. Dissolved 5.4 g NaCl, 30.6 g Agar, 4.5 g Bacto peptone in 1.8 L ddH<sub>2</sub>O in 2 L bottle. Solution autoclaved and cooled to ~55°C, then 45 mL 1M pH 6.0 KH<sub>2</sub>PO<sub>4</sub>, 1.8 mL 1M MgSO<sub>4</sub>, 1.8 mL 1M CaCl<sub>2</sub> and 1.8 mL 5mg/mL EtOH cholesterol were all added sequentially. Plates were left for around 72 hours on bench top before adding 250 µL of OP50 to the centre. These were left approximately for a further 72 hours before use.

### 2.6.2. Synchronisation

~15 N2 day 1 adult worms were transferred to each OP50 NGM plate. Five plates were set up in total which were left at 20°C for 72 hours. Population was checked under Leica bench top dissecting microscope. 1 mL M9 solution (Table 2.2) was used to wash worms into solution before being added to two 1.5 mL Eppendorf tubes. The tubes were then centrifuged using a SciSpin Mini centrifuge for 10-15 seconds at set  $x$   $g$ . Supernatant was then discarded and pellet left undisturbed. 1 mL of bleaching solution (Table 2.2) was then added to each tube which were shaken by hand for approximately 4 minutes or until majority of population appeared to have broken up. Eppendorf tubes were then centrifuged for 10-15 seconds, supernatant was discarded using a pipette and was replaced with 1 mL M9 solution to resuspend the pellet. After another wash with M9, the pellet was resuspended in 200 µL of M9 before being added in drops to fresh OP50 plates. These were then allowed to dry at room

temperature on bench top before being placed in a 20°C incubator for approximately 60 hours or until the population of worms had reached L4 stage.

### 2.6.3. *P. aeruginosa* Infection

NGM plates were seeded with *P. aeruginosa* PA14, SM381 and SM383 strains approximately 72 hours before transfer. 200 L4 worms were used for each condition across 4 NGM plates. Plates were kept at 20°C in a separate box from maintenance plates to avoid cross contamination. The *P. aeruginosa* worms were transferred at day 1 and day 3 adult stage using platinum wire.

### 2.6.4. Microscopy

Microscope slides had 2.5% (w/v) agar added as a drop onto centre of slide. 7 µL tetramisole (25mM in M9) was added to centre of the pad. Five day 3 adult worms added to puddle and microscope slide was placed on top. Slides were then looked at under a Leica DMR microscope with UV lamp and filter. Images were taken using a CellCam Rana 200CR camera on Micromanager. Filter used was GFP, Ex450-490 nm, Em 500-550 nm and images were adjusted using Fiji/ImageJ.

## 2.7. Biofilm Assay

*P. aeruginosa* PA14, SM381 and SM383 were streaked onto LB agar plates from -80°C glycerol stocks and left at 37°C overnight. Single colonies inoculated 7 mL LB media in 15 mL tube and were incubated at 37°C overnight at 180 RPM. 1 mL aliquots of each

culture were added to sterile 1.5 mL Eppendorf tubes, and centrifuged at 16000 x g for 1 minute at 20°C in the VWR Micro Star 1TR centrifuge. Supernatant was discarded and pellets were washed three times using 1x PBS. After the final wash, pellet was resuspended in 1 mL MHB and OD<sub>600nm</sub> reading was taken using a QuickDrop spectrophotometer. Each culture was then standardised to an OD<sub>600nm</sub> of ~0.2 using the above method. Once standardised, fresh and sterile Greiner bio-one CellStar clear 96-well culture plates were used to add 10 µL of culture to 10 wells in a row. This was done for the 3 samples. 190 µL of fresh MHB media was added to each well and 200 µL was added to 10 wells in a new row. The plate was then left at 37°C in the static incubator for 2 hours. After this time, the media was pipetted out of the well, discarded and replaced by 200 µL of fresh MHB media. The plate was left static at 37°C for 24 hours. The plate lid was removed and plate was inverted to remove the media and was dried by patting the plate on folded paper towels. 200 µL of sterile 1x PBS was added to each well. Fluorescence readings were taken using the FLUOstar omega microplate reader. From here the plate was inserted into the reader and the JOR-GFP program was selected. Number of multichromatics =1, excitation filter = 485-12, emission filter = EM520, orbital averaging = on, bottom optic, setting time = 0.2s, measurement start time = 0.0, number of flashes per well = 20. The gain adjustment was set to 50% of the first well in the SM381 column. The data was opened using MARS where it was transferred to an Excel document for analysis in Prism.

## 2.8. Recombinant DNA Assembly

### 2.8.1. Software DNA Analysis

The plasmid was designed using a combination of NEBuilder (<https://nebuilder.neb.com>) and Benchling (<https://www.benchling.com/>). The vector back bone and RFP DNA sequences were downloaded from AddGene with the *rhIA* promoter region being obtained from [www.pseudomonas.com](http://www.pseudomonas.com) (Table 2.8.1). Once all fragments were obtained, they were visualised using SnapGene Viewer.

**Table 2.8.1.** Names of each component used to design the RFP construct. ID numbers included for backbone and RFP gene reflect entries on Addgene, promoter region ID given for TransRegBase.

Name	Purpose	ID Number
<i>pUCP22</i>	Backbone	U07166
<i>rhIA</i> promoter region	Promoter region	76629
<i>mScarlet-I</i>	RFP gene	#163756

### 2.8.2 Primer Design

Primers were designed using NEBuilder and purchased from IDT.

The purchased primers are as follows (Table 2.8.2).

**Table 2.8.2.1.** Table shows primer ID, name of the primer and the sequence of the primer. Colour of text represents the fragment that sequence came from, red = *pUCP22*, yellow = *rhIA* promoter region and blue = *mScarlet-I*. Uppercase = anneal to DNA target, lowercase = addition to primer from previous fragment.

ID	Primer Name	Primer Sequence
P1	<i>pUCP22_F</i>	gctgcccgggctgctgctaaATTGCGTTGCGCTC ACTG
P2	<i>pUCP22_R</i>	AATAGCGAAGAGGCCCGC
P3	<i>rhIA-prom_F</i>	gtgcgggcctcttcgctattGAGGCCTGCGAAGTG TCC
P4	<i>rhIA-prom_R</i>	CTCACACCTCCAAAAATTTTCG

P5	mScarlet-I_F	aaatthttgggaggtgtgagATGGTGTCCAAGGG CGAGG
P6	mScarlet-I_R	TTAGCAGCAGCCCGGGCA

Designed primers were prepared as follows (Table 2.8.2.2):

**Table 2.8.2.2.** Table shows the name, nMol amount and volume of ddH<sub>2</sub>O required to make 100 µM.

ID	Sequence	nMol
P1	gctgcccgggctgtgctctaaATTGCGTTGCGCTCACTG	26.2
P2	AATAGCGAAGAGGCCCGC	28.1
P3	gtgcgggcctcttcgctattGAGGCCTGCGAAGTGTCC	19.8
P4	CTCACACCTCCCAAAAATTTTCG	26.6
P5	aaatthttgggaggtgtgagATGGTGTCCAAGGGCGAGG	19.8
P6	TTAGCAGCAGCCCGGGCA	25.5

DNA was dissolved in ddH<sub>2</sub>O to a stock concentration of 100 µM. For PCR, the primers were diluted in ddH<sub>2</sub>O to 10 µM working stock.

## 2.9. Recombinant DNA cloning

### 2.9.1. Preparation of chemically competent cells

DH10β competent *E. coli* cells were streaked onto an LB plate from glycerol stock stored at -80°C. A single colony was picked and inoculated into 5 mL of LB broth in a 50 mL tube which was then incubated at 37°C, 180 rpm for 16 hours. Then, 1 mL of overnight culture was subcultured into 50 mL fresh LB in a baffled flask (250 mL). This was incubated at 37°C, 225 rpm in the shaking incubator for 2-3 hours (until OD 0.3-0.4). Once the desired OD<sub>600nm</sub> was reached, cells were cooled on ice for 10 minutes and transferred to a sterile 50 mL tube. Cells were centrifuged at 4°C, 3000 x g for 10 minutes. The supernatant was decanted, and the cells were re-suspended in 2 mL of chilled Transformation and Storage Solution

(TSS) (Table 2.2). Cells were incubated on ice for 15 minutes.

Following this, 200  $\mu\text{L}$  aliquots in sterile 1.5 mL were stored at  $-80^{\circ}\text{C}$ .

### 2.9.2. Transformation of chemically competent cells

50  $\mu\text{L}$  competent cells were mixed with 2  $\mu\text{L}$  (212.1 ng/ $\mu\text{L}$ ) of plasmid and were incubated on ice for 20 minutes. Cells were heat shocked for 50 seconds at  $42^{\circ}\text{C}$ . Cells were incubated on ice for 2 minutes and 200  $\mu\text{L}$  of LB was added. Cells were incubated at  $37^{\circ}\text{C}$  for 1 hour, before being spread onto an LB plate containing appropriate antibiotic and incubated overnight at  $37^{\circ}\text{C}$ .

### 2.9.3. Plasmid purification

A single colony was picked from selective plate and added to a 50 mL tube containing 5 mL with antibiotic selection. Culture was then incubated at  $37^{\circ}\text{C}$  at 180 RPM for 16 hours. Culture was centrifuged at  $3000 \times g$ ,  $4^{\circ}\text{C}$  for 10 minutes, supernatant was decanted and pellet was resuspended in 250  $\mu\text{L}$  Buffer P1 provided and transferred to a 1.5 mL Eppendorf tube. 250  $\mu\text{L}$  Buffer P2 was added, tube was inverted several times to mix and allowed to sit at room temperature for 5 minutes. Next, 350  $\mu\text{L}$  Buffer N3 was added and tube inverted again to mix. Solution centrifuged at 13,000 RPM for 10 minutes, 800  $\mu\text{L}$  supernatant was transferred to a provided spin column. Spin column was then centrifuged at 13,000 RPM for 60 seconds and flow through discarded. 500  $\mu\text{L}$  Buffer PB was added to the spin column before being centrifuged again for 60 seconds. Flow through was discarded again and 750  $\mu\text{L}$  Buffer PE was added and spin column

was centrifuged for another 60 seconds. Flow through was discarded and the empty spin column was centrifuged again for 60 seconds to remove any residual buffer. The column was removed and placed into a fresh 1.5 mL Eppendorf tube, 50  $\mu$ L Buffer EB was added to the spin column where it incubated at room temperature for 60 seconds. The spin column was centrifuged at 13,000 RPM for 60 seconds.

#### 2.9.4. DNA concentration estimation by Nanodrop absorbance

1  $\mu$ L Buffer EB was added to Nanodrop sensor, lid closed and Nanodrop was blanked. Sensor was dabbed clean using paper towel. 1  $\mu$ L of undiluted plasmid DNA was then added to the sensor and concentration was read using Nanodrop.

#### 2.9.5. Gel Electrophoresis of DNA

DNA fragment separation ensured plasmid had been extracted successfully. A 1% (w/v) agarose gel was prepared using TAE buffer (See Table 2.2) and SYBRsafe (1x concentrate in DMSO). Table 2.9.3. shows composition of digest mix.

**Table 2.9.3.** Components for DNA double restriction digest.

<b>Component Name</b>	<b>Volume (<math>\mu</math>L)</b>
Buffer	2
Enzyme 1 (10 u/ $\mu$ L)	1
Enzyme 2 (10 u/ $\mu$ L)	1
DNA	5
ddH <sub>2</sub> O	11

Digests were incubated for 2 hours at 37°C then 10x Blue Juice Gel Loading Buffer was added and solutions were mixed. 1kb Plus DNA

Ladder used for marker. Solutions were loaded and a voltage of 100V was applied for 30 minutes to allow the DNA fragments to migrate to the anode. DNA was detected using a UV light box.

#### 2.9.6. *P. aeruginosa* gDNA Purification

*P. aeruginosa* PA14 streaked onto LB plate from -80°C glycerol stocks and incubated for 16 hours at 37°C. Single colony picked and inoculated into 5 mL LB in 50 mL tube, this was incubated at 37°C, 180 RPM for 16 hours. Culture centrifuged at 3000 rpm, 4°C for 10 minutes. The supernatant was decanted, pellet resuspended in 90 µL cold PBS and transferred to 1.5 mL Eppendorf tube. 10 µL Lysozymes added and mixture vortexed, then 100 µL Tissue Lysis Buffer added. Mixture incubated for 5 minutes at 37°C. 10 µL Proteinase K was added before being vortexed again to mix. The solution was incubated in thermomixer at 56°C for 30 minutes at 1400 RPM. After, 3 µL RNase A was added and mixed using vortex. The suspension was incubated in the thermomixer for 5 minutes at 56°C, 1400RPM. 400 µL gDNA Binding Buffer was added then mixture was transferred to spin column. Spin column was centrifuged at 13,000 RPM for 10 minutes, flow through was discarded. 500 µL gDNA wash was added and the spin column cap was closed before inverting 3 times to mix. Mixture was centrifuged at 13000 RPM for 5 minutes and flow through was discarded. Wash and centrifuge steps were repeated. After second wash, centrifuged the empty column to ensure residual buffer was removed. Spin column was added to fresh 1.5 mL Eppendorf and 100 µL 60°C ddH<sub>2</sub>O was added. This

incubated at room temperature for 5 minutes before being centrifuged at 13000 RPM for 5 minutes.

### 2.9.7. PCR

In order to generate fragments for Gibson Assembly, PCR was used. The PCR mixtures to generate the *mScarlet-I* gene, *rhlA* promoter and vector backbone are as follows (Table 2.9.7.1). PCR conditions listed below (Table 2.9.7.2).

**Table 2.9.7.1.** Composition of the mScarlet-I PCR mixture and the volumes of each component.

mScarlet-I PCR Composition	
Name of Component	Amount ( $\mu\text{L}$ )
5x Q5 Buffer	5
5 x DNA Enhancer	5 (Optional)
Primer one	1
Primer two	1
DNA	0.5
dNTPs	0.5
Q5 polymerase (2000 u/ $\mu\text{L}$ )	0.25
dH <sub>2</sub> O	Fill to 25 $\mu\text{L}$

**Table 2.9.7.2.** PCR cycling conditions

mScarlet-I PCR Conditions		
Temperature ( $^{\circ}\text{C}$ )	Time (s)	Number of Cycles
98	30	1
98	10	30
57-72	20	
72	15s/kb	
72	120	1
16	Infinite	1

Once the PCR reactions were completed, the products were separated by gel electrophoresis as described earlier (see 2.9.5).

### 2.9.8. Gel Extraction of DNA

The Zymo Research DNA Clean & Concentrator – 5 kit was used to extract the DNA from the gel. Band excised from gel using scalpel,

weighed and added to a 1.5 mL Eppendorf tube. Three times the mass of the excised band in  $\mu\text{L}$  of Buffer QC was added to the tube. The tube was then added to heat block set to  $42^{\circ}\text{C}$  to dissolve the gel piece into solution. Optional step – add 1 volume isopropanol if size is  $<200$  bp or  $>6$  kb. The DNA was then transferred to a spin column and centrifuged at 13000 RPM for 1 minute. Flowthrough discarded and  $500 \mu\text{L}$  Buffer QC added to column which was centrifuged at 13000 RPM for 1 minute. Flowthrough removed and  $750 \mu\text{L}$  Buffer PE was added to spin column before being centrifuged at 13000 RPM for 10 seconds. Flowthrough was discarded and the empty column was centrifuged for 3 more minutes at 13000 RPM. Spin column was transferred to fresh 1.5 mL Eppendorf tube and  $30 \mu\text{L}$  ddH<sub>2</sub>O was added to the column. The reaction was left at room temperature for 5 minutes. The tube was spun at 13000 RPM for 1 minute, contents was quantified using nanodrop.

### 2.9.9. Gibson Assembly

To understand the Gibson Assembly composition the following formula was used via NEB Bio Calculator

(<https://nebiocalculator.neb.com>):

*Required mass (ng)*

*= Insert:Vector \* Mass of vector (ng)*

*\* Insert length: Vector length*

A 3:1 insert to vector ratio was decided upon which required  $\sim 13.8$  ng promoter insert and  $\sim 19.1$  ng of RFP insert. From this information,

the volume of each fragment was converted into  $\mu\text{L}$  using the obtained concentrations. The final Gibson Assembly composition is shown below (Table 2.9.8).

**Table 2.9.8.** Composition for *pUCP22-rhIA-mScarlet-I* and control Gibson Assembly reactions.

<b>pTdk-rhIA-mScarlet-I</b>		<b>Control</b>	
<b>Component Name</b>	<b>Volume (<math>\mu\text{L}</math>)</b>	<b>Component Name</b>	<b>Volume (<math>\mu\text{L}</math>)</b>
<i>pUCP22</i>	3	<i>pUCP22</i>	3
<i>rhIA</i>	0.5	ddH <sub>2</sub> O	2
<i>mScarlet-I</i>	0.5	buffer	5
ddH <sub>2</sub> O	1		
buffer	5		

Gibson Assembly reactions incubated at 50°C for 1 hour.

## 2.10. DNA Sequencing

Once the Gibson Assembly reactions were complete, DH10 $\beta$  cells were transformed and plated onto selective agar for the newly constructed *pUCP22-rhIA-mScarlet-I* plasmid (see 2.9.2). Two single colonies were minipreped (see 2.9.3). Aliquots of the new construct (HM08 & HM09) were diluted 1:4 DNA:ddH<sub>2</sub>O into 20  $\mu\text{L}$  solutions. HM08 (60.17 ng/ $\mu\text{L}$ ) and HM09 (64.04 ng/ $\mu\text{L}$ ) solutions were sent to the sequencing company Plasmidsaurus.

## 2.11. Transformation of *P. aeruginosa*

### 2.11.1. *E. coli* ET12567 Conjugation

A plate of *E. coli* ET12567 was streaked from -80°C glycerol stocks onto LB containing appropriate antibiotic and incubated at 37°C overnight. Single colonies inoculated into two cultures of 6 mL LB

containing antibiotics. Cultures incubated at 37°C overnight shaking at 180 RPM. 1 mL of cultures were subcultured into 100 mL LB in a 250 mL Erlenmeyer flask. The cultures were made competent (see 2.9.1). an aliquot of competent ET12567 was transformed with HM09 (see 2.9.2). Transformed and untransformed ET12567 cells were spread onto a selective and non-selective LB plate respectively and both were incubated at 37°C overnight. Single colonies were picked from each plate and made into flowing cultures (Table 2.11.1).

**Table 2.11.1.** Culture composition for conjugation.

<b>Name</b>	<b>Media</b>
PA14	LB
ET12567 (HM09)	LB + chloramphenicol (35 µg/mL) + kanamycin (25 µg/mL) + gentamicin (50 µg/mL)
ET12567	LB + chloramphenicol (35 µg/mL) + kanamycin (25 µg/mL)

All incubated at 37°C, 180 RPM overnight. 500 µL overnight culture added to 9.5 mL LB + required antibiotic in 50 mL tube twice. (Figure 2.11.1.1) shows the culture conditions of each newly established culture.

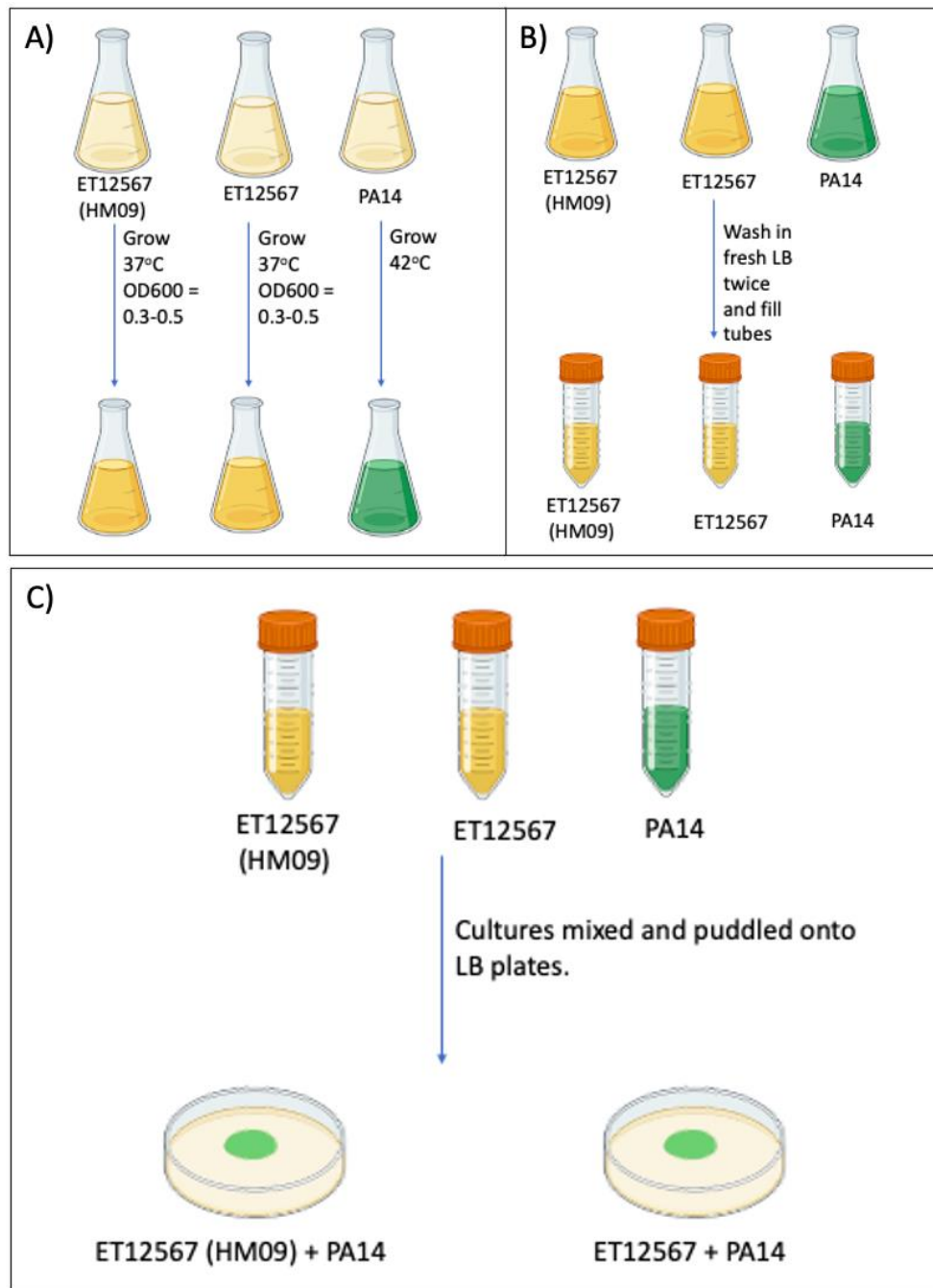


**Figure 2.11.1.1.** Shows the first steps in the conjugation experiment. A) Overnight cultures are subcultured into Erlenmeyer flasks and allowed to grow until OD<sub>600nm</sub> reached. B) Once certain OD<sub>600nm</sub> achieved, the cultures are washed in LB before being transferred to Falcon tubes. C) ET12567 (HM09), ET12567 and PA14 cultures are spun down and mixed before being puddled onto the centre of an LB agar plate.

OD<sub>600nm</sub> readings were taken and once required OD<sub>600nm</sub> reached, opened cultures were discarded and the sealed cultures were centrifuged at 4000 RPM, 4°C for 10 minutes. Cultures were washed

twice in LB and resuspended in 3 mL LB media (Figure 2.11.1.1). 1.5 mL of untransformed and transformed ET12567 were added to sterile Eppendorf tubes and two 0.5 mL PA14 tubes were made. These were centrifuged at 10,000 x *g* for 5 minutes and the supernatant was discarded. Pellets resuspended in 50  $\mu$ L LB. Both PA14 resuspensions were added to ET12567 and ET12567 (HM09). 100  $\mu$ L of mixed cultures were puddled onto the centre of an LB plate and left at 30°C overnight (Figure 2.11.1.1). The puddled mixed cultures were scraped into 1x PBS using a sterile loop and resuspended (Figure 2.11.1.2).

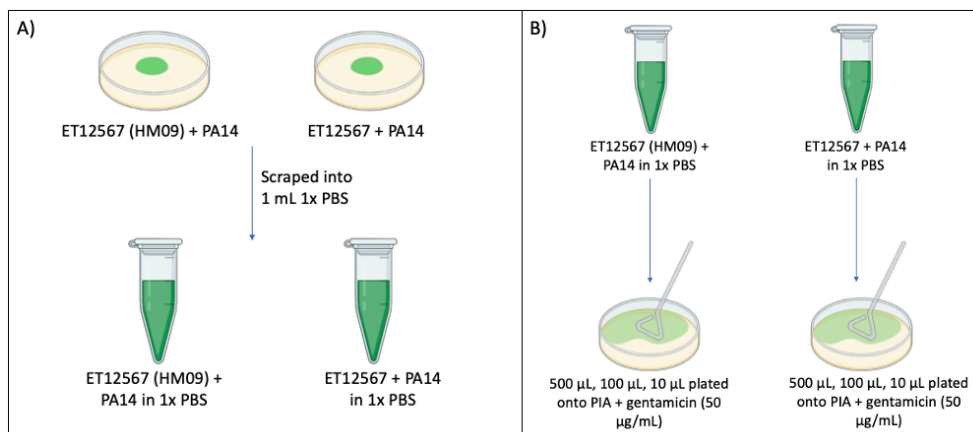


**Figure 2.11.1.2.** Shows conjugation experimental steps for the following day. A) Overnight plates are removed from incubator and colonies are scraped into 1x PBS. B) Specified amounts of mixed cultures are plated onto PIA plates containing gentamicin (50  $\mu$ g/mL).

Aliquots were spread onto Pseudomonas Isolation Agar (PIA) plates containing antibiotics (Figure 2.11.1.2b). These plates were then left at 37°C for 24 hours.

### 2.11.2 *E. coli* S17 Conjugation

Plate of *E. coli* S17 streaked from glycerol stocks and incubated at 37°C. Single colonies selected and grown in LB without antibiotic.

S17 made competent and transformed (see 2.9.1 & 2.9.2). Once competent S17 transformed with HM09, single colonies grown in 5 mL media as follows (Table 2.11.2)

**Table 2.11.2.** Shows the name of bacteria cultured and media each culture is made of. Antibiotic concentration and name shown also.

Name	Media
PA14	LB
S17 (HM09)	LB + gentamicin (50 µg/mL)
S17	LB

Same procedure followed as above (see 2.11.2).

### 2.11.3. Electroporation

Overnight PA14 cultures were left at 37°C overnight shaking at 180 RPM. The cultures were removed from the incubator the following day and 3 mL culture was split between two 1.5 mL Eppendorf tubes. These were centrifuged at 16000 x g for 1 minute at 20°C. The supernatant was discarded, and each tube was washed twice using sterile 300 mM sucrose solution. Cells were resuspended in 50 µL 300 mM sucrose. Combined two tubes into one for a final volume of 100 µL cells. 5 µL of HM09 (320.2 ng/µL) added to 100 µL cells, this was added to fresh 2 mm electrocuvette. Electrocuvette placed in electroporator and the *P. aeruginosa* pre-set program was run. Immediately after, 1 mL LB was added, electrocuvette was placed at 37°C for 1 hour shaking at 180 RPM. 250 µL culture was spread onto LB containing selective marker which were allowed to dry at room temperature then placed at 37°C overnight.

## 2.12. *In Vitro* & *In Vivo* Testing of *P. aeruginosa* HM09

### 2.12.1. Ensuring Biofilm Control of HM09

Overnight cultures of *P. aeruginosa* PA14, SM381, SM383 and HM09 were inoculated and grown at 37°C 180 RPM. 10 mL LB containing 40 µM, 20 µM, 10 µM, 5 µM, 2.5 µM and 0 µM C4-HSL individually were inoculated from 0.1 mL of each overnight culture in 50 mL tubes. The cultures were left at 37°C for 24 hours 180 RPM. 100 µL of each culture was added to black 96-well plate and 96-well clear plate where each column represented a different concentration. The black plates were then read using the following settings on the CLARIOstar. Excitation – 560-10, emission – 595-10, top optic, orbital averaging for detection of mScarlet-I (Khosla & Nelson, 2020). Excitation filter = 485-12, emission filter = EM520, orbital averaging = on and top optics settings were used for GFP detection. Clear plates were read using OD<sub>600nm</sub> setting on the same machine where absorbance is taken at OD<sub>600nm</sub> after a blank reading. The readings were converted to Excel where they were later analysed using Prism10.

### 2.12.2. Microscopy Images of *P. aeruginosa* HM09 on LB Agar Containing C4-HSL

*P. aeruginosa* PA14 and HM09 streaked onto LB agar and LB agar containing antibiotic selection plates respectively with each containing 20 µM C4-HSL. Plates were then left at 37°C overnight in

static incubator. Plates were imaged using the dissecting scope and the CellCam Rana 200CR camera on Micromanager camera.

### 2.12.3. *C. elegans* Imaging on *P. aeruginosa* HM09

Overnight cultures of *P. aeruginosa* HM09 and *P. aeruginosa* PA14 were grown at 37°C 180 RPM. The HM09 culture was then washed twice in 1x PBS and resuspended in same volume of LB. Once resuspended, 250 µL of culture was added to the centre of NGM plate 24 hours before use. N2 worms were synchronised according (see 2.6.2). 400 N2 L4 stage worms were added total per condition across five NGM plates. N2 worms were kept at 25°C and transferred daily. Images were taken at day 3 and day 4 adult stages. For microscopy see 2.6.4.

## Chapter 3: Results

### 3.1. Existing GFP biofilm reporter *P. aeruginosa* strains showed significantly more GFP production when compared to PA14 in vitro but signal lost when imaging *C. elegans* intestine

From the project outset, we wanted to design and construct a biosensor which is under the control of a biofilm promoter specific to *P. aeruginosa* PA14. We then wanted to test our construct *in vivo* in the model organism *C. elegans* by feeding the transformed bacteria to the worms and visualising them using fluorescence microscopy to see whether a biofilm had formed. *C. elegans* is one of the most widely used model organisms when investigating biofilms due to the fact that there is a large genetic similarity between *C. elegans* and humans allowing host-microbe interactions to be understood and the transparent body make biofilm imaging easier to see (Atkinson et al., 2011; Corsi et al., 2018).

Before we could consider the composition of the plasmid construct, we looked at previously used, readily available *P. aeruginosa* strains which had been investigated previously by a student in the Ezcurra lab. The strains in question, *P. aeruginosa* SM381 and SM383, were created by Mukherjee and colleagues (Mukherjee et al., 2017).

SM381 contains the *prhIA-mNeonGreen* plasmid which causes green fluorescence when the *rhIA* gene is transcribed following detection of C4-HSL by RhIR via the Rhl quorum sensing pathway. The SM383

strain contains the same biosensor construct but also has the *rhIR* gene knocked out meaning quorum sensing capabilities of the strain are greatly reduced. Mukherjee et al. were able to show in their research that when the plasmid was activated, a biofilm was formed suggesting fluorescence intensity correlated with biofilm formation. The group did show *in vitro* work regarding the SM381 and SM383 strains and how the biofilm architecture was affected yet they did not try to visualise the biofilm *in vivo*. The previous research conducted by a student in the Ezcurra lab had investigated the *P. aeruginosa* SM381, SM383 and PA14 strains to quantify their fluorescence after a biofilm assay *in vitro* and whether they fluoresce in *glp-1 C. elegans*. The student found SM381 significantly brighter than PA14 and SM383 and saw clear fluorescence within the lumen of the worm intestine which indicated potential biofilm formation (Ragno, 2023). We originally started by replicating the 96-well plate biofilm assay. To quantify fluorescence, we used the FluoStar Omega Microplate Reader by doing an *in vitro* assay in a 96-well plate. Our results show that SM381 was significantly brighter than the other two strains. SM381 was 7.5x brighter than the PA14 strain and was 4.44x brighter than the SM383 strain, while there was no significant difference in fluorescence intensity as SM383 was 1.69x brighter than PA14.

## Average Fluorescence of *P. aeruginosa* Strains

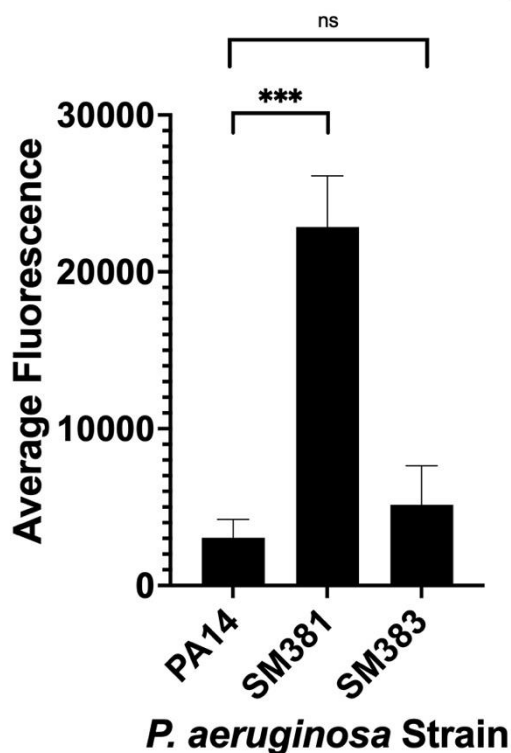


**Figure 3.1.1: SM381 was significantly brighter than PA14 ( $p<0.0002$ ) and SM383 ( $p<0.0003$ ) while there was no significant difference between SM383 and PA14 ( $p=0.58$ ).** Biofilms grown over 24 hours in 96 well plates. Fluorescence emitted by biofilms read using omega plate reader. Stats and graph plotted using Prism10.  $n=29$  across 3 replicates. \*\*\* means  $p<0.001$  when conducting a one-way ANOVA.

After seeing the significant difference between SM381 and the other two strains, we conducted infection imaging in N2 wild-type *C. elegans*. Below shows day 3 adult N2 *C. elegans* worms under the Leica DMR microscope using 20x and 40x magnifications from which we can see some fluorescence in the lumen of the SM381-fed N2 worms which isn't apparent in the PA14 or SM383-fed worm intestines.

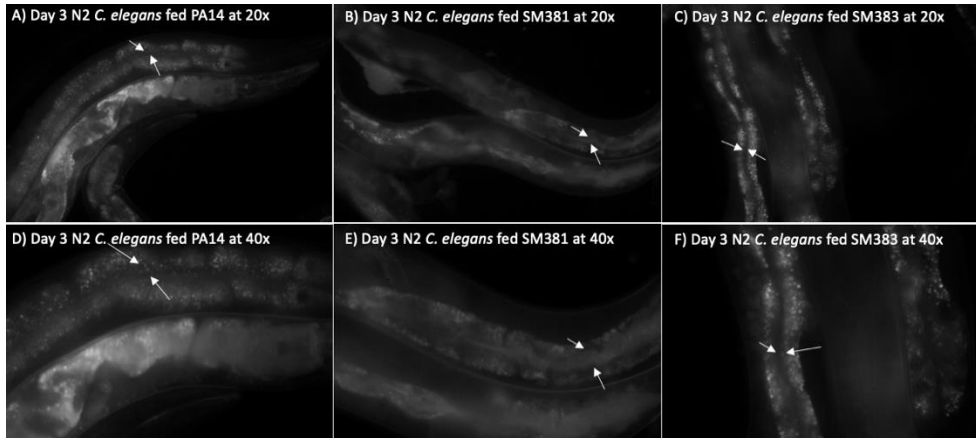


**Figure 3.1.2. Day 3 N2 adults show intestinal fluorescence after being fed SM381 but do not show fluorescence after being fed SM383 or PA14.** Arrows point to intestinal lumen. Images taken on Leica DMR microscope using Micromanager at 20x (A-C) and 40x (D-F) and were adjusted on ImageJ. A, D) Intestinal lumen of the worms fed wild type *P. aeruginosa* PA14 appear empty. B, E) Intestinal lumen shows fluorescence indicating biofilm formation in intestinal lumen of the worms fed *P. aeruginosa* SM381. C, F) Intestinal lumen of the *C. elegans* fed *P. aeruginosa* SM383 clear and only background fluorescence seen. Arrows show the intestinal lumen in all images.

After finding it difficult to discern between *P. aeruginosa* fluorescence and intestinal lumen autofluorescence, it was decided to move ahead with creating a new biofilm reporter strain containing an RFP.

## 3.2. Constructing *prhIA-mScarlet-I* using Gibson Assembly

### 3.2.1. RFP bioreporter was designed using Benchling

A theoretical structure for our bioreporter was designed as a starting point. From the initial tests, the *rhlA* promoter was chosen as a good candidate to use to keep our bioreporter under the control of a biofilm dependent promoter. The backbone and RFP components were readily available in the lab and hence were used to create the design (Figure 3.2.1).



**Figure 3.2.1. The initial design of the biofilm biosensor accompanied by the different components used to create it.**

A) pTdk-GFP is an already existing *P. aeruginosa* plasmid which was selected for the origin of replication specific to *P. aeruginosa* that contains gentamicin resistance. B) The RFP gene which is intended to be used for the biosensor is the *mScarlet-I* which was obtained from the *pTU1-SP44-PET-mScarlet-I* plasmid. C) The *rhIA* promoter region can be found between the *dcd* and *rhIA* genes of the *P. aeruginosa* genome and would mean the new plasmid is only active when a biofilm is formed. D) Gibson Assembly of the three highlighted regions in each component. Assembly run on Benchling.

With a plasmid map produced, we could refer to this in the moving forward to ensure assemblies and transformations had succeeded. The next step was to try to assemble the theoretical plasmid using the parts selected.

### 3.2.2. Bioreporter fragments were collected by PCR and agarose gel extraction successfully

Once the bioreporter structure was determined, the method of assembly was selected as Gibson Assembly. To start, the fragments highlighted in Figure 3.2.1. were loaded into NEBbuilder and the displayed overlapping primers were ordered. Once the primers had arrived, the *pTU1-SP44-PET-mScarlet-I*, *pTdk-GFP* plasmids and the *P. aeruginosa* PA14 genome were extracted. Once the 3 parts were extracted, a PCR reaction mixture was established and run to create large quantities of the fragments with overlapping sequences using the developed primers. Once the PCR reactions were complete, the end product was run on a 1% agarose gels (Figure 3.2.2.1, 3.2.2.2 & 3.2.2.3).

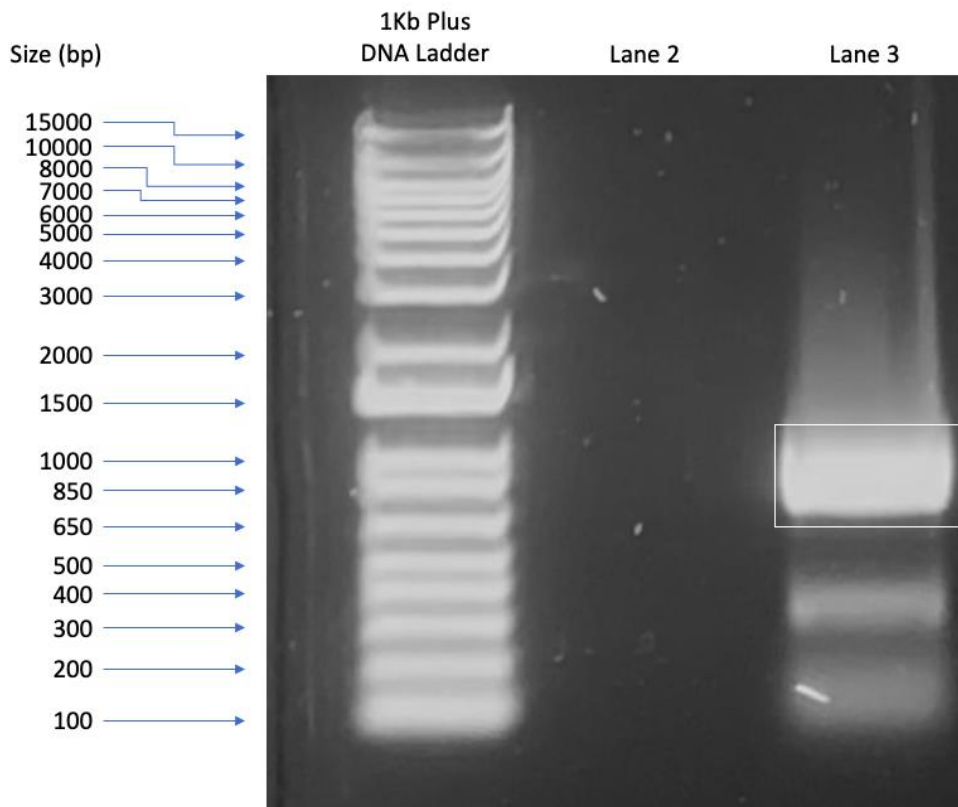


**Figure 3.2.2.1. Brightest band from the *pTU1-SP44-PET-mScarlet-I* PCR is equal to the size of the *mScarlet-I* gene.** Lane 1 = 1 Kb Plus DNA Ladder, Lane 2 was left empty and Lane 3 = *mScarlet-I* PCR product. There are 3 bands following the digest with varying sizes of approximately 100 bp, 300 bp and 700 bp. The highlighted band represents the *mScarlet-I* gene which is 696 bp in length.

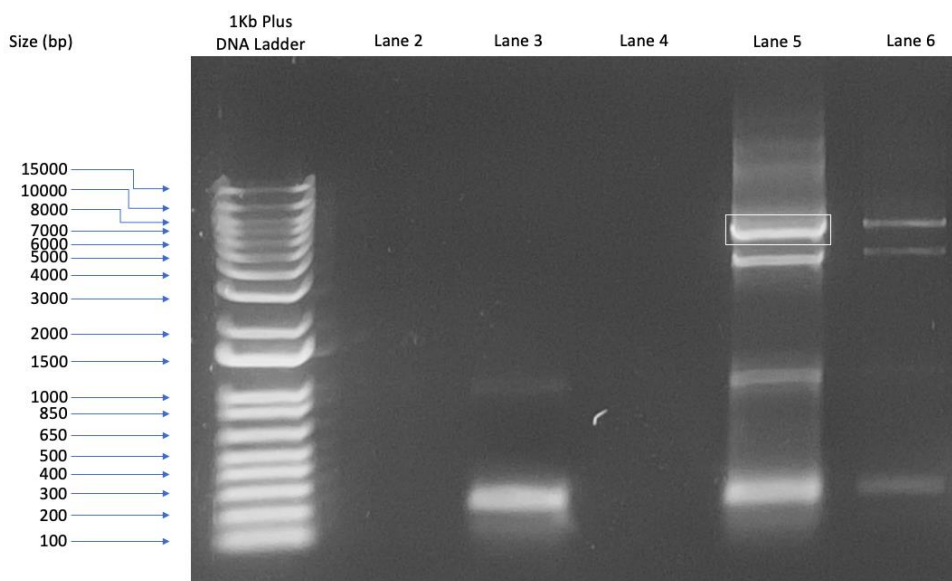


**Figure 3.2.2.2. *pTdk-GFP* PCR product from JP2 had run successfully and the highlighted band was excised.** Lane 1 = 1 Kb Plus DNA Ladder, Lane 3 = *pTdk-GFP* (JP1) PCR product, Lane 5 = *pTdk-GFP* (JP2) PCR product and Lanes 2, 4 and 6 were left empty. Lane 3 has 2 bands of varying sizes being 250 bp and 1000 bp. Lane 5 has 4 bands of varying sizes being 250 bp, 1000 bp, 4500 bp and 7000 bp. The highlighted band is the band excised for Gibson Assembly (See 2.9.7).

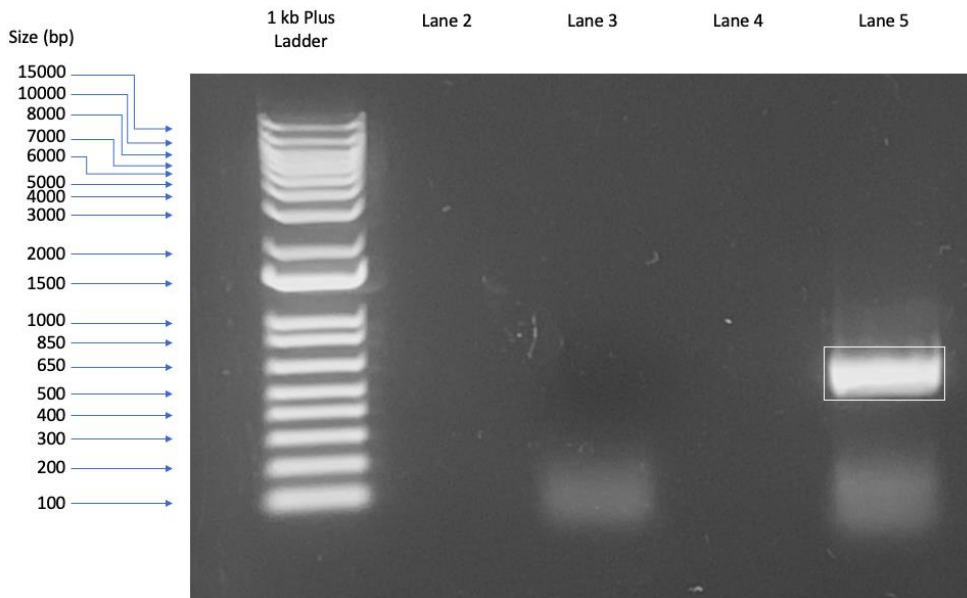
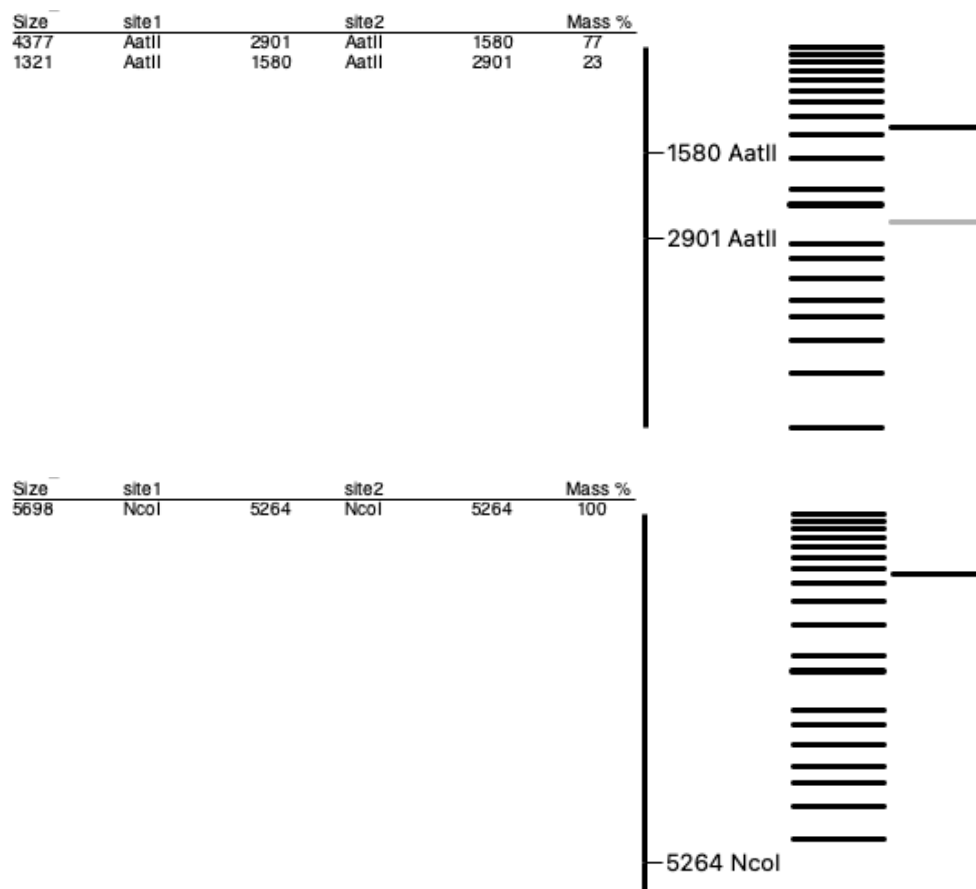


**Figure 3.2.2.3. The *rhIA* promoter region PCR containing the GC enhancer successfully ran and the highlighted band at approximately 500bp was extracted.** Lane 1 = 1 Kb Plus DNA Ladder, Lane 3 = *rhIA* promoter region PCR product, Lane 5 = *rhIA* promoter region PCR product with GC enhancer present and Lanes 2 and 4 were left empty. Lane 3 has one band 100 bp in size. Lane 5 has two bands 100 bp and 550 bp in size. The highlighted band is approximately 500 bp which is the same size as the *rhIA* containing region which is required for the biofilm control of the biosensor.

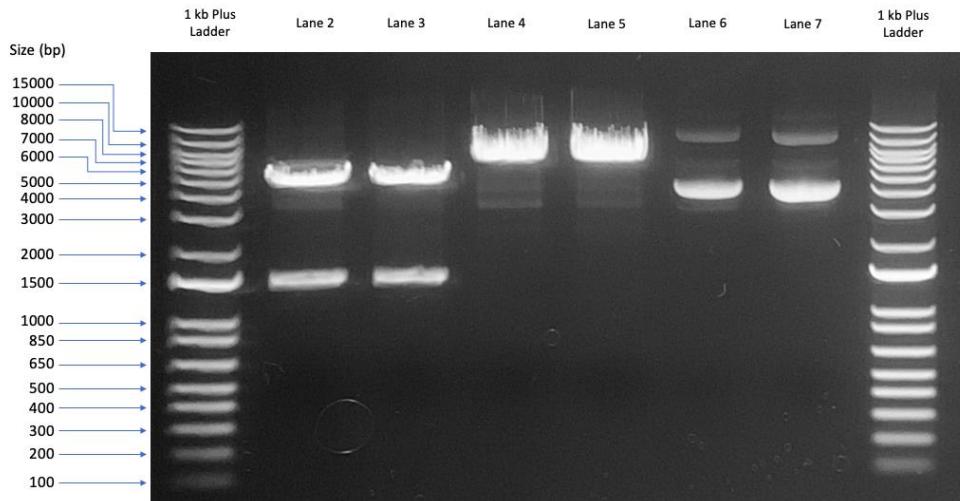
Once the PCR products had been run on agarose gels, the highlighted bands were extracted using a gel extraction kit. This meant Gibson Assembly could then commence in order to build the construct.

### 3.2.3. Successful Gibson Assembly of the RFP bioreporter

Once the parts highlighted were obtained from PCR reaction, the biosensor was assembled using the Gibson Assembly method as previously detailed (Gibson et al., 2009). Once assembled, DH10 $\beta$  *E. coli* cells were transformed with the reporter plasmid in order to generate a stock of plasmid to be tested before being sent for sequencing. Once the plasmid was extracted, two aliquots (HM08 & HM09) were then digested using AatII and NcoI in two separate reactions. Once digested, the reactions were run on the same agarose gel along with the undigested plasmids (Figure 3.2.2 & Figure 3.2.3).



**3.2.2. The AatII digest results in 2 bands 4377 and 1321 bp in size and the NcoI digest results in 1 band 5698 bp in size.** Sequence taken from design made on Benchling. Digest predicted on ApE software.



**3.2.3. AatII reaction shows 2 bands for both HM08 and HM09 at around 5,500 bp and 1,500 bp in size. NcoI shows a single band in each case approximately between 6,000 bp and 7000 bp in size.** Digests run on 1% agarose gel. Lanes 1 and 8 = 1 Kb Plus DNA Ladder, Lane 2 = HM08 cut with AatII, Lane 3 = HM09 cut with AatII, Lane 4 = HM08 cut with NcoI, Lane 5 = HM09 cut with NcoI, Lane 6 = Uncut HM08 and Lane 7 = uncut HM09.

The banding patterns of the above gels suggested that the construct had been created as intended and such was ready to be sent for sequencing before moving forward with transformation.

### 3.3. Sequencing showed successfully constructed biofilm reporter

Once digest reactions had been run, HM08 and HM09 were sent for sequencing using Plasmidsaurus. Once fully sequenced, Plasmidsaurus provided a plasmid map (Figure 3.3.1).

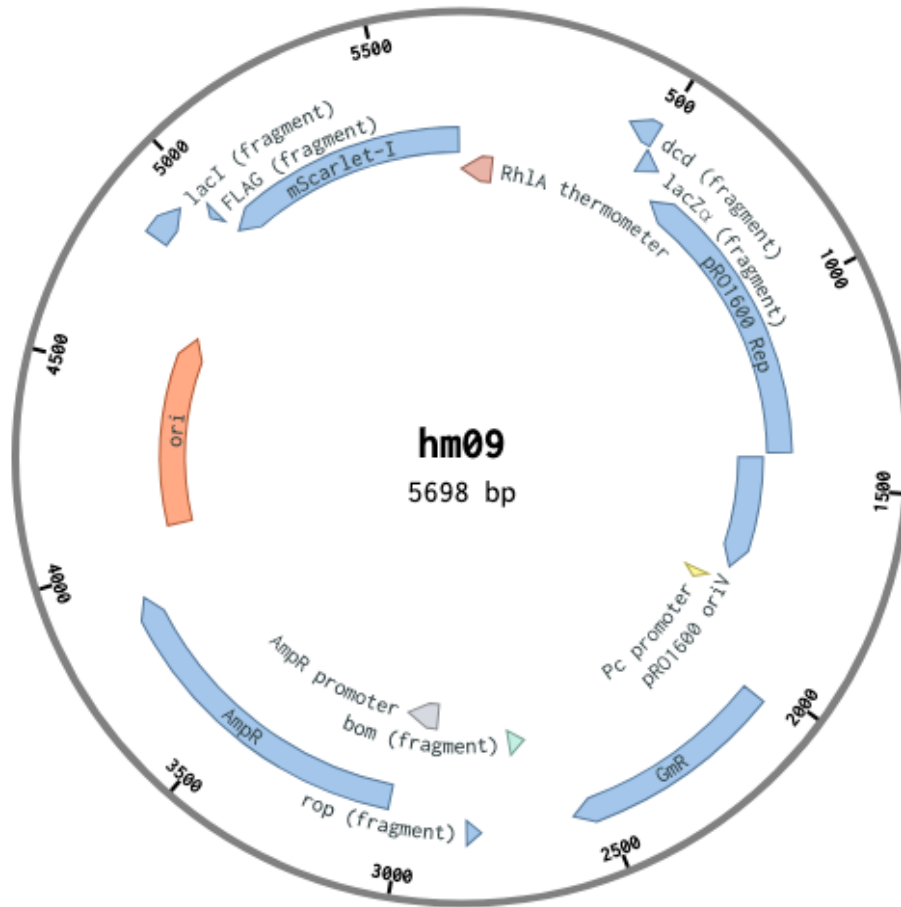


**Figure 3.3.1. Plasmid map of the HM09 plasmid.** Biosensor contains gentamicin resistance as well as the *mScarlet-I* gene which is under the control of the *rhIA* promoter region. Map taken from Benchling.

The annotated plasmid map matched what was designed and meant there could be confidence that the construct was built as intended hence transformation could move ahead as planned.

### 3.4. Successful transformation of *P. aeruginosa* PA14

Once the sequence of the plasmid was confirmed to contain the correct biofilm reporter and RFP gene, attention was then turned to transforming *P. aeruginosa* PA14 with the newly synthesised biosensor.

### 3.4.1. Initial conjugation transformation of *P. aeruginosa* PA14 was unsuccessful

Initially, conjugation was attempted to transform the *P. aeruginosa* PA14. Conjugation is a well-defined method which has been reported to work widely within the literature (Hmelo et al., 2015). Conjugation relies on a donor strain of *E. coli* containing the synthesised construct to donate the plasmid through a pilus into the recipient *P. aeruginosa* PA14 strain, then selecting for specifically the *P. aeruginosa* through selective media (Hmelo et al., 2015). The *E. coli* ET12567 strain was made competent and transformed to contain the HM09 plasmid. Once this was complete, the conjugation protocol was followed (See 2.11.1). Once the mixed cultures were plated and left to grow overnight, they were checked for presence of colonies (Figure 3.4.1.1).

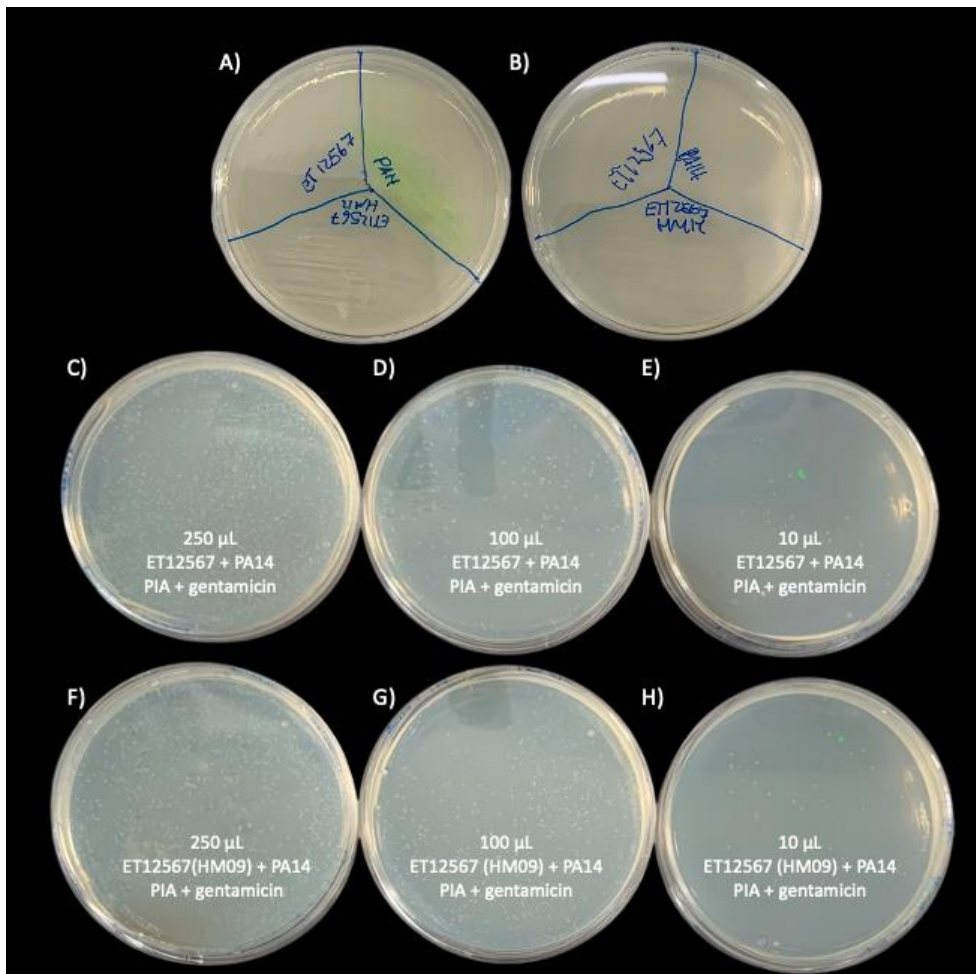


**Figure 3.4.1.1. PIA trial and conjugation images of *E. coli* ET12567 control and ET12567 (HM09) mixed cultures plated on PIA + gentamicin plates all showing single colony growth.** A) PIA plate with *E. coli* ET12567, ET12567 (HM09) and *P. aeruginosa* PA14 streaked onto it. Plate shows no growth for the *E. coli* strains and single colony formation of the PA14 streak. B) PIA plate containing gentamicin (50 µg/mL) which had the 2 *E. coli* strains and *P. aeruginosa* PA14 streaked onto it. This condition showed no growth across the 3 strains indicating the PIA gentamicin to be selective for the transformed colonies after conjugation. C-E) The antibiotic selective PIA plates have the ET12567 and PA14 mixed culture spread onto it in varying volumes. Each plate under this condition had single colonies growing despite the fact the plasmid should not be present. F-H) The PIA plates containing gentamicin have the transformed ET12567 strain in mixed culture with the wild type *P. aeruginosa* PA14 spread onto them in varying volumes. Each of the plates under this condition also have increasing amounts of single colony formations as volume of culture spread increased.

Despite colonies being present in both the control and test conditions, a different *E. coli* donor was used (S17-1) which had been cited within the literature (Strand et al., 2014). The same protocol was followed and the plates were checked again (Figure 3.4.1.2). Once again, single colonies were present in both the control and test plates at all volumes spread.

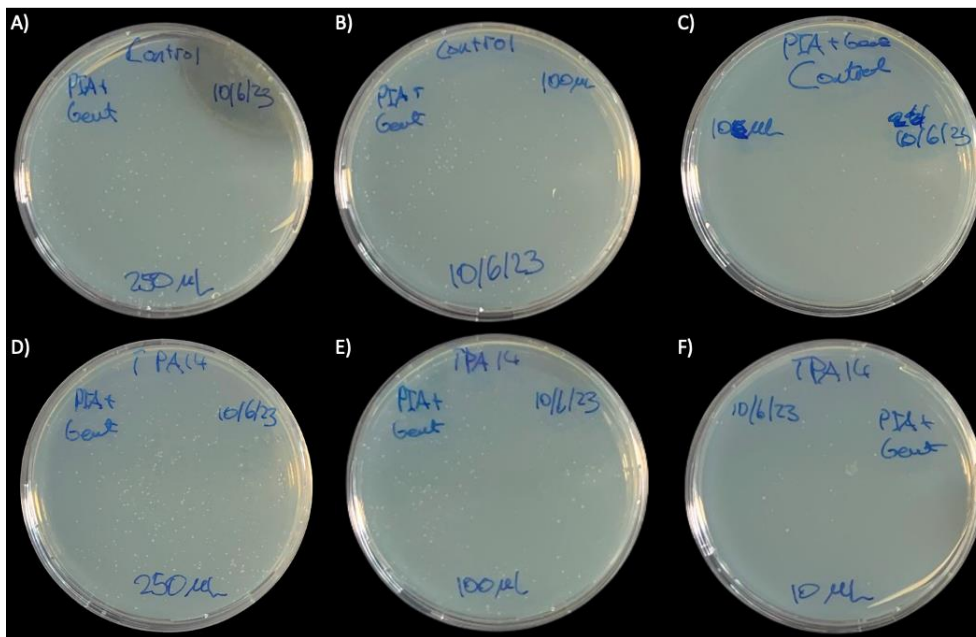


**Figure 3.4.1.2. Plate images following conjugation of *E. coli* S17-1 and *E. coli* S17-1 (HM09) with *P. aeruginosa* PA14 plated on PIA + gentamicin plates. A-C) The PIA + gentamicin plates under the control condition, single colony formation still present. D-F) Under the transformed condition, single colony formation was also seen.**

In light of the fact that single colonies were present when conjugating with two different donor strains and the fact the plasmid had not been inserted into *P. aeruginosa* PA14, it was decided to try a different transformation method.

### 3.4.2. Alternate transformation method (electroporation) of *P.*

*aeruginosa* PA14 successfully produced RFP bioreporter *P.*

*aeruginosa* strain

After several conjugation attempts, the electroporation method of transformation was selected as an alternative. Electroporation works by using an electrical current in order to form pores in a bacterial cell membrane which then allows the plasmid into the cell before the pores are closed during the recovery stage (Potter & Heller, 2018).

PA14 overnight cultures were washed with 300mM sucrose, the culture was then split and had the HM09 DNA added and was electroporated using an electrocuvette on the *P. aeruginosa* program in the electroporator. After the recovery period the cells were plated on LB agar plates containing gentamicin (50 µg/mL) (Figure 3.4.2.1).

To ensure equipment working correctly, an *E. coli* DH5α culture was transformed using the same method and the *pTU1-SP44-PET-mScarlet-1* plasmid. From the electroporation there was a clear difference between the transformed and control plates. The HM09 transformed *P. aeruginosa* condition showed clear individual colonies on the selective agar which the control *P. aeruginosa* PA14 did not. In both cases, the PA14 cells grew on non-selective LB agar plates indicating that both were viable after electroporation and recovery.

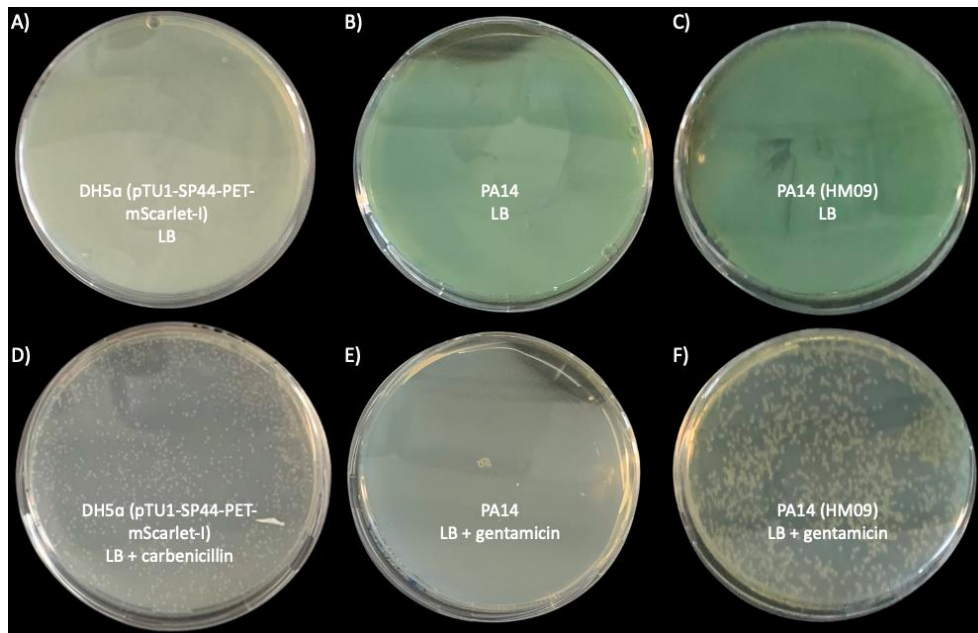


**Figure 3.4.2.1. Plate images of *P. aeruginosa* PA14 WT and PA14 (HM09) spread onto LB + gentamicin (50 µg/mL) following electroporation.** A, D) Electroporation transformation of *E. coli* DH5α with the established *pTU1-SP44-PET-mScarlet-I* plasmid. A) Lawn of *E. coli* shows the cells were viable after electroporation. D) Single colonies present on the LB + carbenicillin (100 µg/mL) plate are pink in appearance indicating successful transformation. B, E) *P. aeruginosa* PA14 electroporated with water control. B) Green lawn indicates the cells were viable after electroporation procedure. E) LB + gentamicin agar plate shows no bacterial growth meaning that the PA14 remained untransformed. C, F) PA14 was transformed successfully with the HM09 plasmid. C) Green lawn present on plate means cells survived electroporation successfully. E) Single colony formation was seen across the LB + gentamicin plate indicating successful transformation of the *P. aeruginosa*.

The images above suggest that the electroporation protocol worked as intended due to the presence of *P. aeruginosa* growth on gentamicin containing LB plates. The next step was to work with the newly formed RFP strain to ensure the strain worked as intended.

### 3.5. HM09 biofilm reporter in *P. aeruginosa* PA14 produces proportional fluorescence depending on the amount of C4-HSL

Upon binding to autoinducers, e.g., C4-HSL, the RhlR receptor protein forms a complex which binds to the *rhlA* promoter region and allows *rhlA* transcription (Morici et al., 2007). Once transcribed and translated, the RhlA protein plays a role in the biosynthesis of rhamnolipids by catalysing the synthesis of 3-(3-hydroxyalkanoxy) alkanolic acid (HAA) which is a key component of an extracellular glycolipid surfactant on *P. aeruginosa* (Zhu & Rock, 2008). After transformation of the *P. aeruginosa* PA14 strain with HM09 plasmid it was tested to ensure it was under the control of the *rhlA* quorum sensing promoter. To do this, varying concentrations (0  $\mu$ M, 2.5  $\mu$ M, 5  $\mu$ M, 10  $\mu$ M, 20  $\mu$ M and 40  $\mu$ M) of the quorum sensing molecule C4-HSL were used to test the level of biofilm control. The set values were added to individual cultures of *P. aeruginosa* PA14, HM09, SM381 and SM383. All were left at 37°C for 24 hours and then were transferred to black and clear 96-well plates before having the red and green fluorescence measured by the microplate reader. The values were standardised based on OD<sub>600</sub> reading and plotted (Figure 3.5.1 & Figure 3.5.2). When measuring RFP, the HM09 strain exhibited much higher levels of fluorescence than the other three strains. Under the GFP measuring conditions, the SM381 strain exhibits higher fluorescence values than the other 3 strains present. However, when comparing the two conditions, the signal to noise

ratio is lower in the GFP reading than the RFP. Under RFP monitoring conditions, HM09 is up to 56 times brighter than other strains being looked at. Although it is important to note this occurred off of a single repeat of the experiment.

### Red Fluorescence of *P. aeruginosa* Strains with Different Amounts of C4-HSL Added

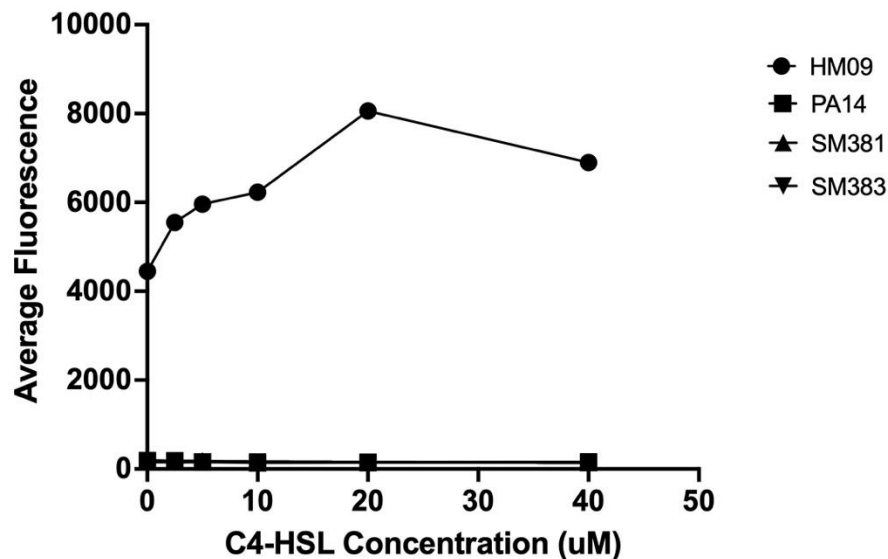


**Figure 3.5.1. HM09 *P. aeruginosa* was brighter than the 3 other tested strains at all concentrations.** Overnight bacterial cultures were grown in varying concentrations of C4-HSL. mScarlet-I fluorescence measured using CLARIOstar microplate reader, excitation – 560-10, emission – 595-10, top optic, orbital averaging for detection of mScarlet-I (Khosla & Nelson, 2020). HM09 strain was the brightest fluorescing strain and showed a peak fluorescence at 20 mM C4-HSL concentration. It is important to consider the data shown is only after a single run and such more repeats are needed before a definitive conclusion can be reached and stats applied.

### Green Fluorescence of *P. aeruginosa* Strains with Different Amounts of C4-HSL Added

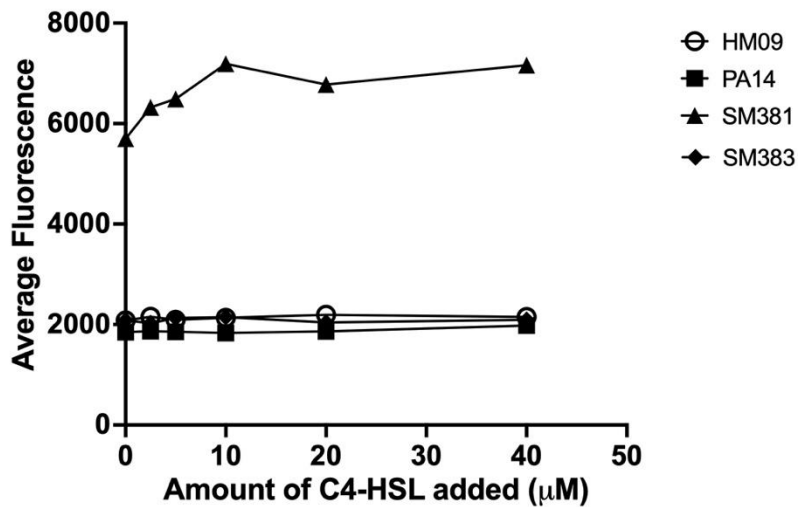


**Figure 3.5.2. SM381 was the brightest strain when measuring green fluorescence of the 4 strains.** The CLARIOstar was set to excitation filter = 485-12, emission filter = EM520, orbital averaging = on and top optics settings. The SM381 showed to be the brightest fluorescing strain when measuring green fluorescence. However, as opposed to the red fluorescence, the other 3 strains measured exhibited high levels of background green fluorescence.

From the above results, there is a much greater fold increase in fluorescence in the red strain when looking at RFP than the green fluorescing strains when looking at GFP. This result was based off of a single replicate and such needs further work to be conclusive. Along with these, qualitative data was collected using fluorescent microscopy.

### 3.6. Fluorescent microscopy of HM09 colonies showed brighter red fluorescence when compared to PA14 in the presence of C4-HSL

Once the HM09 *P. aeruginosa* strain had been tested with autoinducer, colony images were taken using the Leica dissecting

microscope and camera using micromanager to see the red fluorescence. This allowed us to visualise the difference in fluorescence that could be expected when comparing HM09 vs PA14 *in vivo*. LB agar plates were made containing C4-HSL (20 mM) and one containing gentamicin (50 µg/mL). *P. aeruginosa* PA14 and HM09 were streaked onto LB and LB + gentamicin plates respectively. The plates were incubated overnight and imaged using the Leica Dissecting Microscope using the RFP filter on the UV lamp. Images were taken using Micromanager.

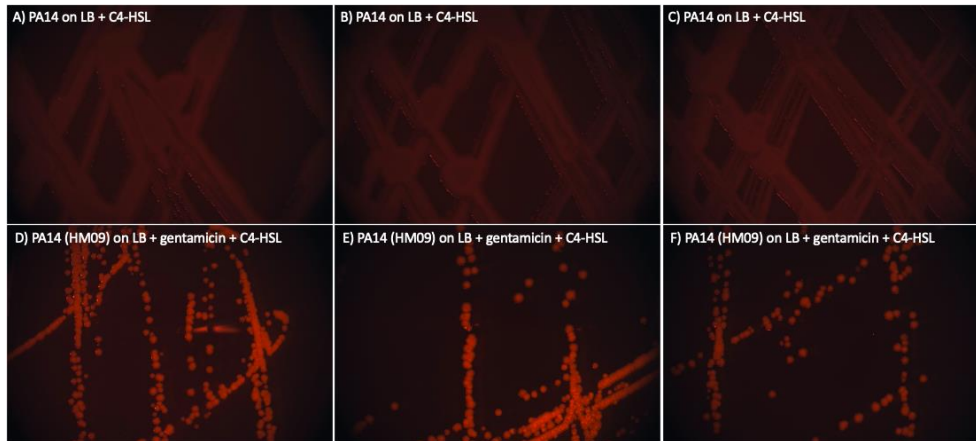


**Figure 3.6.1. HM09 was noticeably brighter than the wild-type alternative under the Leica dissecting microscope.** The plates were visualised under the RFP filter on the Leica Dissecting Microscope. Images taken using Micromanager. The above images show that *P. aeruginosa* HM09 appeared much brighter than the wildtype *P. aeruginosa* PA14 strain when looking down the scope and in the images.

The images taken on the microscope provide a visual representation showing that the HM09 strain fluoresces red brighter than the wild type, this meant the reporter strain was taken forward to be used *in vivo* in *C. elegans* worms.

### 3.7. HM09 fed *C. elegans* showed inconclusive red fluorescence in intestinal lumen when compared to PA14 fed *C. elegans*

Upon attaining that the HM09 *P. aeruginosa* strain appeared bright under the fluorescent microscope, we imaged the *C. elegans* after feeding them *P. aeruginosa* HM09 and PA14 to image biofilm formation *in vivo*. The procedure for this section was similar to 3.1. The worms were synchronised and fed *E. coli* OP50 until the worms had reached L4 stage. Once L4 had been reached, the worms were transferred to *P. aeruginosa* PA14 and HM09 plates. To try and limit biofilm formation occurring on the NGM plate, the NGM plates were seeded 24 hours before use each day. At day 3 and day 4 adult stage, five N2 adults were immobilised and mounted on a microscope slide using tetramisole (25 mM). Images taken of day 3 adult (Figure 3.7.1) and day 4 adult (Figure 3.7.2) stages. When comparing the day 3 adult PA14 fed to the HM09 fed *C. elegans*, very little differences could be noticed. Day 4 infected worms were different as the HM09 fed day worms appeared to have low levels of fluorescence in the intestinal lumen. The difference between the RFP and GFP images could be attributed to the fact the GFP plates were seeded several days in advance. It is also important to note that only one trial was performed.

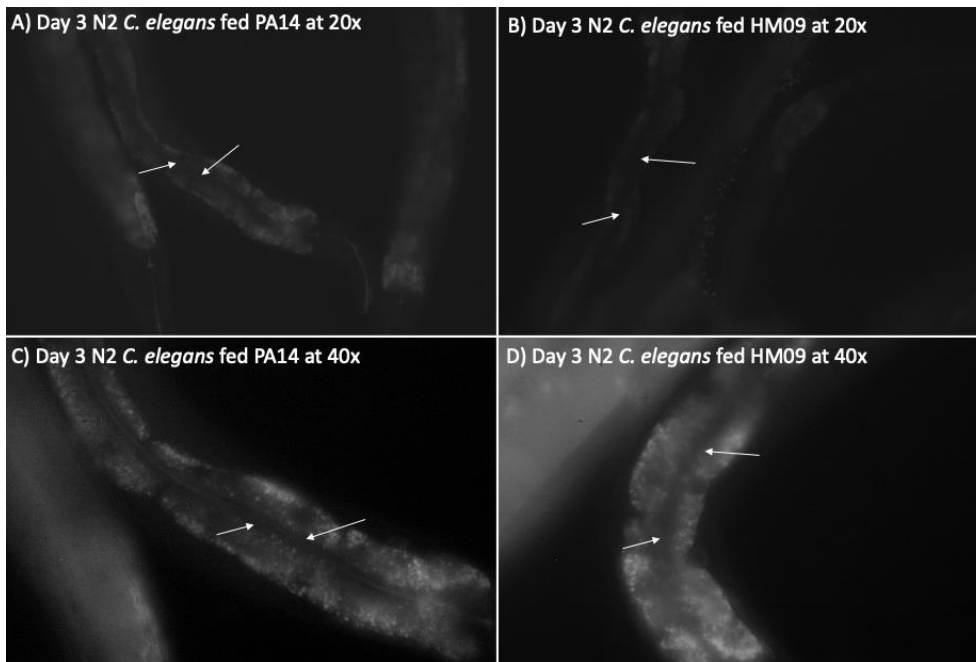


**Figure 3.7.1. Day 3 adult N2 *C. elegans* showed no intestinal fluorescence when using an RFP filter.** Five N2 worms were selected for each condition. Images were taken using Leica DMR microscope set to RFP filter, which registers excitation at 515 nm – 560 nm and emission at LP590 nm, via the Micromanager program. In both the PA14 and HM09 fed *C. elegans* there was a lack of fluorescence in the intestinal lumen which is highlighted by the white arrows in the images.

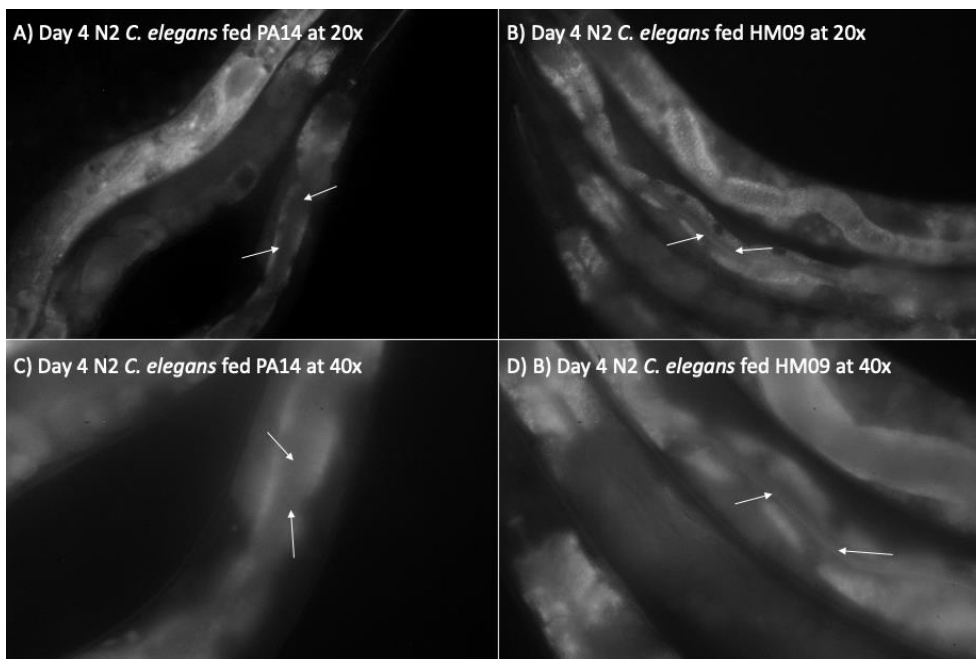


**Figure 3.7.2. Day 4 adult N2 *C. elegans* showed low levels of intestinal fluorescence when under an RFP filter.** Five N2 worms were imaged as in Figure 3.7.1. Under the microscope there was a low level of red fluorescence in the intestinal lumen of the HM09 fed worms as highlighted by the white arrows. In the PA14 fed worms this fluorescence wasn't noticed, however as this is only from a single run more replicates are required before a definitive conclusion can be reached.

From the above images, there is some initial evidence that the HM09 could prove to be a useful tool in *C. elegans* research, however further repeats are needed to draw any certain conclusions.

## Chapter 4: Discussion

The aim of this project was to develop a novel biosensor tool which allowed *P. aeruginosa* biofilms to be studied. This is important as current *in vivo* methods of researching biofilms lack the standardised protocols making them widely available. We started by engineering a plasmid to produce a red fluorescence protein in response to biofilm formation via the quorum sensing signalling cascade in *P. aeruginosa*. Upon induction, in principle, the cells should fluoresce red through production of the mScarlet-I protein, which is an engineered variant of monomeric red fluorescing protein (mRFP). Once built we worked with the newly developed strain through a series of *in vitro* and *in vivo* trials to monitor biofilm formation.

### 4.1. The current state of *in-vitro* and *in-vivo* modelling for biofilm study

Biofilms are bacterial communities which attach to surfaces and grow into a 3D complex architecture that form over 5 distinct stages. The biofilm is surrounded by a matrix which has set components such as eDNA, proteins, water, extracellular polysaccharides and RNA (Tuon et al., 2022). The biofilm matrix provides the biofilm with a way to distribute nutrients evenly throughout and offers protection to the microbial community against antimicrobials and the host environment (Roy et al., 2018). Biofilm forming bacteria are a major concern to public health and more needs to be done in terms of trying to

understanding biofilm interactions and finding new way to combat them.

Studying biofilms is of increasing interest in two different senses. The majority of the techniques used to detect biofilms are currently *in vitro* where the models can be split between static and dynamic models (Su et al., 2022). The most common current static models are the microtiter plate assay, the Calgary biofilm device and the biofilm ring test (Crivello et al., 2023). There are some visualisation methods using different types of microscopies such as confocal laser scanning microscopy and scanning electron microscopy (Vyas & Mai-Prochnow, 2022). The dynamic models are supposed to reproduce the environmental stress a biofilm would experience *in vivo* without the use of a model organism (Gabriliska & Rumbaugh, 2015). The commonly used dynamic models are flow-cell systems, Robbins devices, drip flow reactor and microfluidic platforms (Gabriliska & Rumbaugh, 2015).

There is a wider willing to move to using more *in vivo* based methods to try and mimic the biofilm forming conditions when inside a host, despite the current lack of widely accepted standard techniques (Weigelt et al., 2021). Currently, non-mammalian and mammalian models are used to study biofilms (Lebeaux et al., 2013). Non-mammalian model organisms include *C. elegans*, *Drosophila melanogaster* (fruit fly) and *Danio rerio* (zebrafish) and mammalian models are *Mus musculus* (mouse), *Oryctolagus cuniculus* (rabbits), *Sus scrofa* (pigs) and *Rattus norvegicus* (rats) (Lebeaux et al., 2013;

Guzmán-Soto et al., 2021). Both types of model organism are extremely useful yet lack the standardised procedure which makes them widely adoptable. We aim to begin filling this gap by producing a widely accessible *P. aeruginosa* strain which is compatible across the host of different model organisms.

#### 4.2. Green fluorescing *P. aeruginosa* as a tool for studying biofilms

Mukherjee and colleagues have developed two mutant strains we initially investigated to quantify fluorescence when a biofilm is formed *in vitro* and visualise *in vivo*. *P. aeruginosa* SM381 expressed the *prhIA-mNeonGreen* plasmid meaning the strain should fluoresce green when a biofilm is formed. *P. aeruginosa* SM383 contained the biofilm reporter plasmid also but had the *rhIR* gene knocked out making it difficult for a biofilm to form. At this early stage of investigation, wild-type N2 *C. elegans* worms were fed the different *P. aeruginosa* strains from L4 stage of development and then they were immobilised and imaged.

The results presented in 3.1. show that at day 3 adult stage, the SM381 fed worms had green fluorescence coming from the intestinal lumen. This fluorescence was missing in the N2 worms fed the SM383 and PA14 strains which was to be expected due to the lack of *rhIR* gene and construct respectively. This suggests that the SM381 strain was better at forming a biofilm than the SM383. This idea was further supported by the *in vitro* biofilm assay conducted. A natural

biofilm was allowed to form in a 96-well plate by each of the three mentioned strains and the GFP fluorescence was monitored using a plate reader. This showed SM381 to have a significantly greater fluorescence than SM383 ( $p < 0.0003$ ) and PA14 ( $p < 0.0002$ ), SM383 and PA14 showed no significant difference ( $p = 0.58$ ).

The SM381 was better at forming biofilms than SM383 which was not a surprise as it is widely documented that the *rhIR* gene is required for quorum sensing, biofilm formation and correct biofilm architecture (Lin & Cheng, 2019). *rhIR* knockout studies in model organisms have shown that a lack of the gene results in lower virulence in murine, *C. elegans* and *D. melanogaster* models (Sánchez-Jiménez et al., 2023; Haller et al., 2018). The data provided attempts to show using reporter *P. aeruginosa* strains that are controlled by QS activation could be an extremely useful tool and build upon studies using constitutively active reporter strains that have been attempted previously. Previous studies have largely focussed on identifying antimicrobial activity of compounds. Zhang et al., 2022 tested Xuebijing which contains five traditional Chinese medicines into one injection and is administered to patients to treat sepsis caused by *P. aeruginosa*. The group infected *C. elegans* worms with *P. aeruginosa* PA14:GFP, which is a strain that contains a constitutively active GFP, then the worms were treated with varying concentrations of Xuebijing and fluorescent microscopy images were taken to see whether green fluorescence lowered (Zhang et al., 2022). Through this method, the group found that increasing treatment led to a reduction of *P.*

*aeruginosa* in the *C. elegans* intestinal lumen. Wang et al. used the same method to research paeoniflorin which is a natural product originally extracted from the *Paeonia lactiflora* plant and found in other *Paeonia* plants. The group infected *C. elegans* with the same PA14:GFP strain and treated the worms with varying concentrations of paeoniflorin and monitored intestinal fluorescence and life span. After treatment, the group found that fluorescence in the lumen decreased and lifespan increased indicating paeoniflorin has antimicrobial activity (Wang et al., 2023). In both of the highlighted instances, the groups used a non-specific strain of *P. aeruginosa* GFP which gives an arbitrary result whether the tested compounds have antimicrobial properties. However, by using a strain that is under biofilm control it is possible to determine whether the tested compound has a biofilm disrupting mechanism thus providing a greater mechanistic understanding.

The drawback of using *P. aeruginosa* expressing GFP is that autofluorescence occurs *in vitro* and *in vivo* through *P. aeruginosa* producing phenazines which are green and the *C. elegans* gut granules which fluoresce green (Teuscher & Ewald, 2018). However, by creating a *P. aeruginosa* strain which expresses an RFP biosensor you eliminate the autofluorescence issue entirely.

### 4.3. Using synthetic biology to create a red fluorescing *P. aeruginosa* strain for studying biofilms

Synthetic biology is defined as the engineering of biology towards a new function (National Human Genome Research Institute, 2019). In our investigation, *P. aeruginosa* PA14 needs to be reprogrammed so that an RFP is produced when a biofilm is formed. We chose to construct a biosensor specific to *P. aeruginosa*. Biosensors detect biological reactions and produce a proportional reporter in response (Bhalla et al., 2016). To construct the plasmid, we used Gibson DNA Assembly (Gibson et al., 2009). We required several components to build a functional shuttle vector for molecular cloning in *E. coli* and expression in *P. aeruginosa*. This included the *pUCP22* backbone, *rhlA* promoter region and *mScarlet-I* gene as three fragments (see Table 2.8.1. Each fragment was extracted and a PCR was run. DNA was extracted from the gels and the plasmid was assembled using Gibson DNA assembly.

### 4.4. Causes for unsuccessful *P. aeruginosa* conjugation

After the plasmid was fully sequenced, we attempted to transform *P. aeruginosa* using established protocols for electroporation and conjugation. First, conjugation was attempted. For this we used *P. aeruginosa* PA14 as the recipient, and *E. coli* ET12567 and S17-1 as the donor strains. We saw that in both donor strains instances the *P. aeruginosa* grew on the selective PIA agar plates containing antibiotics when there was plasmid and no plasmid added which was

unexpected. The results suggest that a change was occurring within the *P. aeruginosa* PA14 during the conjugation process due to the spontaneous resistance developing to gentamicin. This result went against the literature available as conjugation has been shown to work with the S17-1 strain (Hmelo et al., 2015). The effects of the antibiotics triclosan and gentamicin were investigated. Triclosan was selected for its ability to kill *E. coli* cells when the mixed cultures were plated. Triclosan works to slow biochemical reactions in the *E. coli* cells causing cell death (Westfall et al., 2019). Gentamicin was used in the conjugation in order to select against the non-transformed *P. aeruginosa* cells in the mixed cultures. Gentamicin works by inhibiting protein synthesis of *P. aeruginosa* (Martin & Beveridge, 1986). We studied the literature on the interactions between the two antibiotics and found that they work in a synergistic manner to stop *P. aeruginosa* growth in a more efficient manner (Maiden et al., 2018). We also studied the literature on the donor strains as we hypothesised potentially the donor plasmid could be getting donated however in both cases the plasmids used are non-transmissible (Kim et al., 2017; Mahapatra et al., 2003). When growing the initial subculture of *P. aeruginosa* the temperature is set to 42°C rather than the typical 37°C (Figure 2.11.1.1a). The change in growth temperature at this stage was another option considered, yet the literature states that there are no known issues at this temperature (LaBauve & Wargo, 2015). To test this in the future, we would try growing *P. aeruginosa* for several hours at 42°C then attempting to

grow the strain on PIA + gentamicin and monitoring growth. It could be possible to order the PIA agar powder premade in order to see if the process of making the agar is inactivating the selective antibiotics, however we did account for this in our initial media tests.

#### 4.5. *P. aeruginosa* HM09 red fluorescence was proportional to autoinducer concentration indicating biofilm control

After attempting conjugation, the *P. aeruginosa* PA14 was successfully transformed using the electroporation method. The newly transformed strain was then tested to ensure the biosensor was under biofilm control as intended. When monitoring red fluorescence (Figure 3.5.1), the HM09 strain was by far the brightest of the 4 being tested (HM09, PA14, SM381 and SM383) by a decent margin with its fluorescence appearing to increase with increasing concentrations of C4-HSL. When monitoring green fluorescing conditions (Figure 3.5.2), the SM381 strain was brighter than the rest, however the other 3 strains exhibited much brighter background fluorescence. This once again highlights the issue that using GFP isn't as effective in *P. aeruginosa* because of the naturally produced phenazines causing the background interference making it difficult to determine whether a biofilm has formed (DeBritto et al., 2020). The HM09 strain provided a much higher reading than the other 3 strains reflecting that the strain could be working as intended.

This idea is further backed up by the single colony images taken of the HM09 vs PA14 under the RFP filter of the dissecting microscope

(Figure 3.6.1). In the images it can be seen that the HM09 strain shows bright red-fluorescing single colonies whereas the PA14 strain shows very little if any fluorescence. This suggests the overall aim of this investigation has been achieved and that a red fluorescing biosensor under biofilm control has been inserted into the *P. aeruginosa* PA14 strain to make the HM09 strain.

A drawback of the data presented in 3.5. was that it was obtained only from a single run. This means two more distinct biological replicates are required before a firm conclusion can be drawn to the extent of control the varying concentrations of C4-HSL has on fluorescence. Also, when similar procedures have been conducted previously a much larger range of autoinducer has been used to get a larger range of fluorescence (Di Veroli et al., 2015; Manoil et al., 2022). This provides a wider spread in data when looking at fluorescence and shows ideal concentration ranges better than in the data we have provided, thus wider ranges of C4-HSL concentrations could be something to change when investigating further.

#### 4.6. *In-vivo* modelling for studying red fluorescing *P. aeruginosa* biofilms

*C. elegans* worms were fed the newly manufactured strain and biofilm formation was compared to the PA14 strain at day 3 and day 4 adult stages. From the images taken on day 3 (Figure 3.7.1) no fluorescence was seen in either condition at 20x or 40x magnification in the intestinal lumen under the RFP filter. At day 4 adult stage

(Figure 3.7.2), there was some low-level red fluorescence which was noticed in the lumen of the *C. elegans* intestine which is highlighted using the white arrows. This result suggests QS was occurring and a biofilm was beginning to form in the intestine of the *C. elegans*. Previous studies have shown in a murine model, biofilms were noticed as early as 8 hours after infection, *in vitro* biofilm assay grown in minimal media showed early biofilm development occurred between 1-14 hours before the later biofilm maturing after 1-5 days and *D. melanogaster* showed biofilm formation 24 hours after oral infection. (Schaber et al., 2007; Rasamiravaka et al., 2015; Mulcahy et al., 2011). Based on our results presented, we are seeing the biofilms are becoming visible after 4 days of daily transfers which would put it on the higher end in comparison to other biofilm study models. This could be explained by the change in seeding times, in trying to avoid biofilm formation on plate the bacterial culture may not be able to form a biofilm as easily as a dried seeded plate. The change in seeding time means that the results presented here are not comparable to the green fluorescence monitored images in 3.1. In other research studies, plates were seeded 1-3 days before and NGM plates were incubated between 25°C – 30°C (Wang et al., 2021; Kang & Kirienko, 2017; Smolentseva et al., 2017). Upon reflection we should have stuck with the original seeding times and placed the plates in an incubator to better prepare the plates for the biofilm assay.

Another detail to mention is that this data is also based off of a single run and such more replicates are needed using this strain. When considering what to study in the future with this strain we would seed plates, then move them to 25°C for 24 hours as previous groups have done. Work would also have to be done in order to try and optimise the amount of time the *C. elegans* are alive.

#### 4.7. Conclusions and future research

The results presented in this work show that we have successfully been able to create an RFP biosensor which is under the control of the *P. aeruginosa* Rhl quorum sensing pathway and have successfully inserted this biosensor into the *P. aeruginosa* PA14 strain. Once the strain was successfully produced, we ensured that activation of RFP transcription was under biofilm control and saw that on all concentrations of HM09 was significantly brighter than the other 3 strains tested and that fluorescence increased with increasing concentrations of C4-HSL. We also attempted to use the newly constructed HM09 strain in *in vivo* *C. elegans* assays where fluorescence microscopy was used in order to visualise biofilm formation in the intestine, some low levels of red fluorescence was noticed in the intestinal lumen. However, in both the biofilm control and *in vivo* assays, only a single run of each was managed and such further research is needed in order to be certain of the result.

In the future, it is important to conduct more replicates of the C4-HSL biofilm control dose-response experiment to be certain that the

results obtained are correct. Optimisation of the *in vivo C. elegans* assay would also allow for a standardised method to be developed to study biofilm interactions in a model organism allowing it to be more widely adopted. From this point, the strain could be used in a host of biofilm study methods such as finding new antimicrobials in *in vitro* biofilm assay then testing toxicity and biofilm disruption *in vivo*. Joint biofilm studies are of increasing interest to better understand co-infections which our strain could be used for *in vivo* and *in vitro*. Overall, we have provided a promising tool which has the ability to play a key role in the expansion of *in vivo* biofilm study methods which can be built upon in the future.

## 5. References:

Abdel-Mawgoud, A. M., Lépine, F. & Déziel, E. (2010) Rhamnolipids: diversity of structures, microbial origins and roles. *Appl Microbiol Biotechnol*, 86(5), 1323-36. 10.1007/s00253-010-2498-2.

AbdulWahab, A., Zahraidin, K., Sid Ahmed, M. A., Jarir, S. A., Muneer, M., Mohamed, S. F., Hamid, J. M., Hassan, A. A. I. & Ibrahim, E. B. (2017) The emergence of multidrug-resistant *Pseudomonas aeruginosa* in cystic fibrosis patients on inhaled antibiotics. *Lung India*, 34(6), 527-531. 10.4103/lungindia.lungindia\_39\_17.

American Society for Microbiology. (2023). The Role of Bacterial Biofilms in Antimicrobial Resistance. Available at: <https://asm.org/Articles/2023/March/The-Role-of-Bacterial-Biofilms-in-Antimicrobial-Re#:~:text=The%20biofilm%20structure's%20complexity%2C%20which,reach%20the%20bacterial%20target%20within> (Accessed July 2023).

Antunes, L. C., Ferreira, R. B., Lostroh, C. P. & Greenberg, E. P. (2008) A mutational analysis defines *Vibrio fischeri* LuxR binding sites. *J Bacteriol*, 190(13), 4392-7. 10.1128/jb.01443-07.

Arango MT, Quintero-Ronderos P, Castiblanco J, et al. Cell culture and cell analysis. In: Anaya JM, Shoenfeld Y, Rojas-Villarraga A, et al., editors. *Autoimmunity: From Bench to Bedside* [Internet]. Bogota (Colombia): El Rosario University Press; 2013 Jul 18. Chapter 45. Available from: <https://www.ncbi.nlm.nih.gov/books/NBK459464/>

Atkinson, S., Goldstone, R. J., Joshua, G. W., Chang, C. Y., Patrick, H. L., Cámara, M., Wren, B. W. & Williams, P. (2011) Biofilm development on *Caenorhabditis elegans* by *Yersinia* is facilitated by quorum sensing-dependent repression of type III secretion. *PLoS Pathog*, 7(1), e1001250. 10.1371/journal.ppat.1001250.

Baeshen, N. A., Baeshen, M. N., Sheikh, A., Bora, R. S., Ahmed, M. M., Ramadan, H. A., Saini, K. S. & Redwan, E. M. (2014) Cell factories for insulin production. *Microb Cell Fact*, 13, 141. 10.1186/s12934-014-0141-0.

Barequet, I. S., Ben Simon, G. J., Safrin, M., Ohman, D. E. & Kessler, E. (2004) *Pseudomonas aeruginosa* LasA protease in treatment of experimental staphylococcal keratitis. *Antimicrob Agents Chemother*, 48(5), 1681-7. 10.1128/aac.48.5.1681-1687.2004.

Bastaert, F., Kheir, S., Saint-Criq, V., Villeret, B., Dang, P. M., El-Benna, J., Sirard, J. C., Voulhoux, R. & Sallenave, J. M. (2018) *Pseudomonas aeruginosa* LasB Subverts Alveolar Macrophage Activity by Interfering With Bacterial Killing Through Downregulation of Innate Immune Defense, Reactive Oxygen Species Generation,

- and Complement Activation. *Front Immunol*, 9, 1675. 10.3389/fimmu.2018.01675.
- Bhalla, N., Jolly, P., Formisano, N. & Estrela, P. (2016a) Introduction to biosensors. *Essays Biochem*, 60(1), 1-8. 10.1042/ebc20150001.
- Boyd, A. & Chakrabarty, A. M. (1995) *Pseudomonas aeruginosa* biofilms: role of the alginate exopolysaccharide. *J Ind Microbiol*, 15(3), 162-8. 10.1007/bf01569821.
- Brophy, J. A. & Voigt, C. A. (2014) Principles of genetic circuit design. *Nat Methods*, 11(5), 508-20. 10.1038/nmeth.2926.
- Buhmann, M. T., Stiefel, P., Maniura-Weber, K. & Ren, Q. (2016) In Vitro Biofilm Models for Device-Related Infections. *Trends Biotechnol*, 34(12), 945-948. 10.1016/j.tibtech.2016.05.016.
- Bustamante-Marin, X. M. & Ostrowski, L. E. (2017) Cilia and Mucociliary Clearance. *Cold Spring Harb Perspect Biol*, 9(4). 10.1101/cshperspect.a028241.
- Byrd, M. S., Sadovskaya, I., Vinogradov, E., Lu, H., Sprinkle, A. B., Richardson, S. H., Ma, L., Ralston, B., Parsek, M. R., Anderson, E. M., Lam, J. S. & Wozniak, D. J. (2009) Genetic and biochemical analyses of the *Pseudomonas aeruginosa* Psl exopolysaccharide reveal overlapping roles for polysaccharide synthesis enzymes in Psl and LPS production. *Mol Microbiol*, 73(4), 622-38. 10.1111/j.1365-2958.2009.06795.x.
- Caenorhabditis Genetics Centre. (2023). Caenorhabditis Genetics Centre. Available at: <https://cgc.umn.edu/>. (Accessed: August 2023).
- Caiazza, N. C., Shanks, R. M. & O'Toole, G. A. (2005) Rhamnolipids modulate swarming motility patterns of *Pseudomonas aeruginosa*. *J Bacteriol*, 187(21), 7351-61. 10.1128/jb.187.21.7351-7361.2005.
- Cameron, D. R., Shan, Y., Zalis, E. A., Isabella, V. & Lewis, K. (2018) A Genetic Determinant of Persister Cell Formation in Bacterial Pathogens. *J Bacteriol*, 200(17). 10.1128/jb.00303-18.
- Cathcart, G. R., Quinn, D., Greer, B., Harriott, P., Lynas, J. F., Gilmore, B. F. & Walker, B. (2011) Novel inhibitors of the *Pseudomonas aeruginosa* virulence factor LasB: a potential therapeutic approach for the attenuation of virulence mechanisms in pseudomonas infection. *Antimicrob Agents Chemother*, 55(6), 2670-8. 10.1128/aac.00776-10.
- Cezairliyan, B., Vinayavekhin, N., Grenfell-Lee, D., Yuen, G. J., Saghatelyan, A. & Ausubel, F. M. (2013) Identification of *Pseudomonas aeruginosa* phenazines that kill *Caenorhabditis elegans*. *PLoS Pathog*, 9(1), e1003101. 10.1371/journal.ppat.1003101.
- Chasnov, J. R. (2013) The evolutionary role of males in *C. elegans*. *Worm*, 2(1), e21146. 10.4161/worm.21146.

Chen, S., Chen, X., Su, H., Guo, M. & Liu, H. (2023) Advances in Synthetic-Biology-Based Whole-Cell Biosensors: Principles, Genetic Modules, and Applications in Food Safety. *Int J Mol Sci*, 24(9). 10.3390/ijms24097989.

Chong, H. & Li, Q. (2017) Microbial production of rhamnolipids: opportunities, challenges and strategies. *Microb Cell Fact*, 16(1), 137. 10.1186/s12934-017-0753-2.

Ciofu, O. & Tolker-Nielsen, T. (2019) Tolerance and Resistance of *Pseudomonas aeruginosa* Biofilms to Antimicrobial Agents-How *P. aeruginosa* Can Escape Antibiotics. *Front Microbiol*, 10, 913. 10.3389/fmicb.2019.00913.

Coffey, B. M. & Anderson, G. G. (2014) Biofilm formation in the 96-well microtiter plate. *Methods Mol Biol*, 1149, 631-41. 10.1007/978-1-4939-0473-0\_48.

Coin, D., Louis, D., Bernillon, J., Guinand, M. & Wallach, J. (1997) LasA, alkaline protease and elastase in clinical strains of *Pseudomonas aeruginosa*: quantification by immunochemical methods. *FEMS Immunol Med Microbiol*, 18(3), 175-84. 10.1111/j.1574-695X.1997.tb01043.x.

Colvin, K. M., Gordon, V. D., Murakami, K., Borlee, B. R., Wozniak, D. J., Wong, G. C. & Parsek, M. R. (2011) The pel polysaccharide can serve a structural and protective role in the biofilm matrix of *Pseudomonas aeruginosa*. *PLoS Pathog*, 7(1), e1001264. 10.1371/journal.ppat.1001264.

Coquant, G., Grill, J. P. & Seksik, P. (2020) Impact of N-Acyl-Homoserine Lactones, Quorum Sensing Molecules, on Gut Immunity. *Front Immunol*, 11, 1827. 10.3389/fimmu.2020.01827.

Corsi, A. K., Wightman, B. & Chalfie, M. (2015) A Transparent Window into Biology: A Primer on *Caenorhabditis elegans*. In: *Genetics*. United States: Copyright © 2015 Corsi, Wightman, and Chalfie.

Costerton, J. W., Lewandowski, Z., Caldwell, D. E., Korber, D. R. & Lappin-Scott, H. M. (1995) Microbial biofilms. *Annu Rev Microbiol*, 49, 711-45. 10.1146/annurev.mi.49.100195.003431.

Coulson, A., Kozono, Y., Lutterbach, B., Shownkeen, R., Sulston, J. & Waterston, R. (1991) YACs and the *C. elegans* genome. *Bioessays*, 13(8), 413-7. 10.1002/bies.950130809.

Crivello, G., Fracchia, L., Ciardelli, G., Boffito, M. & Mattu, C. (2023) In Vitro Models of Bacterial Biofilms: Innovative Tools to Improve Understanding and Treatment of Infections. *Nanomaterials (Basel)*, 13(5). 10.3390/nano13050904.

da Silva, A. J., Cunha, J. S., Hreha, T., Micocci, K. C., Selistre-de-Araujo, H. S., Barquera, B. & Koffas, M. A. G. (2021) Metabolic

- engineering of *E. coli* for pyocyanin production. *Metab Eng*, 64, 15-25. 10.1016/j.ymben.2021.01.002.
- Darch, S. E., West, S. A., Winzer, K. & Diggle, S. P. (2012) Density-dependent fitness benefits in quorum-sensing bacterial populations. *Proc Natl Acad Sci U S A*, 109(21), 8259-63. 10.1073/pnas.1118131109.
- Das, T. & Manefield, M. (2012) Pyocyanin promotes extracellular DNA release in *Pseudomonas aeruginosa*. *PLoS One*, 7(10), e46718. 10.1371/journal.pone.0046718.
- Davey, M. E., Caiazza, N. C. & O'Toole, G. A. (2003) Rhamnolipid surfactant production affects biofilm architecture in *Pseudomonas aeruginosa* PAO1. *J Bacteriol*, 185(3), 1027-36. 10.1128/jb.185.3.1027-1036.2003.
- DeBritto, S., Gajbar, T. D., Satapute, P., Sundaram, L., Lakshmikantha, R. Y., Jogaiah, S. & Ito, S. I. (2020) Isolation and characterization of nutrient dependent pyocyanin from *Pseudomonas aeruginosa* and its dye and agrochemical properties. *Sci Rep*, 10(1), 1542. 10.1038/s41598-020-58335-6.
- Dekimpe, V. & Déziel, E. (2009) Revisiting the quorum-sensing hierarchy in *Pseudomonas aeruginosa*: the transcriptional regulator RhIR regulates LasR-specific factors. *Microbiology (Reading)*, 155(Pt 3), 712-723. 10.1099/mic.0.022764-0.
- Delaviz, Y., Santerre, J. P., Cvitkovitch, D. G., Barnes, L. & Cooper, I. R. (2015) 11 - Infection resistant biomaterials. In: *Biomaterials and Medical Device - Associated Infections*. Oxford: Woodhead Publishing.
- Desalermos, A., Muhammed, M., Glavis-Bloom, J. & Mylonakis, E. (2011) Using *C. elegans* for antimicrobial drug discovery. *Expert Opin Drug Discov*, 6(6), 645-652. 10.1517/17460441.2011.573781.
- Di Veroli, G. Y., Fornari, C., Goldlust, I., Mills, G., Koh, S. B., Bramhall, J. L., Richards, F. M. & Jodrell, D. I. (2015) An automated fitting procedure and software for dose-response curves with multiphasic features. *Sci Rep*, 5, 14701. 10.1038/srep14701.
- Diggle, S. P., Stacey, R. E., Dodd, C., Cámara, M., Williams, P. & Winzer, K. (2006) The galactophilic lectin, LecA, contributes to biofilm development in *Pseudomonas aeruginosa*. *Environ Microbiol*, 8(6), 1095-104. 10.1111/j.1462-2920.2006.001001.x.
- Dinarello, C. A. (2018) Overview of the IL-1 family in innate inflammation and acquired immunity. *Immunol Rev*, 281(1), 8-27. 10.1111/imr.12621.
- Duperthuy, M. (2020) Antimicrobial Peptides: Virulence and Resistance Modulation in Gram-Negative Bacteria. *Microorganisms*, 8(2). 10.3390/microorganisms8020280.

- Fong, J. N. C. & Yildiz, F. H. (2015) Biofilm Matrix Proteins. *Microbiol Spectr*, 3(2). 10.1128/microbiolspec.MB-0004-2014.
- Fu, O., Pukin, A. V., Quarles van Ufford, H. C., Kemmink, J., de Mol, N. J. & Pieters, R. J. (2015) Functionalization of a Rigid Divalent Ligand for LecA, a Bacterial Adhesion Lectin. *ChemistryOpen*, 4(4), 463-70. 10.1002/open.201402171.
- Fuqua, W. C., Winans, S. C. & Greenberg, E. P. (1994) Quorum sensing in bacteria: the LuxR-LuxI family of cell density-responsive transcriptional regulators. *J Bacteriol*, 176(2), 269-75. 10.1128/jb.176.2.269-275.1994.
- Gabrilska, R. A. & Rumbaugh, K. P. (2015) Biofilm models of polymicrobial infection. *Future Microbiol*, 10(12), 1997-2015. 10.2217/fmb.15.109.
- Garrison, A. T., Abouelhassan, Y., Yang, H., Yousaf, H. H., Nguyen, T. J. & Huigens Iii, R. W. (2017) Microwave-enhanced Friedländer synthesis for the rapid assembly of halogenated quinolines with antibacterial and biofilm eradication activities against drug resistant and tolerant bacteria. *Medchemcomm*, 8(4), 720-724. 10.1039/c6md00381h.
- Gibson, D. G., Young, L., Chuang, R. Y., Venter, J. C., Hutchison, C. A., 3rd & Smith, H. O. (2009) Enzymatic assembly of DNA molecules up to several hundred kilobases. *Nat Methods*, 6(5), 343-5. 10.1038/nmeth.1318.
- Gibson, E. G., Oviatt, A. A. & Osheroff, N. (2020) Two-Dimensional Gel Electrophoresis to Resolve DNA Topoisomers. *Methods Mol Biol*, 2119, 15-24. 10.1007/978-1-0716-0323-9\_2.
- González, J. F., Hahn, M. M. & Gunn, J. S. (2018) Chronic biofilm-based infections: skewing of the immune response. *Pathog Dis*, 76(3). 10.1093/femspd/fty023.
- Gonçalves, T. & Vasconcelos, U. (2021) Colour Me Blue: The History and the Biotechnological Potential of Pyocyanin. *Molecules*, 26(4). 10.3390/molecules26040927.
- Groleau, M. C., de Oliveira Pereira, T., Dekimpe, V. & Déziel, E. (2020) PqsE Is Essential for RhIR-Dependent Quorum Sensing Regulation in *Pseudomonas aeruginosa*. *mSystems*, 5(3). 10.1128/mSystems.00194-20.
- Gruber, J. D., Chen, W., Parnham, S., Beauchesne, K., Moeller, P., Flume, P. A. & Zhang, Y. M. (2016) The role of 2,4-dihydroxyquinoline (DHQ) in *Pseudomonas aeruginosa* pathogenicity. *PeerJ*, 4, e1495. 10.7717/peerj.1495.
- Gunn, J. S., Bakaletz, L. O. & Wozniak, D. J. (2016) What's on the Outside Matters: The Role of the Extracellular Polymeric Substance of Gram-negative Biofilms in Evading Host Immunity and as a Target

for Therapeutic Intervention. *J Biol Chem*, 291(24), 12538-12546. 10.1074/jbc.R115.707547.

Guzmán-Soto, I., McTiernan, C., Gonzalez-Gomez, M., Ross, A., Gupta, K., Suuronen, E. J., Mah, T. F., Griffith, M. & Alarcon, E. I. (2021) Mimicking biofilm formation and development: Recent progress in in vitro and in vivo biofilm models. *iScience*, 24(5), 102443. 10.1016/j.isci.2021.102443.

Hall, S., McDermott, C., Anoopkumar-Dukie, S., McFarland, A. J., Forbes, A., Perkins, A. V., Davey, A. K., Chess-Williams, R., Kiefel, M. J., Arora, D. & Grant, G. D. (2016) Cellular Effects of Pyocyanin, a Secreted Virulence Factor of *Pseudomonas aeruginosa*. *Toxins (Basel)*, 8(8). 10.3390/toxins8080236.

Haller, S., Franchet, A., Hakkim, A., Chen, J., Drenkard, E., Yu, S., Schirmeier, S., Li, Z., Martins, N., Ausubel, F. M., Liégeois, S. & Ferrandon, D. (2018) Quorum-sensing regulator RhIR but not its autoinducer RhII enables *Pseudomonas* to evade opsonization. *EMBO Rep*, 19(5). 10.15252/embr.201744880.

Hall-Stoodley, L., Rayner, J.C., Stoodley, P., Lappin-Scott, H.M. (1999). Establishment of Experimental Biofilms Using the Modified Robbins Device and Flow Cells. In: Edwards, C. (eds) *Environmental Monitoring of Bacteria. Methods in Biotechnology*, vol 12. Humana Press, Totowa, NJ. <https://doi.org/10.1385/0-89603-566-2:307>

Hazan, R., Que, Y. A., Maura, D., Strobel, B., Majcherczyk, P. A., Hopper, L. R., Wilbur, D. J., Hreha, T. N., Barquera, B. & Rahme, L. G. (2016) Auto Poisoning of the Respiratory Chain by a Quorum-Sensing-Regulated Molecule Favors Biofilm Formation and Antibiotic Tolerance. *Curr Biol*, 26(2), 195-206. 10.1016/j.cub.2015.11.056.

Heesterbeek, D. A., Bardoel, B. W., Parsons, E. S., Bennett, I., Ruyken, M., Doorduijn, D. J., Gorham, R. D., Jr., Berends, E. T., Pyne, A. L., Hoogenboom, B. W. & Rooijackers, S. H. (2019) Bacterial killing by complement requires membrane attack complex formation via surface-bound C5 convertases. *Embo j*, 38(4). 10.15252/emboj.201899852.

Heesterbeek, D. A. C., Angelier, M. L., Harrison, R. A. & Rooijackers, S. H. M. (2018) Complement and Bacterial Infections: From Molecular Mechanisms to Therapeutic Applications. *J Innate Immun*, 10(5-6), 455-464. 10.1159/000491439.

Hemmati, F., Salehi, R., Ghotaslou, R., Samadi Kafil, H., Hasani, A., Gholizadeh, P., Nouri, R. & Ahangarzadeh Rezaee, M. (2020) Quorum Quenching: A Potential Target for Antipseudomonal Therapy. *Infect Drug Resist*, 13, 2989-3005. 10.2147/idr.s263196.

Herndon, L.A., Wolkow, C.A., Driscoll, M. and Hall, D.H. 2018. Introduction to Aging in *C. elegans*. In *WormAtlas*. [doi:10.3908/wormatlas.8.4](https://doi.org/10.3908/wormatlas.8.4)

- Heuschkel, I., Hanisch, S., Volke, D. C., Löfgren, E., Hoschek, A., Nickel, P. I., Karande, R. & Bühler, K. (2021) *Pseudomonas taiwanensis* biofilms for continuous conversion of cyclohexanone in drip flow and rotating bed reactors. *Eng Life Sci*, 21(3-4), 258-269. 10.1002/elsc.202000072.
- Hmelo, L. R., Borlee, B. R., Almblad, H., Love, M. E., Randall, T. E., Tseng, B. S., Lin, C., Irie, Y., Storek, K. M., Yang, J. J., Siehnel, R. J., Howell, P. L., Singh, P. K., Tolker-Nielsen, T., Parsek, M. R., Schweizer, H. P. & Harrison, J. J. (2015b) Precision-engineering the *Pseudomonas aeruginosa* genome with two-step allelic exchange. *Nat Protoc*, 10(11), 1820-41. 10.1038/nprot.2015.115.
- Holt, J. E., Houston, A., Adams, C., Edwards, S. & Kjellerup, B. V. (2017) Role of extracellular polymeric substances in polymicrobial biofilm infections of *Staphylococcus epidermidis* and *Candida albicans* modelled in the nematode *Caenorhabditis elegans*. *Pathog Dis*, 75(5). 10.1093/femspd/ftx052.
- iGEM. (2023). *Build Stage*. Available at: <https://technology.igem.org/engineering/build>. (Accessed: August 2023).
- Irorere, V. U., Tripathi, L., Marchant, R., McClean, S. & Banat, I. M. (2017) Microbial rhamnolipid production: a critical re-evaluation of published data and suggested future publication criteria. *Appl Microbiol Biotechnol*, 101(10), 3941-3951. 10.1007/s00253-017-8262-0.
- Jennings, L. K., Dreifus, J. E., Reichhardt, C., Storek, K. M., Secor, P. R., Wozniak, D. J., Hisert, K. B. & Parsek, M. R. (2021) *Pseudomonas aeruginosa* aggregates in cystic fibrosis sputum produce exopolysaccharides that likely impede current therapies. *Cell Rep*, 34(8), 108782. 10.1016/j.celrep.2021.108782.
- Jennings, L. K., Storek, K. M., Ledvina, H. E., Coulon, C., Marmont, L. S., Sadovskaya, I., Secor, P. R., Tseng, B. S., Scian, M., Filloux, A., Wozniak, D. J., Howell, P. L. & Parsek, M. R. (2015) Pel is a cationic exopolysaccharide that cross-links extracellular DNA in the *Pseudomonas aeruginosa* biofilm matrix. *Proc Natl Acad Sci U S A*, 112(36), 11353-8. 10.1073/pnas.1503058112.
- Jing, C., Liu, C., Liu, Y., Feng, R., Cao, R., Guan, Z., Xuan, B., Gao, Y., Wang, Q., Yang, N., Ma, Y., Lan, L., Feng, J., Shen, B., Wang, H., Yu, Y. & Yang, G. (2021) Antibodies Against *Pseudomonas aeruginosa* Alkaline Protease Directly Enhance Disruption of Neutrophil Extracellular Traps Mediated by This Enzyme. *Front Immunol*, 12, 654649. 10.3389/fimmu.2021.654649.
- Kamath, S., Kapatral, V. & Chakrabarty, A. M. (1998) Cellular function of elastase in *Pseudomonas aeruginosa*: role in the cleavage of nucleoside diphosphate kinase and in alginate synthesis. *Mol Microbiol*, 30(5), 933-41. 10.1046/j.1365-2958.1998.01121.x.

- Kaplan, J. B. (2010) Biofilm dispersal: mechanisms, clinical implications, and potential therapeutic uses. *J Dent Res*, 89(3), 205-18. 10.1177/0022034509359403.
- Kelly, C. L., Taylor, G. M., Šatkutė, A., Dekker, L. & Heap, J. T. (2019) Transcriptional Terminators Allow Leak-Free Chromosomal Integration of Genetic Constructs in Cyanobacteria. *Microorganisms*, 7(8). 10.3390/microorganisms7080263.
- Khan, F., Jain, S. & Oloketuyi, S. F. (2018) Bacteria and bacterial products: Foe and friends to *Caenorhabditis elegans*. *Microbiol Res*, 215, 102-113. 10.1016/j.micres.2018.06.012.
- Khosla, A. & Nelson, D. C. (2020) Ratiometric Measurement of Protein Abundance after Transient Expression of a Transgene in *Nicotiana benthamiana*. *Bio Protoc*, 10(17), e3747. 10.21769/BioProtoc.3747.
- Kim, H., Ju, J., Lee, H. N., Chun, H. & Seong, J. (2021) Genetically Encoded Biosensors Based on Fluorescent Proteins. *Sensors (Basel)*, 21(3). 10.3390/s21030795.
- Kim, M. S., Cho, W. J., Song, M. C., Park, S. W., Kim, K., Kim, E., Lee, N., Nam, S. J., Oh, K. H. & Yoon, Y. J. (2017) Engineered biosynthesis of milbemycins in the avermectin high-producing strain *Streptomyces avermitilis*. *Microb Cell Fact*, 16(1), 9. 10.1186/s12934-017-0626-8.
- Kim, S. K. & Lee, J. H. (2016) Biofilm dispersion in *Pseudomonas aeruginosa*. *J Microbiol*, 54(2), 71-85. 10.1007/s12275-016-5528-7.
- Kim, W., Conery, A. L., Rajamuthiah, R., Fuchs, B. B., Ausubel, F. M. & Mylonakis, E. (2015) Identification of an Antimicrobial Agent Effective against Methicillin-Resistant *Staphylococcus aureus* Persists Using a Fluorescence-Based Screening Strategy. *PLoS One*, 10(6), e0127640. 10.1371/journal.pone.0127640.
- Kiss, K., Ng, W. T. & Li, Q. (2017) Production of rhamnolipids-producing enzymes of *Pseudomonas* in *E. coli* and structural characterization. *Frontiers of Chemical Science and Engineering*, 11(1), 133-138. 10.1007/s11705-017-1637-z.
- Kitano, S., Lin, C., Foo, J. L. & Chang, M. W. (2023) Synthetic biology: Learning the way toward high-precision biological design. *PLoS Biol*, 21(4), e3002116. 10.1371/journal.pbio.3002116.
- Laarman, A. J., Bardoel, B. W., Ruyken, M., Fernie, J., Milder, F. J., van Strijp, J. A. & Rooijackers, S. H. (2012) *Pseudomonas aeruginosa* alkaline protease blocks complement activation via the classical and lectin pathways. *J Immunol*, 188(1), 386-93. 10.4049/jimmunol.1102162.
- LaBauve, A. E. & Wargo, M. J. (2012) Growth and laboratory maintenance of *Pseudomonas aeruginosa*. *Curr Protoc Microbiol*, Chapter 6, Unit 6E.1. 10.1002/9780471729259.mc06e01s25.

Lakshmanan, U., Yap, A., Fulwood, J., Yichun, L., Hoon, S. S., Lim, J., Ting, A., Sem, X. H., Kreisberg, J. F., Tan, P., Tan, G. & Flotow, H. (2014) Establishment of a novel whole animal HTS technology platform for melioidosis drug discovery. *Comb Chem High Throughput Screen*, 17(9), 790-803. 10.2174/1386207317666141019195031.

Le Mauff, F., Razvi, E., Reichhardt, C., Sivarajah, P., Parsek, M. R., Howell, P. L. & Sheppard, D. C. (2022) The Pel polysaccharide is predominantly composed of a dimeric repeat of  $\alpha$ -1,4 linked galactosamine and N-acetylgalactosamine. *Commun Biol*, 5(1), 502. 10.1038/s42003-022-03453-2.

Lebeaux, D., Chauhan, A., Rendueles, O. & Beloin, C. (2013) From in vitro to in vivo Models of Bacterial Biofilm-Related Infections. *Pathogens*, 2(2), 288-356. 10.3390/pathogens2020288.

Lee, J., Wu, J., Deng, Y., Wang, J., Wang, C., Chang, C., Dong, Y., Williams, P. & Zhang, L. H. (2013) A cell-cell communication signal integrates quorum sensing and stress response. *Nat Chem Biol*, 9(5), 339-43. 10.1038/nchembio.1225.

Lee, J. & Zhang, L. (2015) The hierarchy quorum sensing network in *Pseudomonas aeruginosa*. *Protein Cell*, 6(1), 26-41. 10.1007/s13238-014-0100-x.

Leonelli, S. & Ankeny, R. A. (2013) What makes a model organism? *Endeavour*, 37(4), 209-12. 10.1016/j.endeavour.2013.06.001.

Li, X. H. & Lee, J. H. (2019) Quorum sensing-dependent post-secretional activation of extracellular proteases in *Pseudomonas aeruginosa*. *J Biol Chem*, 294(51), 19635-19644. 10.1074/jbc.RA119.011047.

Liao, C., Huang, X., Wang, Q., Yao, D. & Lu, W. (2022) Virulence Factors of *Pseudomonas Aeruginosa* and Antivirulence Strategies to Combat Its Drug Resistance. *Front Cell Infect Microbiol*, 12, 926758. 10.3389/fcimb.2022.926758.

Lin, J. & Cheng, J. (2019). Quorum Sensing in *Pseudomonas aeruginosa* and Its Relationship to Biofilm Development. 10.1021/bk-2019-1323.ch001

Lin, J., Cheng, J., Wang, Y. & Shen, X. (2018) The *Pseudomonas* Quinolone Signal (PQS): Not Just for Quorum Sensing Anymore. *Front Cell Infect Microbiol*, 8, 230. 10.3389/fcimb.2018.00230.

Liu, R., Bassalo, M. C., Zeitoun, R. I. & Gill, R. T. (2015) Genome scale engineering techniques for metabolic engineering. *Metab Eng*, 32, 143-154. 10.1016/j.ymben.2015.09.013.

Létoffé, S., Wu, Y., Darch, S. E., Beloin, C., Whiteley, M., Touqui, L. & Ghigo, J. M. (2022) *Pseudomonas aeruginosa* Production of Hydrogen Cyanide Leads to Airborne Control of *Staphylococcus*

- aureus Growth in Biofilm and In Vivo Lung Environments. *mBio*, 13(5), e0215422. 10.1128/mbio.02154-22.
- Mahapatra, N. R., Ghosh, S., Sarkar, P. K. & Banerjee, P. C. (2003) Generation of novel plasmids in *Escherichia coli* S17-1(pSUP106). *Curr Microbiol*, 46(5), 318-23. 10.1007/s00284-002-3835-1.
- Maiden, M. M., Hunt, A. M. A., Zachos, M. P., Gibson, J. A., Hurwitz, M. E., Mulks, M. H. & Waters, C. M. (2018) Triclosan Is an Aminoglycoside Adjuvant for Eradication of *Pseudomonas aeruginosa* Biofilms. *Antimicrob Agents Chemother*, 62(6). 10.1128/aac.00146-18.
- Mann, E. E. & Wozniak, D. J. (2012) *Pseudomonas* biofilm matrix composition and niche biology. *FEMS Microbiol Rev*, 36(4), 893-916. 10.1111/j.1574-6976.2011.00322.x.
- Manoil, D., Parga, A., Hellesen, C., Khawaji, A., Brundin, M., Durual, S., Özenci, V., Fang, H. & Belibasakis, G. N. (2022) Photo-oxidative stress response and virulence traits are co-regulated in *E. faecalis* after antimicrobial photodynamic therapy. *J Photochem Photobiol B*, 234, 112547. 10.1016/j.jphotobiol.2022.112547.
- Martin, N. L. & Beveridge, T. J. (1986) Gentamicin interaction with *Pseudomonas aeruginosa* cell envelope. *Antimicrob Agents Chemother*, 29(6), 1079-87. 10.1128/aac.29.6.1079.
- Martínez-García, E., Benedetti, I., Hueso, A. & De Lorenzo, V. (2015) Mining Environmental Plasmids for Synthetic Biology Parts and Devices. *Microbiol Spectr*, 3(1), Plas-0033-2014. 10.1128/microbiolspec.PLAS-0033-2014.
- Maunder, E. & Welch, M. (2017) Matrix exopolysaccharides; the sticky side of biofilm formation. *FEMS Microbiol Lett*, 364(13). 10.1093/femsle/fnx120.
- McCready, A. R., Paczkowski, J. E., Cong, J. P. & Bassler, B. L. (2019) An autoinducer-independent RhIR quorum-sensing receptor enables analysis of RhIR regulation. *PLoS Pathog*, 15(6), e1007820. 10.1371/journal.ppat.1007820.
- McGhee, J. D. (2007) The *C. elegans* intestine. *WormBook*, 1-36. 10.1895/wormbook.1.133.1.
- Meirelles, L. A. & Newman, D. K. (2018) Both toxic and beneficial effects of pyocyanin contribute to the lifecycle of *Pseudomonas aeruginosa*. *Mol Microbiol*, 110(6), 995-1010.
- Meneely, P. M., Dahlberg, C. L., & Rose, J. K. (2019). Working with worms: *Caenorhabditis elegans* as a model organism. *Current Protocols Essential Laboratory Techniques*, 19, e35. doi: [10.1002/cpet.35](https://doi.org/10.1002/cpet.35)

- Miller, C. & Gilmore, J. (2020) Detection of Quorum-Sensing Molecules for Pathogenic Molecules Using Cell-Based and Cell-Free Biosensors. *Antibiotics (Basel)*, 9(5). 10.3390/antibiotics9050259.
- Miranda, S. W., Asfahl, K. L., Dandekar, A. A. & Greenberg, E. P. (2022) *Pseudomonas aeruginosa* Quorum Sensing. *Adv Exp Med Biol*, 1386, 95-115. 10.1007/978-3-031-08491-1\_4.
- Montagut, E. J., Raya, J., Martin-Gomez, M. T., Vilaplana, L., Rodriguez-Urretavizcaya, B. & Marco, M. P. (2022) An Immunochemical Approach to Detect the Quorum Sensing-Regulated Virulence Factor 2-Heptyl-4-Quinoline N-Oxide (HQNO) Produced by *Pseudomonas aeruginosa* Clinical Isolates. *Microbiol Spectr*, 10(4), e0107321. 10.1128/spectrum.01073-21.
- Moradali, M.F., Rehm, B.H.A. (2019). The Role of Alginate in Bacterial Biofilm Formation. In: Cohen, E., Merzendorfer, H. (eds) *Extracellular Sugar-Based Biopolymers Matrices. Biologically-Inspired Systems*, vol 12. Springer, Cham.  
[https://doi.org/10.1007/978-3-030-12919-4\\_13](https://doi.org/10.1007/978-3-030-12919-4_13)
- Morici, L. A., Carterson, A. J., Wagner, V. E., Frisk, A., Schurr, J. R., Höner zu Bentrup, K., Hassett, D. J., Iglewski, B. H., Sauer, K. & Schurr, M. J. (2007) *Pseudomonas aeruginosa* AlgR represses the Rhl quorum-sensing system in a biofilm-specific manner. *J Bacteriol*, 189(21), 7752-64. 10.1128/jb.01797-06.
- Moser, C., Pedersen, H. T., Lerche, C. J., Kolpen, M., Line, L., Thomsen, K., Høiby, N. & Jensen, P. (2017) Biofilms and host response - helpful or harmful. *Apmis*, 125(4), 320-338. 10.1111/apm.12674.
- Mukherjee, S., Moustafa, D., Smith, C. D., Goldberg, J. B. & Bassler, B. L. (2017) The RhlR quorum-sensing receptor controls *Pseudomonas aeruginosa* pathogenesis and biofilm development independently of its canonical homoserine lactone autoinducer. *PLoS Pathog*, 13(7), e1006504. 10.1371/journal.ppat.1006504.
- Mulcahy, H., Sibley, C. D., Surette, M. G. & Lewenza, S. (2011) *Drosophila melanogaster* as an animal model for the study of *Pseudomonas aeruginosa* biofilm infections in vivo. *PLoS Pathog*, 7(10), e1002299. 10.1371/journal.ppat.1002299.
- Mullan, A. Marsh, A. (2019). *Advantages of using Caenorhabditis Elegans as a Model Organism*. Available at: <https://andor.oxinst.com/learning/view/article/advantages-of-using-caenorhabditis-elegans-as-a-model-organism>. (Accessed: August 2023).
- National Human Genome Research Institute. (2013). *1998: Genome of Roundworm C. elegans Sequenced*. Available at: <https://www.genome.gov/25520394/online-education-kit-1998-genome-of-roundworm-c-elegans-sequenced>. (Accessed: August 2023).

National Human Genome Research Institute. (2019). *Synthetic Biology*. Available at: <https://www.genome.gov/about-genomics/policy-issues/Synthetic-Biology>. (Accessed: August 2023).

Nigon, V. M. & Félix, M. A. (2017) History of research on *C. elegans* and other free-living nematodes as model organisms. *WormBook*, 2017, 1-84. 10.1895/wormbook.1.181.1.

Nora, L. C., Westmann, C. A., Martins-Santana, L., Alves, L. F., Monteiro, L. M. O., Guazzaroni, M. E. & Silva-Rocha, R. (2019) The art of vector engineering: towards the construction of next-generation genetic tools. *Microb Biotechnol*, 12(1), 125-147. 10.1111/1751-7915.13318.

Olczyk, P., Mencner, Ł. & Komosinska-Vassev, K. (2015) Diverse Roles of Heparan Sulfate and Heparin in Wound Repair. *Biomed Res Int*, 2015, 549417. 10.1155/2015/549417.

Olivares, E., Badel-Berchoux, S., Provot, C., Jaulhac, B., Prévost, G., Bernardi, T. & Jehl, F. (2016) The BioFilm Ring Test: a Rapid Method for Routine Analysis of *Pseudomonas aeruginosa* Biofilm Formation Kinetics. *J Clin Microbiol*, 54(3), 657-61. 10.1128/jcm.02938-15.

Palikaras K and Tavernarakis N, *Caenorhabditis elegans* (Nematode). In: Stanley Maloy and Kelly Hughes, editors. *Brenner's Encyclopedia of Genetics* 2nd edition, Vol 1. San Diego: Academic Press; 2013. p. 404–408.

Pamp, S. J., Sternberg, C. & Tolker-Nielsen, T. (2009) Insight into the microbial multicellular lifestyle via flow-cell technology and confocal microscopy. *Cytometry A*, 75(2), 90-103. 10.1002/cyto.a.20685.

Papenfort, K. & Bassler, B. L. (2016) Quorum sensing signal-response systems in Gram-negative bacteria. *Nat Rev Microbiol*, 14(9), 576-88. 10.1038/nrmicro.2016.89.

Park, P. W., Reizes, O. & Bernfield, M. (2000) Cell surface heparan sulfate proteoglycans: selective regulators of ligand-receptor encounters. *J Biol Chem*, 275(39), 29923-6. 10.1074/jbc.R000008200.

Parsons, J. F., Greenhagen, B. T., Shi, K., Calabrese, K., Robinson, H. & Ladner, J. E. (2007) Structural and functional analysis of the pyocyanin biosynthetic protein PhzM from *Pseudomonas aeruginosa*. *Biochemistry*, 46(7), 1821-8. 10.1021/bi6024403.

Patel, H., Buchad, H. & Gajjar, D. (2022) *Pseudomonas aeruginosa* persister cell formation upon antibiotic exposure in planktonic and biofilm state. *Sci Rep*, 12(1), 16151. 10.1038/s41598-022-20323-3.

Pesci, E. C., Milbank, J. B., Pearson, J. P., McKnight, S., Kende, A. S., Greenberg, E. P. & Iglewski, B. H. (1999) Quinolone signaling in the cell-to-cell communication system of *Pseudomonas aeruginosa*.

Proc Natl Acad Sci U S A, 96(20), 11229-34.  
10.1073/pnas.96.20.11229.

Pessi, G. & Haas, D. (2000) Transcriptional control of the hydrogen cyanide biosynthetic genes *hcnABC* by the anaerobic regulator ANR and the quorum-sensing regulators LasR and RhIR in *Pseudomonas aeruginosa*. *J Bacteriol*, 182(24), 6940-9. 10.1128/jb.182.24.6940-6949.2000.

Potter, H. & Heller, R. (2018) Transfection by Electroporation. *Curr Protoc Mol Biol*, 121, 9.3.1-9.3.13. 10.1002/cpmb.48.

Price-Whelan, A., Dietrich, L. E. & Newman, D. K. (2007) Pyocyanin alters redox homeostasis and carbon flux through central metabolic pathways in *Pseudomonas aeruginosa* PA14. *J Bacteriol*, 189(17), 6372-81. 10.1128/jb.00505-07.

Quan, K., Hou, J., Zhang, Z., Ren, Y., Peterson, B. W., Flemming, H. C., Mayer, C., Busscher, H. J. & van der Mei, H. C. (2022) Water in bacterial biofilms: pores and channels, storage and transport functions. *Crit Rev Microbiol*, 48(3), 283-302.  
10.1080/1040841x.2021.1962802.

Que, Y. A., Hazan, R., Strobel, B., Maura, D., He, J., Kesarwani, M., Panopoulos, P., Tsurumi, A., Giddey, M., Wilhelmy, J., Mindrinos, M. N. & Rahme, L. G. (2013) A quorum sensing small volatile molecule promotes antibiotic tolerance in bacteria. *PLoS One*, 8(12), e80140. 10.1371/journal.pone.0080140.

Rada, B. & Leto, T. L. (2013) Pyocyanin effects on respiratory epithelium: relevance in *Pseudomonas aeruginosa* airway infections. *Trends Microbiol*, 21(2), 73-81. 10.1016/j.tim.2012.10.004.

Radlinski, L., Rowe, S. E., Kartchner, L. B., Maile, R., Cairns, B. A., Vitko, N. P., Gode, C. J., Lachiewicz, A. M., Wolfgang, M. C. & Conlon, B. P. (2017) *Pseudomonas aeruginosa* exoproducts determine antibiotic efficacy against *Staphylococcus aureus*. *PLoS Biol*, 15(11), e2003981. 10.1371/journal.pbio.2003981.

Ragno, M. 2023. *Development of an in-vivo high throughput assay to monitor biofilm development of the pathogenic microorganism Pseudomonas aeruginosa, in C. elegans*. MSc thesis, University of Kent, Canterbury.

Rajput, A. & Kumar, M. (2017) In silico analyses of conservational, functional and phylogenetic distribution of the LuxI and LuxR homologs in Gram-positive bacteria. *Sci Rep*, 7(1), 6969. 10.1038/s41598-017-07241-5.

Rasamiravaka, T., Labtani, Q., Duez, P. & El Jaziri, M. (2015) The formation of biofilms by *Pseudomonas aeruginosa*: a review of the natural and synthetic compounds interfering with control mechanisms. *Biomed Res Int*, 2015, 759348. 10.1155/2015/759348.

- Rather, M. A., Gupta, K. & Mandal, M. (2021) Microbial biofilm: formation, architecture, antibiotic resistance, and control strategies. *Braz J Microbiol*, 52(4), 1701-1718. 10.1007/s42770-021-00624-x.
- Read, R. C., Roberts, P., Munro, N., Rutman, A., Hastie, A., Shryock, T., Hall, R., McDonald-Gibson, W., Lund, V., Taylor, G. & et al. (1992) Effect of *Pseudomonas aeruginosa* rhamnolipids on mucociliary transport and ciliary beating. *J Appl Physiol* (1985), 72(6), 2271-7. 10.1152/jappl.1992.72.6.2271.
- Reddy, K. C., Hunter, R. C., Bhatla, N., Newman, D. K. & Kim, D. H. (2011) *Caenorhabditis elegans* NPR-1-mediated behaviors are suppressed in the presence of mucoid bacteria. *Proc Natl Acad Sci U S A*, 108(31), 12887-92. 10.1073/pnas.1108265108.
- Reichhardt, C., Jacobs, H. M., Matwichuk, M., Wong, C., Wozniak, D. J. & Parsek, M. R. (2020) The Versatile *Pseudomonas aeruginosa* Biofilm Matrix Protein CdrA Promotes Aggregation through Different Extracellular Exopolysaccharide Interactions. *J Bacteriol*, 202(19). 10.1128/jb.00216-20.
- Reis, R. S., Pereira, A. G., Neves, B. C. & Freire, D. M. (2011) Gene regulation of rhamnolipid production in *Pseudomonas aeruginosa*--a review. *Bioresour Technol*, 102(11), 6377-84. 10.1016/j.biortech.2011.03.074.
- Rouches, M. V., Xu, Y., Cortes, L. B. G. & Lambert, G. (2022) A plasmid system with tunable copy number. *Nat Commun*, 13(1), 3908. 10.1038/s41467-022-31422-0.
- Roy, R., Tiwari, M., Donelli, G. & Tiwari, V. (2018) Strategies for combating bacterial biofilms: A focus on anti-biofilm agents and their mechanisms of action. *Virulence*, 9(1), 522-554. 10.1080/21505594.2017.1313372.
- Rutherford, S. T. & Bassler, B. L. (2012) Bacterial quorum sensing: its role in virulence and possibilities for its control. *Cold Spring Harb Perspect Med*, 2(11). 10.1101/cshperspect.a012427.
- Sauer, K., Stoodley, P., Goeres, D. M., Hall-Stoodley, L., Burmølle, M., Stewart, P. S. & Bjarnsholt, T. (2022) The biofilm life cycle: expanding the conceptual model of biofilm formation. *Nat Rev Microbiol*, 20(10), 608-620. 10.1038/s41579-022-00767-0.
- Schaber, J. A., Triffo, W. J., Suh, S. J., Oliver, J. W., Hastert, M. C., Griswold, J. A., Auer, M., Hamood, A. N. & Rumbaugh, K. P. (2007) *Pseudomonas aeruginosa* forms biofilms in acute infection independent of cell-to-cell signaling. *Infect Immun*, 75(8), 3715-21. 10.1128/iai.00586-07.
- Schweizer, H. P. (1991) *Escherichia-Pseudomonas* shuttle vectors derived from pUC18/19. *Gene*, 97(1), 109-21. 10.1016/0378-1119(91)90016-5.

- Schütz, C. & Empting, M. (2018) Targeting the *Pseudomonas* quinolone signal quorum sensing system for the discovery of novel anti-infective pathoblockers. *Beilstein J Org Chem*, 14, 2627-2645. 10.3762/bjoc.14.241.
- Seed, P. C., Passador, L. & Iglewski, B. H. (1995) Activation of the *Pseudomonas aeruginosa* lasI gene by LasR and the *Pseudomonas* autoinducer PAI: an autoinduction regulatory hierarchy. *J Bacteriol*, 177(3), 654-9. 10.1128/jb.177.3.654-659.1995.
- Seminara, A., Angelini, T. E., Wilking, J. N., Vlamakis, H., Ebrahim, S., Kolter, R., Weitz, D. A. & Brenner, M. P. (2012) Osmotic spreading of *Bacillus subtilis* biofilms driven by an extracellular matrix. *Proc Natl Acad Sci U S A*, 109(4), 1116-21. 10.1073/pnas.1109261108.
- Seviour, T., Winnerdy, F. R., Wong, L. L., Shi, X., Mugunthan, S., Foo, Y. H., Castaing, R., Adav, S. S., Subramoni, S., Kohli, G. S., Shewan, H. M., Stokes, J. R., Rice, S. A., Phan, A. T. & Kjelleberg, S. (2021) The biofilm matrix scaffold of *Pseudomonas aeruginosa* contains G-quadruplex extracellular DNA structures. *NPJ Biofilms Microbiomes*, 7(1), 27. 10.1038/s41522-021-00197-5.
- Silhavy, T. J., Kahne, D. & Walker, S. (2010) The bacterial cell envelope. *Cold Spring Harb Perspect Biol*, 2(5), a000414. 10.1101/cshperspect.a000414.
- Simanek, K. A., Taylor, I. R., Richael, E. K., Lasek-Nesselquist, E., Bassler, B. L. & Paczkowski, J. E. (2022) The PqsE-RhIR Interaction Regulates RhIR DNA Binding to Control Virulence Factor Production in *Pseudomonas aeruginosa*. *Microbiol Spectr*, 10(1), e0210821. 10.1128/spectrum.02108-21.
- Singh, V. K., Almpiani, M., Maura, D., Kitao, T., Ferrari, L., Fontana, S., Bergamini, G., Calcaterra, E., Pignaffo, C., Negri, M., de Oliveira Pereira, T., Skinner, F., Gkikas, M., Andreotti, D., Felici, A., Déziel, E., Lépine, F. & Rahme, L. G. (2022) Tackling recalcitrant *Pseudomonas aeruginosa* infections in critical illness via anti-virulence monotherapy. *Nat Commun*, 13(1), 5103. 10.1038/s41467-022-32833-9.
- Smolentseva, O., Gusarov, I., Gautier, L., Shamovsky, I., DeFrancesco, A. S., Losick, R. & Nudler, E. (2017) Mechanism of biofilm-mediated stress resistance and lifespan extension in *C. elegans*. *Sci Rep*, 7(1), 7137. 10.1038/s41598-017-07222-8.
- Soberón-Chávez, G., González-Valdez, A., Soto-Aceves, M. P. & Cocotl-Yañez, M. (2021) Rhamnolipids produced by *Pseudomonas*: from molecular genetics to the market. *Microb Biotechnol*, 14(1), 136-146. 10.1111/1751-7915.13700.
- Soto-Aceves, M. P., Cocotl-Yañez, M., Servín-González, L. & Soberón-Chávez, G. (2021) The Rhl Quorum-Sensing System Is at the Top of the Regulatory Hierarchy under Phosphate-Limiting

- Conditions in *Pseudomonas aeruginosa* PAO1. *J Bacteriol*, 203(5). 10.1128/jb.00475-20.
- Spencer, J., Murphy, L. M., Conners, R., Sessions, R. B. & Gamblin, S. J. (2010) Crystal structure of the LasA virulence factor from *Pseudomonas aeruginosa*: substrate specificity and mechanism of M23 metallopeptidases. *J Mol Biol*, 396(4), 908-23. 10.1016/j.jmb.2009.12.021.
- Stiernagle, T. (2006) Maintenance of *C. elegans*. *WormBook*, 1-11. 10.1895/wormbook.1.101.1.
- Strand, T. A., Lale, R., Degnes, K. F., Lando, M. & Valla, S. (2014) A new and improved host-independent plasmid system for RK2-based conjugal transfer. *PLoS One*, 9(3), e90372. 10.1371/journal.pone.0090372.
- Straub, H., Eberl, L., Zinn, M., Rossi, R. M., Maniura-Weber, K. & Ren, Q. (2020) A microfluidic platform for in situ investigation of biofilm formation and its treatment under controlled conditions. *J Nanobiotechnology*, 18(1), 166. 10.1186/s12951-020-00724-0.
- Su, Y., Yrastorza, J. T., Matis, M., Cusick, J., Zhao, S., Wang, G. & Xie, J. (2022) Biofilms: Formation, Research Models, Potential Targets, and Methods for Prevention and Treatment. *Adv Sci (Weinh)*, 9(29), e2203291. 10.1002/advs.202203291.
- Sun, J., LaRock, D. L., Skowronski, E. A., Kimmey, J. M., Olson, J., Jiang, Z., O'Donoghue, A. J., Nizet, V. & LaRock, C. N. (2020) The *Pseudomonas aeruginosa* protease LasB directly activates IL-1 $\beta$ . *EBioMedicine*, 60, 102984. 10.1016/j.ebiom.2020.102984.
- Synch, T., Omidvar, R., Ostmann, R. *et al.* The bacterial lectin LecA from *P. aeruginosa* alters membrane organization by dispersing ordered domains. *Commun Phys* **6**, 153 (2023). <https://doi.org/10.1038/s42005-023-01272-3>
- Sánchez-Jiménez, A., Llamas, M. A. & Marcos-Torres, F. J. (2023) Transcriptional Regulators Controlling Virulence in *Pseudomonas aeruginosa*. *Int J Mol Sci*, 24(15). 10.3390/ijms241511895.
- Tacconelli, E., Carrara, E., Savoldi, A., Harbarth, S., Mendelson, M., Monnet, D. L., Pulcini, C., Kahlmeter, G., Kluytmans, J., Carmeli, Y., Ouellette, M., Outtersson, K., Patel, J., Cavalieri, M., Cox, E. M., Houchens, C. R., Grayson, M. L., Hansen, P., Singh, N., Theuretzbacher, U. & Magrini, N. (2018) Discovery, research, and development of new antibiotics: the WHO priority list of antibiotic-resistant bacteria and tuberculosis. *Lancet Infect Dis*, 18(3), 318-327. 10.1016/s1473-3099(17)30753-3.
- Teuscher, A. C. & Ewald, C. Y. (2018) Overcoming Autofluorescence to Assess GFP Expression During Normal Physiology and Aging in *Caenorhabditis elegans*. *Bio Protoc*, 8(14). 10.21769/BioProtoc.2940.

- Thi, M. T. T., Wibowo, D. & Rehm, B. H. A. (2020) *Pseudomonas aeruginosa* Biofilms. *Int J Mol Sci*, 21(22).
- Thomason, M. K., Voichek, M., Dar, D., Addis, V., Fitzgerald, D., Gottesman, S., Sorek, R. & Greenberg, E. P. (2019) A rhII 5' UTR-Derived sRNA Regulates RhlR-Dependent Quorum Sensing in *Pseudomonas aeruginosa*. *mBio*, 10(5). 10.1128/mBio.02253-19.
- Toder, D. S., Ferrell, S. J., Nezezon, J. L., Rust, L. & Iglewski, B. H. (1994) *lasA* and *lasB* genes of *Pseudomonas aeruginosa*: analysis of transcription and gene product activity. *Infect Immun*, 62(4), 1320-7. 10.1128/iai.62.4.1320-1327.1994.
- Toyofuku, M., Roschitzki, B., Riedel, K. & Eberl, L. (2012) Identification of proteins associated with the *Pseudomonas aeruginosa* biofilm extracellular matrix. *J Proteome Res*, 11(10), 4906-15. 10.1021/pr300395j.
- Tsai, C. S. & Winans, S. C. (2010) LuxR-type quorum-sensing regulators that are detached from common scents. *Mol Microbiol*, 77(5), 1072-82. 10.1111/j.1365-2958.2010.07279.x.
- Tuon, F. F., Dantas, L. R., Suss, P. H. & Tasca Ribeiro, V. S. (2022) Pathogenesis of the *Pseudomonas aeruginosa* Biofilm: A Review. *Pathogens*, 11(3). 10.3390/pathogens11030300.
- UK Health Security Agency. (2022). *Bacteraemia cases*. Available at: <https://www.gov.uk/government/statistics/p-aeruginosa-bacteraemia-monthly-data-by-location-of-onset> (Accessed: July 2023).
- van Kessel, J. C., Ulrich, L. E., Zhulin, I. B. & Bassler, B. L. (2013) Analysis of activator and repressor functions reveals the requirements for transcriptional control by LuxR, the master regulator of quorum sensing in *Vibrio harveyi*. *mBio*, 4(4). 10.1128/mBio.00378-13.
- Vessillier, S., Delolme, F., Bernillon, J., Saulnier, J. & Wallach, J. (2001) Hydrolysis of glycine-containing elastin pentapeptides by LasA, a metalloelastase from *Pseudomonas aeruginosa*. *Eur J Biochem*, 268(4), 1049-57. 10.1046/j.1432-1327.2001.01967.x.
- Vyas, H. K. N., Xia, B. & Mai-Prochnow, A. (2022) Clinically relevant in vitro biofilm models: A need to mimic and recapitulate the host environment. *Biofilm*, 4, 100069. 10.1016/j.bioflm.2022.100069.
- Wade, D. S., Calfee, M. W., Rocha, E. R., Ling, E. A., Engstrom, E., Coleman, J. P. & Pesci, E. C. (2005) Regulation of *Pseudomonas* quinolone signal synthesis in *Pseudomonas aeruginosa*. *J Bacteriol*, 187(13), 4372-80. 10.1128/jb.187.13.4372-4380.2005.
- Wagner, S., Hauck, D., Hoffmann, M., Sommer, R., Joachim, I., Müller, R., Imberty, A., Varrot, A. & Titz, A. (2017) Covalent Lectin Inhibition and Application in Bacterial Biofilm Imaging. *Angew Chem Int Ed Engl*, 56(52), 16559-16564. 10.1002/anie.201709368.

- Wang, B., Lin, Y. C., Vasquez-Rifo, A., Jo, J., Price-Whelan, A., McDonald, S. T., Brown, L. M., Sieben, C. & Dietrich, L. E. P. (2021) *Pseudomonas aeruginosa* PA14 produces R-bodies, extendable protein polymers with roles in host colonization and virulence. *Nat Commun*, 12(1), 4613. 10.1038/s41467-021-24796-0.
- Wang, C. & Zheng, C. (2022) Using *Caenorhabditis elegans* to Model Therapeutic Interventions of Neurodegenerative Diseases Targeting Microbe-Host Interactions. *Front Pharmacol*, 13, 875349. 10.3389/fphar.2022.875349.
- Wang, Y., Zhang, L., Yuan, X. & Wang, D. (2023) Treatment with paeoniflorin increases lifespan of *Pseudomonas aeruginosa* infected *Caenorhabditis elegans* by inhibiting bacterial accumulation in intestinal lumen and biofilm formation. *Front Pharmacol*, 14, 1114219. 10.3389/fphar.2023.1114219.
- Wareham, D. W., Papakonstantinou, A. & Curtis, M. A. (2005) The *Pseudomonas aeruginosa* PA14 type III secretion system is expressed but not essential to virulence in the *Caenorhabditis elegans*-*P. aeruginosa* pathogenicity model. *FEMS Microbiol Lett*, 242(2), 209-16. 10.1016/j.femsle.2004.11.018.
- Wargo, M. J. & Hogan, D. A. (2007) Examination of *Pseudomonas aeruginosa* lasI regulation and 3-oxo-C12-homoserine lactone production using a heterologous *Escherichia coli* system. *FEMS Microbiol Lett*, 273(1), 38-44. 10.1111/j.1574-6968.2007.00773.x.
- Waters, C. M. & Goldberg, J. B. (2019) *Pseudomonas aeruginosa* in cystic fibrosis: A chronic cheater. *Proc Natl Acad Sci U S A*, 116(14), 6525-6527. 10.1073/pnas.1902734116.
- Watson, S. A. & McStay, G. P. (2020) Functions of Cytochrome c oxidase Assembly Factors. *Int J Mol Sci*, 21(19). 10.3390/ijms21197254.
- Wei, Q. & Ma, L. Z. (2013) Biofilm matrix and its regulation in *Pseudomonas aeruginosa*. *Int J Mol Sci*, 14(10), 20983-1005.
- Weigelt, M. A., McNamara, S. A., Sanchez, D., Hirt, P. A. & Kirsner, R. S. (2021) Evidence-Based Review of Antibiofilm Agents for Wound Care. *Adv Wound Care (New Rochelle)*, 10(1), 13-23. 10.1089/wound.2020.1193.
- Westfall, C., Flores-Mireles, A. L., Robinson, J. I., Lynch, A. J. L., Hultgren, S., Henderson, J. P. & Levin, P. A. (2019) The Widely Used Antimicrobial Triclosan Induces High Levels of Antibiotic Tolerance In Vitro and Reduces Antibiotic Efficacy up to 100-Fold In Vivo. *Antimicrob Agents Chemother*, 63(5). 10.1128/aac.02312-18.
- Wilder, C. N., Diggle, S. P. & Schuster, M. (2011) Cooperation and cheating in *Pseudomonas aeruginosa*: the roles of the las, rhl and pqs quorum-sensing systems. *Isme j*, 5(8), 1332-43. 10.1038/ismej.2011.13.

- Wilking, J. N., Zaburdaev, V., De Volder, M., Losick, R., Brenner, M. P. & Weitz, D. A. (2013) Liquid transport facilitated by channels in *Bacillus subtilis* biofilms. *Proc Natl Acad Sci U S A*, 110(3), 848-52. 10.1073/pnas.1216376110.
- Wolfaardt, G. M., Lawrence, J. R., Robarts, R. D., Caldwell, S. J. & Caldwell, D. E. (1994) Multicellular organization in a degradative biofilm community. *Appl Environ Microbiol*, 60(2), 434-46. 10.1128/aem.60.2.434-446.1994.
- Wood, T. K., Knabel, S. J. & Kwan, B. W. (2013) Bacterial persister cell formation and dormancy. *Appl Environ Microbiol*, 79(23), 7116-21. 10.1128/aem.02636-13.
- Wood, T. L., Gong, T., Zhu, L., Miller, J., Miller, D. S., Yin, B. & Wood, T. K. (2018) Rhamnolipids from *Pseudomonas aeruginosa* disperse the biofilms of sulfate-reducing bacteria. *NPJ Biofilms Microbiomes*, 4, 22. 10.1038/s41522-018-0066-1.
- Xie, M. & Fussenegger, M. (2018) Designing cell function: assembly of synthetic gene circuits for cell biology applications. *Nat Rev Mol Cell Biol*, 19(8), 507-525. 10.1038/s41580-018-0024-z.
- Yan, H., Asfahl, K. L., Li, N., Sun, F., Xiao, J., Shen, D., Dandekar, A. A. & Wang, M. (2019) Conditional quorum-sensing induction of a cyanide-insensitive terminal oxidase stabilizes cooperating populations of *Pseudomonas aeruginosa*. *Nat Commun*, 10(1), 4999. 10.1038/s41467-019-13013-8.
- Yan, J., Nadell, C. D., Stone, H. A., Wingreen, N. S. & Bassler, B. L. (2017) Extracellular-matrix-mediated osmotic pressure drives *Vibrio cholerae* biofilm expansion and cheater exclusion. *Nat Commun*, 8(1), 327. 10.1038/s41467-017-00401-1.
- Yang, J., Zhao, H. L., Ran, L. Y., Li, C. Y., Zhang, X. Y., Su, H. N., Shi, M., Zhou, B. C., Chen, X. L. & Zhang, Y. Z. (2015) Mechanistic insights into elastin degradation by pseudolysin, the major virulence factor of the opportunistic pathogen *Pseudomonas aeruginosa*. *Sci Rep*, 5, 9936. 10.1038/srep09936.
- Yin, R., Cheng, J., Wang, J., Li, P. & Lin, J. (2022) Treatment of *Pseudomonas aeruginosa* infectious biofilms: Challenges and strategies. *Front Microbiol*, 13, 955286. 10.3389/fmicb.2022.955286.
- Yu, H., Rao, X. & Zhang, K. (2017) Nucleoside diphosphate kinase (Ndk): A pleiotropic effector manipulating bacterial virulence and adaptive responses. *Microbiol Res*, 205, 125-134. 10.1016/j.micres.2017.09.001.
- Yu, Z., Hu, Z., Xu, Q., Zhang, M., Yuan, N., Liu, J., Meng, Q. & Yin, J. (2020) The LuxI/LuxR-Type Quorum Sensing System Regulates Degradation of Polycyclic Aromatic Hydrocarbons via Two Mechanisms. *Int J Mol Sci*, 21(15). 10.3390/ijms21155548.

Zhang, L., Wang, Y., Cao, C., Zhu, Y., Huang, W., Yang, Y., Qiu, H., Liu, S. & Wang, D. (2022) Beneficial effect of Xuebijing against *Pseudomonas aeruginosa* infection in *Caenorhabditis elegans*. *Front Pharmacol*, 13, 949608. 10.3389/fphar.2022.949608.

Zhang, Y. M., Frank, M. W., Zhu, K., Mayasundari, A. & Rock, C. O. (2008) PqsD is responsible for the synthesis of 2,4-dihydroxyquinoline, an extracellular metabolite produced by *Pseudomonas aeruginosa*. *J Biol Chem*, 283(43), 28788-94. 10.1074/jbc.M804555200.

Zhou, Y. M., Shao, L., Li, J. A., Han, L. Z., Cai, W. J., Zhu, C. B. & Chen, D. J. (2011) An efficient and novel screening model for assessing the bioactivity of extracts against multidrug-resistant *Pseudomonas aeruginosa* using *Caenorhabditis elegans*. *Biosci Biotechnol Biochem*, 75(9), 1746-51. 10.1271/bbb.110290.

Zhu, K. & Rock, C. O. (2008) RhIA converts beta-hydroxyacyl-acyl carrier protein intermediates in fatty acid synthesis to the beta-hydroxydecanoyl-beta-hydroxydecanoate component of rhamnolipids in *Pseudomonas aeruginosa*. *J Bacteriol*, 190(9), 3147-54. 10.1128/jb.00080-08.

Zuhra, K. & Szabo, C. (2022) The two faces of cyanide: an environmental toxin and a potential novel mammalian gasotransmitter. *Febs j*, 289(9), 2481-2515. 10.1111/febs.16135.